SHIELDING THEORY OF ENCLOSURES WITH APERTURES

Horacio Augusto Mendez

California Institute of Technology

Prepared for:

Air Force Office of Scientific Research

4 December 1973

UNCLASSIFIED

SECURITY CLASSIFICATION OF THIS PAGE (When Data Entered)

AD-773770

REPORT DOCUMENTATION PAGE		READ INSTRUCTIONS BEFORE COMPLETING FORM
1. REPORT NUMBER AFOSR - TR - 74 - 0100	2. GOVT ACCESSION NO.	3. RECIPIENT'S CATALOG NUMBER
4. TITLE (and Subtitle) SHIELDING THEORY OF ENCLOSURES WITH APERTURES		5. TYPE OF REPORT & PERIOD COVERED Interim
		6. PERFORMING ORG. REPORT NUMBER
7. AUTHOR(s) Horacio A. Mendez		8. CONTRACT OR GRANT NUMBER(s) AFOSR-70-1935
9. PERFORMING ORGANIZATION NAME AND ADDRESS California Institute of Technology Pasadena, California 91109		10. PROGRAM ELEMENT, PROJECT, TASK AREA & WORK UNIT NUMBERS 9768-02 61102F 681306
11. CONTROLLING OFFICE NAME AND ADDRESS AF Office of Scientific Research (NE) 1400 Wilson Blvd. Arlington, VA 22209		12. REPORT DATE Dec 73
		13. NUMBER OF PAGES ~~139~~ 143
14. MONITORING AGENCY NAME & ADDRESS(if different from Controlling Office)		15. SECURITY CLASS. (of this report) UNCLASSIFIED
		15a. DECLASSIFICATION/DOWNGRADING SCHEDULE

16. DISTRIBUTION STATEMENT (of this Report)

Approved for public release; distribution unlimited.

17. DISTRIBUTION STATEMENT (of the abstract entered in Block 20, if different from Report)

18. SUPPLEMENTARY NOTES

19. KEY WORDS (Continue on reverse side if necessary and identify by block number)

20. ABSTRACT (Continue on reverse side if necessary and identify by block number)

Present methods for computing the shielding efficiency of metallic plates with apertures are based on the analysis of a plan wave incident on an infinite conducting sheet. When applied to actual enclosures with internal radiation sources, these methods lose all validity, and obviously fail to predict the measured results. Semi-empirical formulas are available for special cases, but no serious analytic investigation has ever been conducted. This report develops the theory of electromagnetic radiation from metallic enclosures with aperatures, excited by an internal source at frequencies below the fundamental

DD FORM 1 JAN 73 1473 EDITION OF 1 NOV 65 IS OBSOLETE

SECURITY CLASSIFICATION OF THIS PAGE (When Data Entered)

ia

resonance of the enclosure. The enclosure with an aperture is analyzed from two different points of view: as a cavity with a small aperture in a wall; and as a waveguide section short-circuited at one end and open at the other end.

UNCLASSIFIED

Security Classification

DOCUMENT CONTROL DATA · R & D AD-773770

(Security classification of title, body of abstract and indexing annotation must be entered when the overall report is classified)

1 ORIGINATING ACTIVITY (Corporate author)

California Institute of Technology
Pasadena, Calif. 91109

2a. REPORT SECURITY CLASSIFICATION

Unclassified

2b. GROUP

3 REPORT TITLE

SHIELDING THEORY OF ENCLOSURES WITH APERTURES

4 DESCRIPTIVE NOTES (Type of report and inclusive dates)

Interim Technical

5 AUTHOR(S) (First name, middle initial, last name)

Horacio A. Méndez

6 REPORT DATE	7a. TOTAL NO OF PAGES	7b. NO OF REFS
Dec. 1973	139	27

8a CONTRACT OR GRANT NO	9a. ORIGINATOR'S REPORT NUMBER(S)
AFOSR-70-1935	Antenna Laboratory Technical Report No. 68
b. PROJECT NO 9768-02	
c 61102F	9b. OTHER REPORT NO(S) (Any other numbers that may be assigned this report)
d 681305	

10 DISTRIBUTION STATEMENT

Approved for public release; distribution unlimited.

11 SUPPLEMENTARY NOTES	12 SPONSORING MILITARY ACTIVITY
TECH, OTHER	A.F. Office of Scientific Research (NE) 1400 Wilson Blvd. Arlington, Virginia 22209

13 ABSTRACT

Present methods for computing the shielding efficiency of metallic plates with apertures are based on the analysis of a plane wave incident on an infinite conducting sheet. When applied to actual enclosures with internal radiation sources, these methods lose all validity, and obviously fail to predict the measured results. Semi-empirical formulas are available for special cases, but no serious analytic investigation has ever been conducted.

This report develops the theory of electromagnetic radiation from metallic enclosures with apertures, excited by an internal source at frequencies below the fundamental resonance of the enclosure. The enclosure with an aperture is analyzed from two different points of view: as a cavity with a small aperture in a wall; and as a waveguide section short-circuited at one end and open at the other end.

Rectangular geometries are used throughout, since these are by far the most commonly encountered in practical enclosures and cabinets. Using the corresponding dyadic Green functions, the fields generated inside the enclosure by some simple sources are determined. In addition to the case of a Hertzian dipole--the building block for more complicated sources--a center-fed dipole and a square loop antenna are analyzed. The fields radiated through small apertures in a cavity are determined using Bethe's theory of diffraction by small holes. Radiation from an open waveguide is calculated with the help of field equivalence theorems with assumptions applicable to the case of evanescent waves. Expressions for the "Insertion Loss" of the shield are derived, and are numerically evaluated for some representative cases.

This work provides accurate prediction capabilities for the design of shielded enclosures with apertures in the presence of internal or external noise sources.

DD FORM 1473

UNCLASSIFIED

Security Classification

ii

SHIELDING THEORY OF ENCLOSURES WITH APERTURES

Thesis by

Horacio Augusto Méndez

In Partial Fulfillment of the Requirements
for the Degree of
Doctor of Philosophy

California Institute of Technology
Pasadena, California

1974

(Submitted December 4, 1973)

ACKNOWLEDGMENTS

The author wishes to acknowledge the encouragement, interest and understanding demonstrated by his advisor, Professor C. H. Papas, during the course of this task.

The author also would like to thank Professor G. Franceschetti and Dr. N. L. Broome for the many and helpful discussions that provided valuable insight into broad areas of electromagnetic theory.

As is true with most academic activities, this work could not have been accomplished without the love, understanding and cooperation of the author's wife and children.

Finally, the author is especially and doubly indebted to the IBM Corporation. During the course of this research, the author was a participant in the Resident Study Program of IBM's General Products Division (San Jose, California). Moreover, the measurements providing experimental confirmation of the present work, were especially conducted for the author by the Electromagnetic Compatibility Group of IBM's Laboratory in Kingston, New York, under the management of Mr. R. Calcavecchio and the technical supervision of Mr. A. A. Smith, Jr. Their support is gratefully acknowledged.

Special thanks are extended to Kathy Ellison and Karen Current for typing the manuscript.

ABSTRACT

Present methods for computing the shielding efficiency of metallic plates with apertures are based on the analysis of a plane wave incident on an infinite conducting sheet. When applied to actual enclosures with internal radiation sources, these methods lose all validity, and obviously fail to predict the measured results. Semi-empirical formulas are available for special cases, but no serious analytic investigation has ever been conducted.

This dissertation develops the theory of electromagnetic radiation from metallic enclosures with apertures, excited by an internal source at frequencies below the fundamental resonance of the enclosure.

The enclosure with an aperture is analyzed from two different points of view: as a cavity with a small aperture in a wall; and as a waveguide section short-circuited at one end and open at the other end.

Rectangular geometries are used throughout, since these are by far the most commonly encountered in practical enclosures and cabinets.

Using the corresponding dyadic Green's functions, the fields generated inside the enclosure by some simple sources are determined. In addition to the case of a Hertzian dipole - the building block for more complicated sources - a center-fed dipole and a square loop antenna are analyzed. The fields radiated through small apertures in a cavity are determined using Bethe's theory of diffraction

by small holes. The radiation from an open waveguide is calculated with the help of field equivalence theorems, with assumptions applicable to the case of evanescent waves.

The final step is to derive expressions for the "Insertion Loss" of the shield, defined as the ratio of the field strength at a point external to the shield, before and after the insertion of the enclosure. To accomplish this, the effect of the shield upon the input impedance of the antenna is analyzed, and expressions obtained for the applicable cases.

The resulting insertion loss expressions are numerically evaluated for some representative cases, and graphically compared with a series of measurements performed to obtain experimental confirmation. Very good agreement is obtained in all cases, establishing the validity of the analysis.

Thus, this work provides accurate prediction capabilities for the design of shielded enclosures with apertures, in the presence of internal or external noise sources (the latter is a consequence of applying the reciprocity theorem). Hence, it constitutes a useful tool in the solution of electromagnetic interference and susceptibility problems.

TABLE OF CONTENTS

Chapter I

INTRODUCTION

Of all the topics comprising the broad field of Electromagnetic Theory, one of the most relevant but least developed is that of electromagnetic shields. The most obvious reason for this state of affairs is that very few three-dimensional boundary value problems have exact or even approximate mathematical solutions, and those that do, are seldom representative of practical, real-world problems. A less obvious, but not less important reason, is that most engineers and physicists working with electromagnetic waves emphasize the optimization of radiation and the generation and transmission of propagating waves and in so doing, disregard those effects that are of paramount importance in shielding theory.

An excellent example combining both of the above reasons is provided by the theory of waveguides and resonant cavities at frequencies below their fundamental mode. The fact that at low frequencies the waves in these structures become "evanescent", seems to have justified their neglect, except for casual and sometimes misleading statements.

One extremely important application for such a theory, if it were systematically developed, is the prediction of the shielding effects of closed shields with apertures. A typical electronic or electromechanical piece of equipment consists of a collection of circuits and devices, surrounded by a metallic cabinet or by covers.

This cabinet, besides providing obvious physical protection, acts as a double-purpose electromagnetic shield: it protects the sensitive portions of the equipment from the electromagnetic "noise" of the environment, and it contains the "noise" generated in its interior.

The concern about generating unwanted electromagnetic waves ("pollution of the spectrum") has been growing rapidly over the past few years. Germany has taken the lead with its "RFI* Law", which imposes strict limits to electromagnetic emanations from any electrical machine or appliance marketed in that country.

Other countries, including the United States, will soon follow, and manufacturers will need a reliable mean of predicting the degree of shielding afforded by metallic enclosures, so that function and cost may be optimized.

In most situations, the leakage of electromagnetic energy from a metallic enclosure is dominated not by the physical characteristics of the metal, but by the size, shape and location of the apertures that are needed for such various reasons as: input and output connections, control panels, dials, ventilation panels, visual access windows, etc.

Moreover, the mere presence of a conducting enclosure around a radiating source changes--sometimes dramatically--the radiation characteristics of that source. It does so by affecting its input

*Radio-Frequency Interference

impedance and therefore changing its current.

All these things have to be accounted for in a comprehensive theory of shielding applicable to enclosures with apertures.

No serious attempts have been made to date to develop such a theory. The treatment of electromagnetic leakage through apertures has been confined to the case of incident plane waves on an infinite screen, and the various formulas available in shielding handbooks are derived from that case.

In the present work, we develop the theory of electromagnetic radiation from metallic enclosures with apertures, excited by an internal source.

We have confined our treatment to frequencies below the fundamental mode of the enclosure (i.e., below the cutoff frequency of the cavity). For typical cabinets, the "cutoff" frequency is in the tens or hundreds of megahertz, and the radiation spectrum of most noise sources seldom shows a significant contribution at these or higher frequencies. Thus, we are covering a very significant portion of the RFI spectrum. Besides, the inclusion of resonance effects would call for very different techniques from those used here.

We have also limited ourselves to rectangular geometries, which are by far the most typically encountered in cabinets and enclosures. Nevertheless, the techniques here presented may be easily duplicated for other regular geometries.

The approach taken is to treat the enclosure as a resonant cavity below cutoff. This allows us to replace it with a perfectly

conducting cavity, obviously assuming that the wall losses will be small compared to the energy leaking through the aperture.

After finding the fields generated in a rectangular cavity by typical radiation sources, we apply Bethe's theory of diffraction by small holes to determine the fields radiated by the aperture.

In order to cover the case where a whole wall is missing in the enclosure (representing for instance, an open door or missing cover), we develop the theory of typical antennas inside a waveguide section, short-circuited at one end and open at the other end. Field equivalence theorems are then invoked to find the radiation from the waveguide's "mouth".

The effect of the cavity (or waveguide section) upon the antenna is treated next, so that we can derive expressions for the quantity of interest in shielding theory: the "Insertion Loss" of a shield, defined as the ratio of the field strength at a point external to the shield, before and after the insertion of that shield.

Our final task is the development of equations for some specific cases, and the comparison of theoretically predicted results with experimentally measured values.

Throughout this thesis, we will be forced to make approximations and assumptions, some of them justified on purely heuristic grounds. The correlation between predictions arising from the two different approaches, and their experimental confirmation, will provide the final word on their validity.

Chapter II

ELECTROMAGNETIC LEAKAGE FROM A CAVITY WITH SMALL APERTURES

In this chapter we shall find expressions for the electromagnetic fields leaking through small apertures in a perfectly conducting rectangular cavity excited by a source located in its interior.

To accomplish this, we shall first make use of the Green's functions for a rectangular cavity to determine the interior fields produced by simple antennas in the absence of apertures. As is the case throughout this dissertation, we shall only consider frequencies lower than the first resonant frequency of the cavity, i.e., the cavity is excited below cutoff.

Then, we shall make use of Bethe's theory on the "polarizability" of apertures[1], which will allow us to find the electromagnetic fields radiated through the aperture.

II.1 Green's Functions for a Rectangular Cavity

We start by defining the electric scalar potential ϕ and the magnetic vector potential $\vec{A}$ in the usual way

$$\vec{B} = \vec{\nabla} \times \vec{A} \tag{II.1.1}$$

$$\vec{E} = -\vec{\nabla}\phi + j\omega\vec{A} \tag{II.1.2}$$

If we now choose to work in the Lorentz gauge by defining

$$\vec{\nabla} \cdot \vec{A} = j\omega\mu_0\varepsilon_0\phi \tag{II.1.3}$$

the field equations to be solved are the scalar and vector Helmholtz equations

$$\nabla^2\phi + k^2\phi = -\frac{\rho}{\varepsilon_0} \tag{II.1.4}$$

$$\nabla^2\vec{A} + k^2\vec{A} = -\mu_0 \vec{J} \tag{II.1.5}$$

where

$$k = \omega\sqrt{\mu_0\varepsilon_0} = \frac{2\pi}{\lambda} \tag{II.1.6}$$

We are, of course, assuming that the fields are time-harmonic, with a time-dependence given by $e^{j\omega t}$. The corresponding scalar and dyadic Green's functions are the solutions to[2]

$$\nabla^2 G(\vec{r}|\vec{r}_0) + k^2 G(\vec{r}|\vec{r}_0) = -\delta(\vec{r} - \vec{r}_0) \tag{II.1.7}$$

$$\nabla^2\overleftrightarrow{G}(\vec{r}|\vec{r}_0) + k^2\overleftrightarrow{G}(\vec{r}|\vec{r}_0) = -\overleftrightarrow{U}\delta(\vec{r} - \vec{r}_0) \tag{II.1.8}$$

where $\overleftrightarrow{U}$ is the "idemfactor" (unit dyadic).

On the walls of a perfectly conducting cavity, we know that

$$\vec{1}_n \times \vec{E} = 0 \quad \text{on} \quad S \tag{II.1.9}$$

where S is the boundary surface. The corresponding boundary conditions for Eqs. (II.1.7) and (II.1.8) are

$$\left.\begin{aligned} \phi &= 0 \\ \vec{\nabla}\cdot\vec{A} &= 0 \\ \vec{1}_n \times \vec{A} &= 0 \end{aligned}\right\} \quad \text{on} \quad S \tag{II.1.10}$$

The Green's functions thus obtained are then combined with the mathematical representation of the actual sources in the cavity to produce the field potentials

$$\phi(\vec{r}) = \int_{Vol} G(\vec{r}|\vec{r}_o) \frac{\rho(\vec{r}_o)}{\varepsilon_o} d\tau_o \qquad (II.1.11)$$

$$\vec{A}(\vec{r}) = \int_{Vol} \overleftrightarrow{G}(\vec{r}|\vec{r}_o) \cdot \mu_o \vec{J}(\vec{r}_o) d\tau_o \qquad (II.1.12)$$

where $d\tau_o$ is an element of volume.

For a perfectly conducting rectangular cavity of sides a, b and d, associated with the x, y and z directions, the Green functions are found to be[3]

$$G(\vec{r}|\vec{r}_o) = -\frac{4}{ad} \sum_{m,p} \sin\frac{m\pi x}{a} \cdot \sin\frac{p\pi z}{d} \cdot$$

$$\cdot \sin\frac{m\pi x_o}{a} \cdot \sin\frac{p\pi z_o}{d} \cdot \frac{1}{K_{mp}\sin(K_{mp}b)} \cdot$$

$$\cdot \begin{cases} \sin(K_{mp}y_o)\sin[K_{mp}(b-y)] \; ; \text{ if } y > y_o \\ \sin(K_{mp}y)\sin[K_{mp}(b-y_o)] \; ; \text{ if } y < y_o \end{cases} \qquad (II.1.13)$$

$$\overleftrightarrow{G}(\vec{r}|\vec{r}_o) = \frac{1}{ad} \sum_{m,p} \frac{\epsilon_m \epsilon_p}{k^2_{mp}} \left\{ \left[\hat{f}_y \times \vec{\nabla} \psi_{mp}(\vec{r}_o) \right] \right.$$

$$\left[\hat{f}_y \times \vec{\nabla} \psi_{mp}(\vec{r}) \right] f_{mp} +$$

$$+ k^2_{mp} \hat{f}_y \chi_{mp}(\vec{r}_o) \hat{f}_y \chi_{mp}(\vec{r}) g_{mp} +$$

$$\left. + \vec{\nabla} \chi_{mp}(\vec{r}_o) \vec{\nabla} \chi_{mp}(\vec{r}) f_{mp} \right\} \qquad \text{(II.1.14)}$$

where

$$K_{mp} = k - \left[\left(\frac{m\pi}{a} \right)^2 + \left(\frac{p\pi}{d} \right)^2 \right] \qquad \text{(II.1.15)}$$

$$k^2_{mp} = \left(\frac{m\pi}{a} \right)^2 + \left(\frac{p\pi}{d} \right)^2 \qquad \text{(II.1.16)}$$

$$\psi_{mp} = \cos \frac{m\pi x}{a} \cdot \cos \frac{p\pi z}{d} \qquad \text{(II.1.17)}$$

$$\chi_{mp} = \sin \frac{m\pi x}{a} \cdot \sin \frac{p\pi z}{d} \qquad \text{(II.1.18)}$$

$$f_{mp} = \frac{1}{K_{mp} \sin(K_{mp} b)} \cdot \begin{cases} \sin(K_{mp} y_o) \sin[K_{mp}(b-y)] \text{ ; if } y > y_o \\ \sin(K_{mp} y) \sin[K_{mp}(b-y_o)] \text{; if } y < y_o \end{cases} \qquad \text{(II.1.19)}$$

$$g_{mp} = \frac{-1}{K_{mp} \sin(K_{mp} b)} \cdot \begin{cases} \cos(K_{mp} y_o) \cdot \cos[K_{mp}(b-y)] \text{ ; if } y > y_o \\ \cos(K_{mp} y) \cdot \cos[K_{mp}(b-y_o)] \text{ ; if } y < y_o \end{cases} \qquad \text{(II.1.20)}$$

m and n are positive integers ranging from zero to infinity.

ε_m and ε_p are Neumann factors, i.e.,

$$\varepsilon_m = \begin{cases} 1 \ ; \text{ if } m = 0 \\ 2 \ ; \text{ otherwise} \end{cases} \qquad \text{(II.1.21)}$$

(x_0, y_0, z_0) are the source coordinates and (x,y,z) are the field coordinates.

Equivalent forms for $G(\vec{r}|\vec{r}_0)$ and $\overleftrightarrow{G}(\vec{r}|\vec{r}_0)$ may be obtained by cyclic interchange of x, y and z and their associated parameters.

II.2 Electromagnetic Fields in a Rectangular Cavity

In this section we shall make use of the Green functions to find the electromagnetic fields inside a rectangular cavity excited by simple antennas, namely: a Hertzian dipole (or current element), an electrically short thin dipole, and an electrically small loop.

Working in the Lorentz gauge, Eq. (II.1.3), we need only to solve for the vector potential $\vec{A}$ in Eq. (II.1.12), since the electric and magnetic fields are then given by

$$\vec{E} = -\frac{1}{j\omega\mu_0\varepsilon_0}\,\vec{\nabla}(\vec{\nabla}\cdot\vec{A}) + j\omega\vec{A} \qquad \text{(II.2.1)}$$

$$\vec{H} = \frac{1}{\mu_0}\,\vec{\nabla} \times \vec{A} \qquad \text{(II.2.2)}$$

II.2.1 Excitation by a Hertzian Dipole.

Consider a current element of length L, defined by (see Fig. 1)

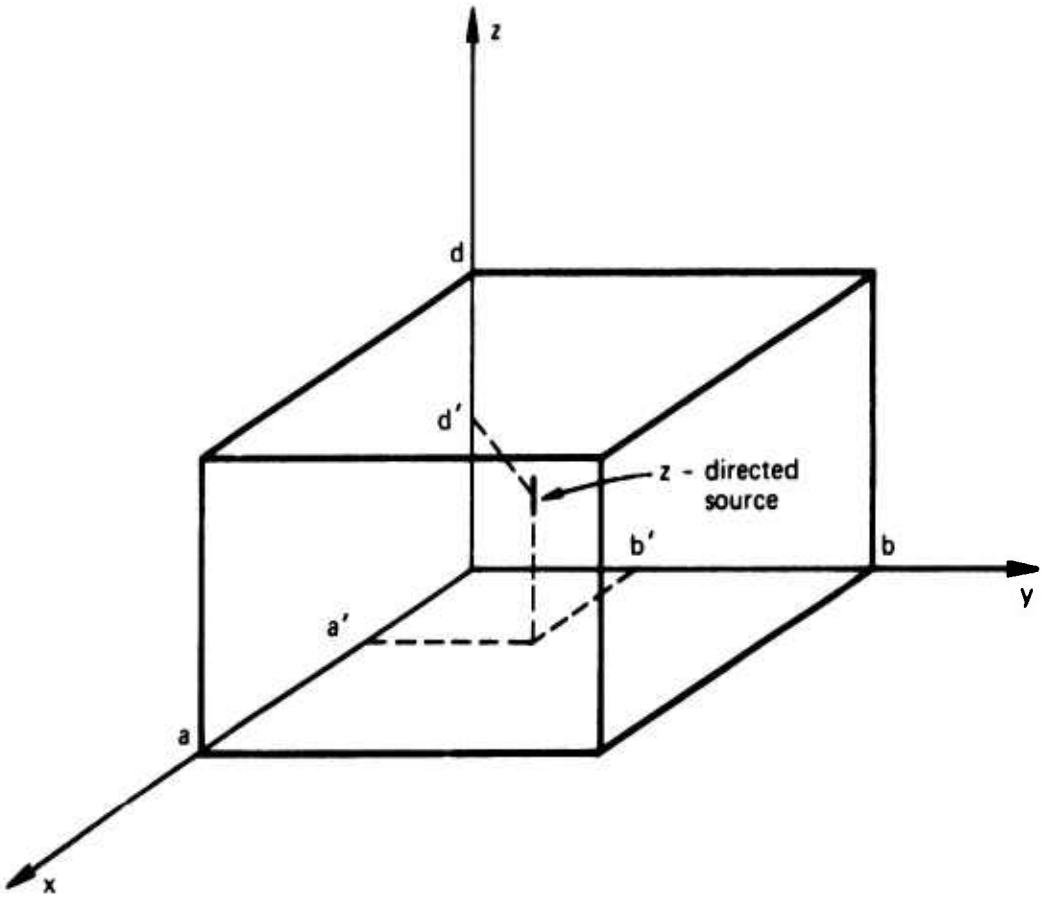

Figure 1
Hertzian dipole in a rectangular cavity

$$\vec{J} = \hat{i}_z J_z = \begin{cases} \hat{i}_z I_0 \delta(x-a') \, \delta(x-b') \; ; \; d' - \frac{L}{2} < z < d' + \frac{L}{2} \\ 0 \qquad\qquad\qquad\qquad ; \; |z - d'| > \frac{L}{2} \end{cases} \tag{II.2.3}$$

The vector potential $\vec{A}$ is given by Eq. (II.1.12), reproduced below

$$\vec{A}(\vec{r}) = \int_{\text{Vol.}} \overleftrightarrow{G}(\vec{r}|\vec{r}_0) \cdot \mu_0 \vec{J}(\vec{r}_0) \, d\tau_0 \tag{II.2.4}$$

Given $\vec{J}$ in the z-direction, the only components of Green's dyadic that may contribute to the answer are

$$G_{xz} \quad , \quad G_{yz} \quad \text{and} \quad G_{zz} \quad .$$

Inspection of Eq. (II.1.14) results in

$$G_{xz} = 0 \tag{II.2.5}$$

$$G_{yz} = 0 \tag{II.2.6}$$

$$G_{zz} = \frac{1}{ad} \sum_{m,p} \varepsilon_m \varepsilon_p \cdot \sin \frac{m\pi x_0}{a} \cdot \cos \frac{p\pi z_0}{d} \cdot$$

$$\cdot \sin \frac{m\pi x}{a} \cdot \cos \frac{p\pi z}{d} \cdot \frac{1}{K_{mp} \sin(K_{mp} b)} \cdot$$

$$\cdot \begin{cases} \sin(K_{mp} y_0) \cdot \sin[K_{mp}(b-y)] \; ; \text{ if } y > y_0 \\ \sin(K_{mp} y) \cdot \sin[K_{mp}(b-y_0)] \; ; \text{ if } y < y_0 \end{cases} \tag{II.2.7}$$

Using Eqs. (II.2.3) and (II.2.7) in (II.2.4) we obtain

$$\vec{A} = \vec{1}_z A_z \tag{II.2.8}$$

$$A_z = \frac{\mu_o I_o}{ad} \sum_{m,p} \epsilon_m \epsilon_p \cdot \sin\frac{m\pi x}{a} \cdot \cos\frac{p\pi z}{d} \cdot$$

$$\cdot \frac{2d}{p\pi} \cdot \sin\frac{m\pi a'}{a} \cdot \cos\frac{p\pi d'}{d} \cdot \sin\frac{p\pi L}{2d} \cdot$$

$$\cdot \frac{1}{K_{mp}\sin(K_{mp}b)} \cdot \begin{cases} \sin(K_{mp}b')\sin[K_{mp}(b-y)] \ ; \ \text{if } y > b' \\ \sin(K_{mp}y)\sin[K_{mp}(b-b')] \ ; \ \text{if } y < b' \end{cases} \tag{II.2.9}$$

The electric field is then found from Eq. (II.2.1), which now becomes

$$\vec{E} = -\frac{1}{j\omega\mu_o\epsilon_o} \vec{\nabla}\left(\frac{\partial A_z}{\partial z}\right) + \vec{1}_z j\omega A_z \tag{II.2.10}$$

resulting in

$$E_x = -j\frac{8I_o}{kad}\sqrt{\frac{\mu_o}{\epsilon_o}} \sum_{m,p} \cos\frac{m\pi x}{a} \cdot \sin\frac{p\pi z}{d} \cdot \frac{m\pi}{a}$$

$$\cdot \sin\frac{m\pi a'}{a} \cdot \cos\frac{p\pi d'}{d} \cdot \sin\frac{p\pi L}{2d} \cdot \frac{1}{K_{mp}\sin(K_{mp}b)} \cdot$$

$$\cdot \begin{cases} \sin(K_{mp}b')\sin[K_{mp}(b-y)] \ ; \ \text{if } y > b' \\ \sin(K_{mp}y)\sin[K_{mp}(b-b')] \ ; \ \text{if } y < b' \end{cases} \tag{II.2.11}$$

$$E_y = -j \frac{8I_o}{kad} \sqrt{\frac{\mu_o}{\varepsilon_o}} \sum_{m,p} \sin \frac{m\pi x}{a} \cdot \sin \frac{p\pi z}{d} \cdot$$

$$\sin \frac{m\pi a'}{a} \cdot \cos \frac{p\pi d'}{d} \cdot \sin \frac{p\pi L}{2d} \cdot \frac{1}{\sin(K_{mp} b)} \cdot$$

$$\cdot \begin{cases} -\sin(K_{mp} b') \cdot \cos [K_{mp}(b-y)] \; ; \text{ if } y > b' \\ \cos(K_{mp} y) \cdot \sin [K_{mp}(b-b') \; ; \text{ if } y < b' \end{cases} \qquad \text{(II.2.12)}$$

$$E_z = -j \frac{4I_o}{kad} \sqrt{\frac{\mu_o}{\varepsilon_o}} \sum_{m,p} \varepsilon_p \cdot \sin \frac{m\pi x}{a} \cdot \cos \frac{p\pi z}{d} \cdot \frac{d}{p\pi} \cdot$$

$$\cdot \sin \frac{m\pi a'}{a} \cdot \cos \frac{p\pi d'}{d} \cdot \sin \frac{p\pi L}{2d} \cdot \frac{\left(\frac{p\pi}{d}\right)^2 - k^2}{K_{mp} \sin(K_{mp} b)} \cdot$$

$$\cdot \begin{cases} \sin(K_{mp} b') \sin[K_{mp}(b-y)] \; ; \text{ if } y > b' \\ \sin(K_{mp} y) \sin[K_{mp}(b-b')] \; ; \text{ if } y < b' \end{cases} \qquad \text{(II.2.13)}$$

The magnetic field is obtained from Eq. (II.2.2), which we can now write as

$$\vec{H} = \frac{1}{\mu_o} \vec{\nabla} \times \vec{A} = \frac{1}{\mu_o} \left(\hat{\imath}_x \frac{\partial A_z}{\partial y} - \hat{\imath}_y \frac{\partial A_z}{\partial x} \right) \qquad \text{(II.2.14)}$$

The cartesian components of this magnetic field are

$$H_x = \frac{4I_o}{ad} \sum_{m,p} \varepsilon_p \cdot \sin\frac{m\pi x}{a} \cdot \cos\frac{p\pi z}{d} \cdot \frac{d}{p\pi} \cdot$$

$$\cdot \sin\frac{m\pi a'}{a} \cdot \cos\frac{p\pi d'}{d} \cdot \sin\frac{p\pi L}{2d} \cdot \frac{1}{\sin(K_{mp}b)} \cdot$$

$$\cdot \begin{cases} -\sin(K_{mp}b') \cdot \cos[K_{mp}(b-y)] \; ; \text{ if } y > b' \\ \cos(K_{mp}y) \cdot \sin[K_{mp}(b-b')] \; ; \text{ if } y < b' \end{cases} \qquad \text{(II.2.15)}$$

$$H_y = -\frac{4I_o}{ad} \sum_{m,p} \varepsilon_p \cos\frac{m\pi x}{a} \cdot \cos\frac{p\pi z}{d} \cdot \frac{m\pi}{a} \cdot$$

$$\cdot \frac{d}{p\pi} \cdot \sin\frac{m\pi a'}{a} \cdot \cos\frac{p\pi d'}{d} \cdot \sin\frac{p\pi L}{2d} \cdot$$

$$\cdot \frac{1}{K_{mp}\sin(K_{mp}b)} \cdot \begin{cases} \sin(K_{mp}b') \cdot \sin[K_{mp}(b-y)] \; ; \text{ if } y > b' \\ \sin(K_{mp}y) \cdot \sin[K_{mp}(b-b')] \; ; \text{ if } y < b' \end{cases}$$

(II.2.16)

$$H_z = 0 \qquad \text{(II.2.17)}$$

II.2.2 Excitation by an Electrically Short Dipole Antenna.

We shall consider the idealized case of a center-driven thin dipole antenna, with the driving emf concentrated at its center. The antenna current is assumed to be

$$\vec{J} = \vec{1}_z J_z = \begin{cases} \vec{1}_z I_o \dfrac{\sin[k(h-|z-d'|)]}{\sin(kh)} \delta(x-a')\delta(y-b') & ; \ |z-d'|<h \\ 0 & ; \ |z-d'|>h \end{cases}$$

(II.2.18)

The overall length of the dipole is 2h.

Repeating the process of part II.2.1, we arrive at the following field components

$$E_x = -j \frac{4I_o}{ad \sin(kh)} \sqrt{\frac{\mu_o}{\varepsilon_o}} \sum_{m,p} \cos\frac{m\pi x}{a} \cdot \sin\frac{p\pi z}{d} \cdot$$

$$\cdot \frac{\frac{m\pi}{a} \cdot \frac{p\pi}{d}}{\left(\frac{p\pi}{d}\right)^2 - k^2} \cdot \sin\frac{m\pi a'}{a} \cdot \cos\frac{p\pi d'}{d} \cdot \left[\cos\frac{p\pi h}{d} - \cos(kh)\right] \cdot$$

$$\cdot \frac{1}{K_{mp}\sin(K_{mp}b)} \cdot \begin{cases} \sin(K_{mp}b') \cdot \sin[K_{mp}(b-y)] & ; \text{ if } y > b' \\ \sin(K_{mp}y) \cdot \sin[K_{mp}(b-b')] & ; \text{ if } y < b' \end{cases}$$

(II.2.19)

$$E_y = -j \frac{4I_o}{ad \sin(kh)} \sqrt{\frac{\mu_o}{\varepsilon_o}} \sum_{m,p} \sin\frac{m\pi x}{a} \cdot \sin\frac{p\pi z}{d} \cdot$$

$$\cdot \frac{\frac{p\pi}{d}}{\left(\frac{p\pi}{d}\right)^2 - k^2} \cdot \sin\frac{m\pi a'}{a} \cdot \cos\frac{p\pi d'}{d} \cdot \left[\cos\frac{p\pi h}{d} - \cos(kh)\right] \cdot$$

$$\cdot \frac{1}{\sin(K_{mp}b)} \cdot \begin{cases} -\sin(K_{mp}b') \cdot \cos[K_{mp}(b-y)] & ; \text{ if } y > b' \\ \cos(K_{mp}y) \cdot \sin[K_{mp}(b-b')] & ; \text{ if } y < b' \end{cases}$$

(II.2.20)

$$E_z = -j \frac{2I_o}{ad \sin(kh)} \sqrt{\frac{\mu_o}{\varepsilon_o}} \sum_{m,p} \varepsilon_p \cdot \sin \frac{m\pi x}{a} \cdot \cos \frac{p\pi z}{d} \cdot$$

$$\cdot \frac{\left(\frac{p\pi}{d}\right)^2 + k^2}{\left(\frac{p\pi}{d}\right)^2 - k^2} \cdot \sin \frac{m\pi a'}{a} \cdot \cos \frac{p\pi d'}{d} \cdot \left[\cos \frac{p\pi h}{d} - \cos(kh)\right] \cdot$$

$$\cdot \frac{1}{K_{mp} \sin(K_{mp} b)} \cdot \begin{cases} \sin(K_{mp} b') \cdot \sin[K_{mp}(b-y)] \; ; \text{ if } y > b' \\ \sin(K_{mp} y) \cdot \sin[K_{mp}(b-b')] \; ; \text{ if } y < b' \end{cases}$$

(II.2.21)

$$H_x = -\frac{2kI_o}{ad \sin(kh)} \sum_{m,p} \varepsilon_p \cdot \sin \frac{m\pi x}{a} \cdot \cos \frac{p\pi z}{d} \cdot$$

$$\cdot \frac{1}{\left(\frac{p\pi}{d}\right)^2 - k^2} \cdot \sin \frac{m\pi a'}{a} \cdot \cos \frac{p\pi d'}{d} \cdot \left[\cos \frac{p\pi h}{d} - \cos(kh)\right] \cdot$$

$$\cdot \frac{1}{\sin(K_{mp} b)} \cdot \begin{cases} -\sin(K_{mp} b') \cdot \cos[K_{mp}(b-y)] \; ; \text{ if } y > b' \\ \cos(K_{mp} y) \cdot \sin[K_{mp}(b-b')] \; ; \text{ if } y < b' \end{cases}$$

(II.2.22)

$$H_y = \frac{2kI_o}{ad \sin(kh)} \sum_{m,p} \varepsilon_p \cdot \cos \frac{m\pi x}{a} \cdot \cos \frac{p\pi z}{d} \cdot$$

$$\cdot \frac{\frac{m\pi}{a}}{\left(\frac{p\pi}{d}\right)^2 - k^2} \cdot \sin \frac{m\pi a'}{a} \cdot \cos \frac{p\pi d'}{d} \left[\cos \frac{p\pi h}{d} - \cos(kh)\right] \cdot$$

$$\frac{1}{K_{mp} \sin(K_{mp} b)} \cdot \begin{cases} \sin(K_{mp} b') \cdot \sin[K_{mp}(b-y)] \; ; \text{ if } y > b' \\ \sin(K_{mp} y) \cdot \sin[K_{mp}(b-b')] \; ; \text{ if } y < b' \end{cases}$$

(II.2.23)

$$H_z = 0 \qquad \text{(II.2.24)}$$

In these expressions, I_o is the current at the input terminals of the antenna.

II.2.3 Excitation by an Electrically Small Loop Antenna.

In order to simplify our already cumbersome expressions, and without loss of generality, we shall evaluate the fields produced by a square loop of sides 2D.

Since we have previously solved the case of a current element, and we are assuming that the loop carries a constant current I_o, the answer is obtained by a straightforward application of the principle of superposition.

From Fig. 2 and Eqs. (II.2.11) through (II.2.17), it is easy to obtain expressions for the fields of a square loop. With the help of trigonometric identities and after rearranging terms, we arrive at the following equations.

$$E_x = j \frac{8kI_o}{ad}\sqrt{\frac{\mu_o}{\varepsilon_o}} \sum_{m,p} \varepsilon_m \cdot \cos\frac{m\pi x}{a} \cdot \sin\frac{p\pi z}{d} \cdot$$

$$\cdot \frac{a}{m\pi} \cdot \cos\frac{m\pi a'}{a} \cdot \cos\frac{p\pi d'}{d} \cdot \sin\frac{m\pi D}{a} \cdot$$

$$\cdot \sin\frac{p\pi D}{d} \cdot \frac{1}{K_{mp}\sin(K_{mp}b)} \cdot$$

$$\cdot \begin{cases} \sin(K_{mp}b') \cdot \sin[K_{mp}(b-y)] \ ; \ \text{if } y > b' \\ \sin(K_{mp}y) \cdot \sin[K_{mp}(b-b')] \ ; \ \text{if } y < b' \end{cases} \qquad \text{(II.2.25)}$$

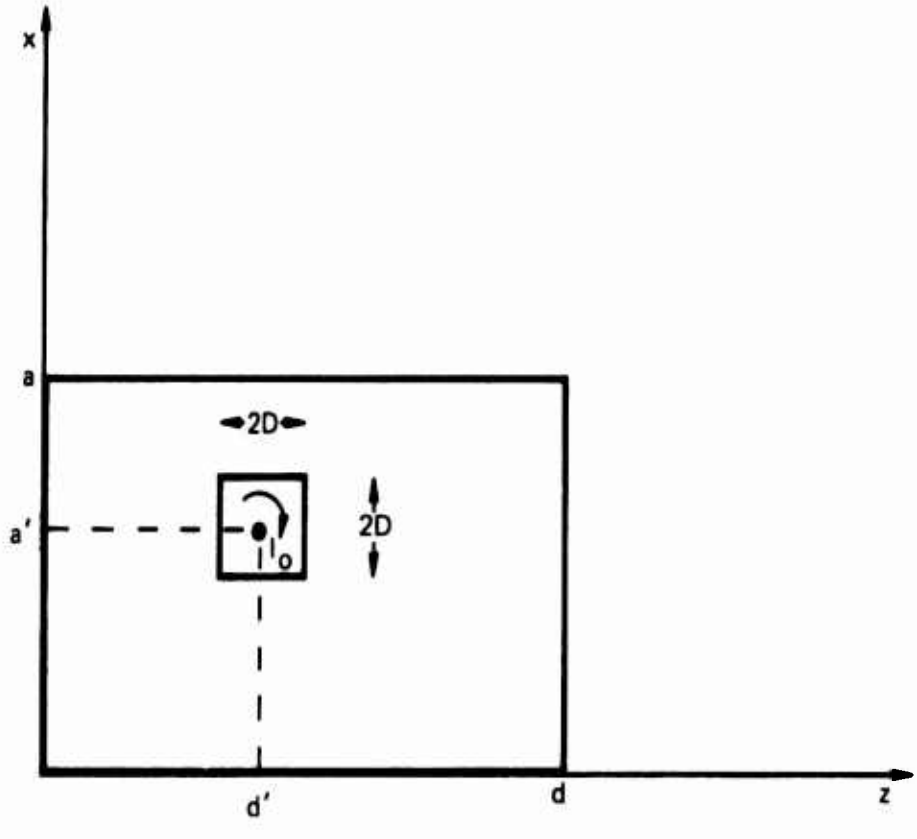

Figure 2
Square loop in a rectangular
cavity (as seen in the plane y=b')

$$E_y = 0 \tag{II.2.26}$$

$$E_z = j \frac{8kI_o}{ad} \sqrt{\frac{\mu_o}{\varepsilon_o}} \sum_{m,p} \varepsilon_p \cdot \sin \frac{m\pi x}{a} \cdot \cos \frac{p\pi z}{d} \cdot$$

$$\cdot \frac{d}{p\pi} \cdot \cos \frac{m\pi a'}{a} \cdot \cos \frac{p\pi d'}{d} \cdot \sin \frac{m\pi D}{a} \cdot$$

$$\cdot \sin \frac{p\pi D}{d} \cdot \frac{1}{K_{mp} \sin(K_{mp} b)} \cdot$$

$$\cdot \begin{cases} \sin(K_{mp} b') \cdot \sin[K_{mp}(b-y)] \; ; \text{ if } y > b' \\ \sin(K_{mp} y) \cdot \sin[K_{mp}(b-b')] \; ; \text{ if } y < b' \end{cases} \tag{II.2.27}$$

$$H_x = \frac{8I_o}{ad} \sum_{m,p} \varepsilon_p \cdot \sin \frac{m\pi x}{a} \cdot \cos \frac{p\pi z}{d} \cdot \frac{d}{p\pi} \cdot$$

$$\cdot \cos \frac{m\pi a'}{a} \cdot \cos \frac{p\pi d'}{d} \cdot \sin \frac{m\pi D}{a} \cdot \sin \frac{p\pi D}{d} \cdot$$

$$\cdot \frac{1}{\sin(K_{mp} b)} \cdot \begin{cases} -\sin(K_{mp} b') \cdot \cos[K_{mp}(b-y)] \; ; \text{ if } y > b' \\ \cos(K_{mp} y) \cdot \sin[K_{mp}(b-b')] \; ; \text{ if } y < b' \end{cases}$$

(II.2.28)

$$H_y = \frac{8I_o}{ad} \sum_{m,p}' \cos\frac{m\pi x}{a} \cdot \cos\frac{p\pi z}{d} \cdot \frac{\epsilon_m \left(\frac{m\pi}{a}\right)^2 - \epsilon_p \left(\frac{p\pi}{d}\right)^2}{\frac{m\pi}{a} \cdot \frac{p\pi}{d}} \cdot$$

$$\cdot \cos\frac{m\pi a'}{a} \cdot \cos\frac{p\pi d'}{d} \cdot \sin\frac{m\pi D}{a} \cdot \sin\frac{p\pi D}{d} \cdot$$

$$\cdot \frac{1}{K_{mp}\sin(K_{mp}b)} \cdot \begin{cases} \sin(K_{mp}b') \cdot \sin[K_{mp}(b-y)] \; ; \text{ if } y > b' \\ \sin(K_{mp}y) \cdot \sin[K_{mp}(b-b')] \; ; \text{ if } y < b' \end{cases}$$

(II.2.29)

$$H_z = -\frac{8I_o}{ad} \sum_{m,p}' \epsilon_m \cdot \cos\frac{m\pi x}{a} \cdot \sin\frac{p\pi z}{d} \cdot \frac{a}{m\pi} \cdot$$

$$\cdot \cos\frac{m\pi a'}{a} \cdot \cos\frac{p\pi d'}{d} \cdot \sin\frac{m\pi D}{a} \cdot \sin\frac{p\pi D}{d} \cdot$$

$$\cdot \frac{1}{\sin(K_{mp}b)} \cdot \begin{cases} -\sin(K_{mp}b') \cdot \cos[K_{mp}(b-y)] \; ; \text{ if } y > b' \\ \cos(K_{mp}y) \cdot \sin[K_{mp}(b-b')] \; ; \text{ if } y < b' \end{cases}$$

(II.2.30)

II.3 Electromagnetic Leakage through Small Apertures in Rectangular Cavities

II.3.1 The "Polarizability" of Apertures

Consider an aperture in a perfectly conducting plane, being illuminated by an electromagnetic field existing in one of the half-spaces defined by that plane.

If the size of the aperture and the wavelength of the field are

such that

$$\ell << \frac{\lambda}{2\pi} \tag{II.3.1}$$

where ℓ is any dimension of the aperture, H. A. Bethe[1] has shown that the field in the vicinity of the hole may be represented approximately by the original internal field $\vec{E}_0$, $\vec{H}_0$ at the location of the aperture (i.e., the fields existing at the site of the hole before it is cut in the wall), plus the fields of an electric and magnetic dipole located at the center of the aperture.

The field transmitted to the other side of the conducting wall may be considered a dipole field and can be calculated from the electric and magnetic dipole moments induced by the incident field on the complementary disk of infinite permeability[4].

An electric dipole moment can be induced only by an electric field which is normal to the plane of the disk (aperture), and a magnetic dipole moment can only be induced by a magnetic field which lies in the plane of the disk.

The resulting electric and magnetic moments are given by

$$\vec{P} = \alpha_e \varepsilon_0 \vec{E}_0 \tag{II.3.2}$$

$$\vec{M} = -\overleftrightarrow{\alpha}_m \vec{H}_0 \tag{II.3.3}$$

where

α_e = electric polarizability scalar

$\overleftrightarrow{\alpha}_m$ = magnetic polarizability tensor

Obviously, for a perfectly conducting plane $\vec{E}_0$ is normal to the surface and $\vec{H}_0$ is tangential.

The values of aperture polarizabilities for different shapes and sizes have been determined by C. G. Montgomery[5] and S. B. Cohn[6], [7]. Table I shows a selection of their results.

II.3.2 Application of Bethe's Method to Rectangular Cavities with Small Apertures

Bethe's treatment of the diffraction through holes, coupled with the field equations we have developed in Sec. 2 of this chapter, provide us with a powerful machinery to evaluate the electromagnetic fields leaked through an aperture in a rectangular cavity.

At frequencies below cutoff, typical cabinet apertures will automatically satisfy condition (III.3.1), making the method applicable.

In the first section of Chapter V we shall make use of these results to find expressions for the insertion loss of rectangular shielding boxes with apertures.

Table I

Polarizability of Apertures

Aperture Shape	α_e	α_{m_1} $\vec{H}$ parallel to long dimension	α_{m_2} $\vec{H}$ normal to long dimension
Circle of diameter d	$\frac{d^3}{6}$	$\frac{1}{3} d^3$	$\frac{1}{3} d^3$
Long narrow ellipse, semi-major axis = a semi-minor axis = b a >> b	$\frac{2}{3} \pi ab^2$	$\frac{2}{3} \pi \frac{a^3}{\ell n(\frac{4a}{b})-1}$	$\frac{2}{3} \pi ab^2$
Long slot of width w and length ℓ	$\frac{\pi}{8} \ell w^2$		$\frac{\pi}{8} \ell w^2$
Square of side ℓ	$0.2274\ \ell^3$	$0.518\ \ell^3$	$0.518\ \ell^3$
Rectangle of length ℓ and width w $\frac{w}{\ell} = 0.75$	$0.1462\ \ell^3$	$0.4192\ \ell^3$	
Rectangle of length ℓ and width w $\frac{w}{\ell} = 0.5$	$0.0740\ \ell^3$	$0.2750\ \ell^3$	
Rectangle of length ℓ and width w $\frac{w}{\ell} = 0.2$	$0.0140\ \ell^3$	$0.1812\ \ell^3$	
Rectangle of length ℓ and width w $\frac{w}{\ell} = 0.1$	$0.0038\ \ell^3$	$0.1290\ \ell^3$	

Chapter III

ELECTROMAGNETIC LEAKAGE FROM AN OPEN CAVITY

In the present chapter we shall investigate the electromagnetic fields leaking from an open rectangular cavity (i.e., a perfectly conducting cavity having one wall missing) when it is excited below cutoff by an internal source.

First, we must find a suitable description of the problem. This is done by considering the open cavity as a section of a rectangular waveguide, short-circuited at one end and open at the other end.

We shall begin by writing the Green function for a semi-infinite rectangular waveguide, and then using it to find expressions for the fields inside the waveguide, generated by simple antennas.

Up to this point, we have paralleled the work done in Chapter II with the closed cavity. But now we must cut open the semi-infinite waveguide and explore the consequences of this truncation. This will lead to an assumed field distribution at the "mouth" of the waveguide.

Then, with the help of the induction and field equivalence theorems, the radiated fields will be determined in an approximation suitable for our purposes.

III.1 Dyadic Green's Function for a Semi-Infinite Rectangular Waveguide

As was seen in Chapter II, when working in the Lorentz gauge (Eq. II.1.3), we need only the dyadic Green's function to determine the

field potentials, and from them, the electric and magnetic fields.

Consider a perfectly conducting, semi-infinite rectangular waveguide of dimensions a and b associated with the x and y directions, short-circuited at the plane z = 0 and extending towards z = +∞.

Its dyadic Green's function corresponding to the boundary conditions (II.1.10) can be easily obtained, by using image theory, from a knowledge of the dyadic Green's function for an infinite waveguide[8]. We have, then, for our semi-infinite waveguide

$$\overleftrightarrow{G}(\vec{r}|\vec{r}_o) = \frac{1}{ab} \sum_{m,n} \frac{\varepsilon_m \varepsilon_n}{k^2_{mn}} \cdot$$

$$\cdot \Big\{ [\vec{1}_z \times \vec{\nabla}\psi_{mn}(\vec{r}_o)]\,[\vec{1}_z \times \vec{\nabla}\psi_{mn}(\vec{r})] +$$

$$+ k^2_{mn}\, \vec{1}_z\, \chi_{mn}(\vec{r}_o)\, \vec{1}_z\, \chi_{mn}(\vec{r}) +$$

$$+ \vec{\nabla}\chi_{mn}(\vec{r}_o)\, \vec{\nabla}\chi_{mn}(\vec{r}) \Big\} \cdot$$

$$\cdot \frac{j}{2K_{mn}} \cdot \left[e^{j|z-z_o|K_{mn}} \pm e^{j(z+z_o)K_{mn}} \right] \qquad \text{(III.1.1)}$$

where the + sign is for longitudinal (z-directed) sources, and the - sign for transverse sources.

The symbols used are defined as follows:

$$K^2_{mn} = k^2 - \left[\left(\frac{m\pi}{a}\right)^2 + \left(\frac{n\pi}{b}\right)^2 \right] \qquad \text{(III.1.2)}$$

$$k^2_{mn} = \left(\frac{m\Pi}{a}\right)^2 + \left(\frac{n\Pi}{b}\right)^2 \qquad \text{(III.1.3)}$$

$$\psi_{mn} = \cos\frac{m\Pi x}{a} \cdot \cos\frac{n\Pi y}{b} \qquad \text{(III.1.4)}$$

$$\chi_{mn} = \sin\frac{m\Pi x}{a} \cdot \sin\frac{n\Pi y}{b} \qquad \text{(III.1.5)}$$

ε_m and ε_n are Neumann factors, defined in (II.1.21).

To remind ourselves that we are dealing with non-propagating modes, we shall find it convenient to define

$$\Gamma^2_{mn} = \left(\frac{m\Pi}{a}\right)^2 + \left(\frac{n\Pi}{b}\right)^2 - k^2 \qquad \text{(III.1.6)}$$

$$K_{mn} = j\Gamma_{mn} \qquad \text{(III.1.7)}$$

The dyadic Green's function (III.1.1) can now be written as

$$\overleftrightarrow{G}(\vec{r}|\vec{r}_o) = \frac{1}{ab}\sum_{m,n}\frac{\varepsilon_m\varepsilon_n}{k^2_{mn}} \cdot$$

$$\cdot\Big\{ [\vec{1}_z \times \vec{\nabla}\psi_{mn}(\vec{r}_o)][\vec{1}_z \times \vec{\nabla}\psi_{mn}(\vec{r})] \cdot$$

$$+ k^2_{mn}\,\vec{1}_z\,\chi_{mn}(\vec{r}_o)\,\vec{1}_z\,\chi_{mn}(\vec{r}) +$$

$$+ \vec{\nabla}\chi_{mn}(\vec{r}_o)\,\vec{\nabla}\chi_{mn}(\vec{r})\Big\} \cdot \frac{1}{\Gamma_{mn}} \cdot$$

$$\cdot\begin{cases} e^{-\Gamma_{mn}z}\begin{pmatrix}\sinh\\ \cosh\end{pmatrix}(\Gamma_{mn}z_o) \;;\; \text{if } z > z_o \\ e^{-\Gamma_{mn}z_o}\begin{pmatrix}\sinh\\ \cosh\end{pmatrix}(\Gamma_{mn}z) \;;\; \text{if } z < z_o \end{cases} \qquad \text{(III.1.8)}$$

where the sinh function is to be used for transverse sources, and the cosh for longitudinal sources.

III.2 Electromagnetic Fields in a Semi-Infinite Rectangular Waveguide

Just as we did in Chapter II for the rectangular cavity, we shall find the fields inside a semi-infinite rectangular waveguide excited by three different sources: a Hertzian dipole, an electrically short thin dipole, and an electrically small loop.

In the present case we must distinguish between transverse and longitudinal sources, which will add up to our already impressive collection of oversize equations. We must ask the reader to bear with this situation, since every one of these expressions will be needed in Chapters IV and V for the determination of the antenna impedance and the insertion loss equations.

III.2.1 Excitation by a Hertzian Dipole.

(A) Transverse Source

Consider a current element of length L, defined by (see Fig. 3)

$$\vec{J} = \vec{1}_x J_x = \begin{cases} \vec{1}_x I_0 \delta(y-b')\delta(z-d'); & a'-\frac{L}{2} < x < a' + \frac{L}{2} \\ 0 & ; \ |x - a'| > \frac{L}{2} \end{cases} \qquad \text{(III.2.1)}$$

Putting expressions (III.1.8) and (III.2.1) into Eq. (II.2.4) repeated below

$$\vec{A}(\vec{r}) = \int_{\text{Vol.}} \overleftrightarrow{G}(\vec{r}|\vec{r}_0) \cdot \mu_0 \vec{J}(\vec{r}_0)\, d\tau_0 \qquad \text{(III.2.2)}$$

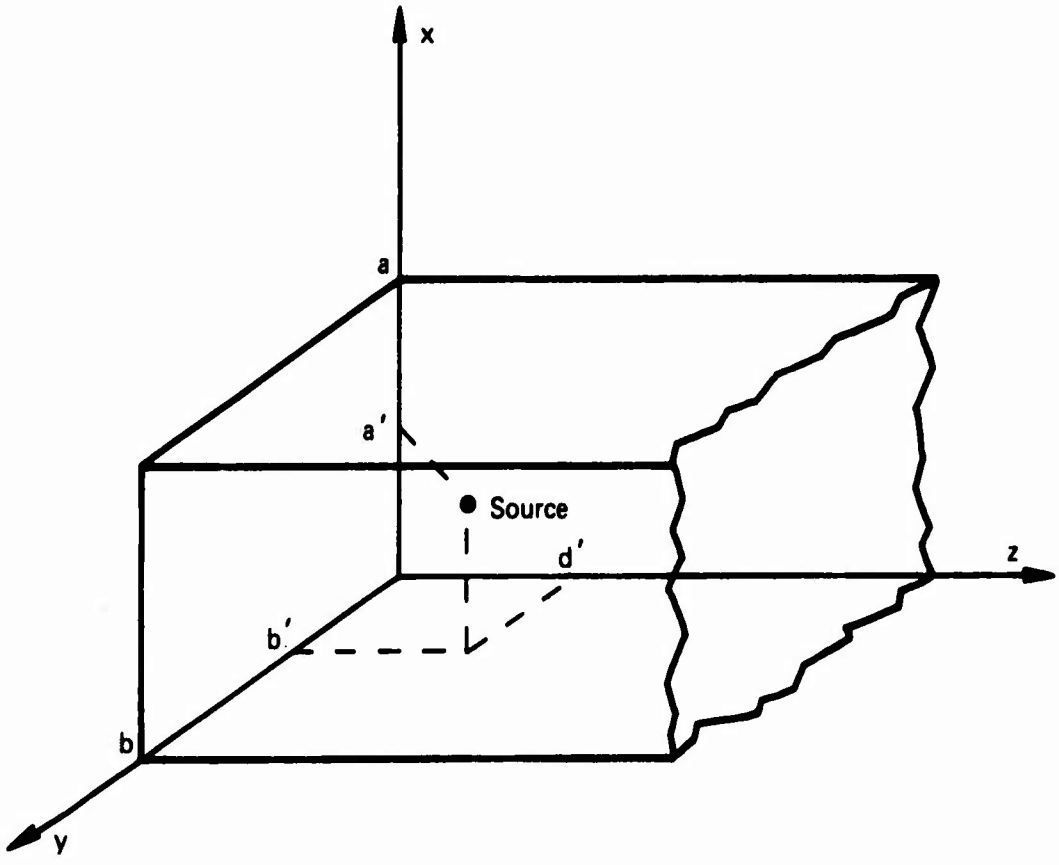

Figure 3
Source in a semi-infinite rectangular waveguide

results in

$$\vec{A} = \vec{1}_x \frac{\mu_o I_o}{ab} \sum_{m,n} \varepsilon_m \varepsilon_n \cos \frac{m\pi x}{a} \cdot \sin \frac{n\pi y}{b} \cdot$$

$$\cdot \frac{2a}{m\pi} \cdot \cos \frac{m\pi a'}{a} \quad \sin \frac{n\pi b'}{b} \quad \sin \frac{m\pi L}{2a}$$

$$\cdot \frac{1}{\Gamma_{mn}} \cdot \begin{cases} e^{-\Gamma_{mn} z} \sinh(\Gamma_{mn} d') \; ; \text{ if } z > d' \\ e^{-\Gamma_{mn} d'} \sinh(\Gamma_{mn} z) \; ; \text{ if } z < d' \end{cases} \qquad \text{(III.2.3)}$$

Thus, from

$$\vec{E} = - \frac{1}{j\omega\mu_o\varepsilon_o} \vec{\nabla}(\vec{\nabla} \cdot \vec{A}) + j\omega\vec{A} \qquad \text{(III.2.4)}$$

and

$$\vec{H} = \frac{1}{\mu_o} \vec{\nabla} \times \vec{A} \qquad \text{(III.2.5)}$$

we obtain

$$E_x = - j \frac{4I_o}{kab} \sqrt{\frac{\mu_o}{\varepsilon_o}} \sum_{m,n} \varepsilon_m \cos \frac{m\pi x}{a} \cdot \sin \frac{n\pi y}{b} \cdot$$

$$\frac{\left(\frac{m\pi}{a}\right)^2 - k^2}{\frac{m\pi}{a}} \cos \frac{m\pi a'}{a} \cdot \sin \frac{n\pi b'}{b} \cdot \sin \frac{m\pi L}{2a} \cdot$$

$$\cdot \frac{1}{\Gamma_{mn}} \cdot \begin{cases} e^{-\Gamma_{mn} z} \sinh(\Gamma_{mn} d') \; ; \text{ if } z > d' \\ e^{-\Gamma_{mn} d'} \sinh(\Gamma_{mn} z) \; ; \text{ if } z < d' \end{cases} \qquad \text{(III.2.6)}$$

$$E_y = -j \frac{8I_o}{kab} \cdot \sqrt{\frac{\mu_o}{\varepsilon_o}} \sum_{m,n} \sin \frac{m\pi x}{a} \cdot \cos \frac{n\pi y}{b} \cdot \frac{n\pi}{b} \cdot$$

$$\cdot \cos \frac{m\pi a'}{a} \cdot \sin \frac{n\pi b'}{b} \cdot \sin \frac{m\pi L}{2a} \cdot$$

$$\cdot \frac{1}{\Gamma_{mn}} \cdot \begin{cases} e^{-\Gamma_{mn} z} \sinh(\Gamma_{mn} d') \; ; \text{ if } z > d' \\ e^{-\Gamma_{mn} d'} \sinh(\Gamma_{mn} z) \; ; \text{ if } z < d' \end{cases} \qquad \text{(III.2.7)}$$

$$E_z = -j \frac{8I_o}{kab} \sqrt{\frac{\mu_o}{\varepsilon_o}} \sum_{m,n} \sin \frac{m\pi x}{a} \cdot \sin \frac{n\pi y}{b} \cdot$$

$$\cdot \cos \frac{m\pi a'}{a} \cdot \sin \frac{n\pi b'}{b} \cdot \sin \frac{m\pi L}{2a} \cdot$$

$$\cdot \begin{cases} -e^{-\Gamma_{mn} z} \sinh(\Gamma_{mn} d') \; ; \text{ if } z > d' \\ -e^{-\Gamma_{mn} d'} \cosh(\Gamma_{mn} z) \; ; \text{ if } z < d' \end{cases} \qquad \text{(III.2.8)}$$

$$H_x = 0 \qquad \text{(III.2.9)}$$

$$H_y = \frac{4I_o}{ab} \sum_{m,n} \varepsilon_m \cos\frac{m\pi x}{a} \cdot \sin\frac{n\pi y}{b} \cdot \frac{a}{m\pi} \cdot$$

$$\cdot \cos\frac{m\pi a'}{a} \cdot \sin\frac{n\pi b'}{b} \cdot \sin\frac{m\pi L}{2a} \cdot$$

$$\cdot \begin{cases} -e^{-\Gamma_{mn} z} \sinh(\Gamma_{mn} d') \; ; \text{ if } z > d' \\ e^{-\Gamma_{mn} d'} \cosh(\Gamma_{mn} z) \; ; \text{ if } z < d' \end{cases} \qquad \text{(III.2.10)}$$

$$H_z = -\frac{4I_o}{ab} \sum_{m,n} \varepsilon_m \cos\frac{m\pi x}{a} \cdot \cos\frac{n\pi y}{b} \cdot \frac{a}{m\pi} \cdot$$

$$\cdot \frac{n\pi}{b} \cdot \cos\frac{m\pi a'}{a} \cdot \sin\frac{n\pi b'}{b} \cdot \sin\frac{m\pi L}{2a} \cdot$$

$$\cdot \frac{1}{\Gamma_{mn}} \cdot \begin{cases} e^{-\Gamma_{mn} z} \sinh(\Gamma_{mn} d') \; ; \text{ if } z > d' \\ e^{-\Gamma_{mn} d'} \sinh(\Gamma_{mn} z) \; ; \text{ if } z < d' \end{cases} \qquad \text{(III.2.11)}$$

For a y-directed source, we can use the same expressions interchanging x, a, a' and m with y, b, b' and n, respectively.

(B) Longitudinal Source

If our source is assumed to be a z-directed current element

$$\vec{J} = \vec{1}_z J_z = \begin{cases} \vec{1}_z I_o \, \delta(x-a') \, \delta(y-b') \; ; \; d' - \frac{L}{2} < z < d' + \frac{L}{2} \\ 0 \qquad\qquad\qquad\qquad ; \; |z-d'| > \frac{L}{2} \end{cases} \qquad \text{(III.2.12)}$$

the electric and magnetic fields are found to be

$$E_x = j \frac{8I_o}{kab}\sqrt{\frac{\mu_o}{\varepsilon_o}} \sum_{m,n} \cos\frac{m\pi x}{a} \cdot \sin\frac{n\pi y}{b} \cdot \frac{m\pi}{a} \cdot$$

$$\cdot \sin\frac{m\pi a'}{a} \cdot \sin\frac{n\pi b'}{b} \cdot \frac{1}{\Gamma_{mn}} \cdot \sinh\left(\Gamma_{mn}\frac{L}{2}\right) \cdot$$

$$\cdot \begin{cases} -e^{-\Gamma_{mn}z}\cosh(\Gamma_{mn}d') \; ; \text{ if } z > d' \\ e^{-\Gamma_{mn}d'}\sinh(\Gamma_{mn}z) \; ; \text{ if } z < d' \end{cases} \qquad \text{(III.2.13)}$$

$$E_y = j \frac{8I_o}{kab}\sqrt{\frac{\mu_o}{\varepsilon_o}} \sum_{m,n} \sin\frac{m\pi x}{a} \cdot \cos\frac{n\pi y}{b} \cdot \frac{n\pi}{b} \cdot$$

$$\cdot \sin\frac{m\pi a'}{a} \cdot \sin\frac{n\pi b'}{b} \cdot \frac{1}{\Gamma_{mn}} \cdot \sinh\left(\Gamma_{mn}\frac{L}{2}\right) \cdot$$

$$\cdot \begin{cases} -e^{-\Gamma_{mn}z}\cosh(\Gamma_{mn}d') \; ; \text{ if } z > d' \\ e^{-\Gamma_{mn}d'}\sinh(\Gamma_{mn}z) \; ; \text{ if } z < d' \end{cases} \qquad \text{(III.2.14)}$$

$$E_z = j \frac{8I_o}{kab}\sqrt{\frac{\mu_o}{\varepsilon_o}} \sum_{m,n} \sin\frac{m\pi x}{a} \cdot \sin\frac{n\pi y}{b} \cdot \sin\frac{m\pi a'}{a} \cdot$$

$$\cdot \sin\frac{n\pi b'}{b} \cdot \sinh\left(\Gamma_{mn}\frac{L}{2}\right) \cdot \frac{\left(\frac{m\pi}{a}\right)^2 + \left(\frac{n\pi}{b}\right)^2}{\Gamma_{mn}^2} \cdot$$

$$\cdot \begin{cases} e^{-\Gamma_{mn}z}\cosh(\Gamma_{mn}d') \; ; \text{ if } z > d' \\ e^{-\Gamma_{mn}d'}\cosh(\Gamma_{mn}z) \; ; \text{ if } z < d' \end{cases} \qquad \text{(III.2.15)}$$

$$H_x = \frac{8I_o}{ab} \sum_{m,n} \cdot \sin \frac{m\pi x}{a} \cdot \cos \frac{n\pi y}{b} \cdot \frac{n\pi}{b} \cdot$$

$$\cdot \sin \frac{m\pi a'}{a} \cdot \sin \frac{n\pi b'}{b} \cdot \frac{1}{\Gamma_{mn}^2} \cdot \sinh(\Gamma_{mn} \frac{L}{2}) \cdot$$

$$\cdot \begin{cases} e^{-\Gamma_{mn} z} \cosh(\Gamma_{mn} d') \; ; \text{ if } z > d' \\ e^{-\Gamma_{mn} d'} \cosh(\Gamma_{mn} z) \; ; \text{ if } z < d' \end{cases} \qquad \text{(III.2.16)}$$

$$H_y = - \frac{8I_o}{ab} \sum_{m,n} \cos \frac{m\pi x}{a} \cdot \sin \frac{n\pi y}{b} \cdot \frac{m\pi}{a} \cdot$$

$$\cdot \sin \frac{m\pi a'}{a} \cdot \sin \frac{n\pi b'}{b} \cdot \frac{1}{\Gamma_{mn}^2} \cdot \sinh(\Gamma_{mn} \frac{L}{2}) \cdot$$

$$\cdot \begin{cases} e^{-\Gamma_{mn} z} \cosh(\Gamma_{mn} d') \; ; \text{ if } z > d' \\ e^{-\Gamma_{mn} d'} \cosh(\Gamma_{mn} z) \; ; \text{ if } z < d' \end{cases} \qquad \text{(III.2.17)}$$

$$H_z = 0 \qquad \text{(III.2.18)}$$

III.2.2 Excitation by an Electrically Short Dipole Antenna

(A) Transverse Source

Assume a dipole antenna current defined by

$$\vec{J} = \hat{i}_x J_x = \begin{cases} \hat{i}_x I_o \dfrac{\sin[k(h-|x-a'|)]}{\sin(kh)} \delta(y-b')\delta(z-d') & ; \ |x-a'|<h \\ 0 & ; \ |x-a'|>h \end{cases} \qquad \text{(III.2.19)}$$

The fields generated by this current in the semi-infinite waveguide are found to be

$$E_x = -j \frac{2I_o}{ab \sin(kh)} \cdot \sqrt{\frac{\mu_o}{\varepsilon_o}} \cdot \sum_{m,n} \varepsilon_m \cos\frac{m\pi x}{a} \cdot \sin\frac{n\pi y}{b} \cdot$$

$$\cdot \frac{\left(\frac{m\pi}{a}\right)^2 + k^2}{\left(\frac{m\pi}{a}\right)^2 - k^2} \cdot \cos\frac{m\pi a}{a} \cdot \sin\frac{n\pi b'}{b} \cdot \left[\cos\frac{m\pi h}{a} - \cos(kh)\right] \cdot$$

$$\cdot \frac{1}{\Gamma_{mn}} \cdot \begin{cases} e^{-\Gamma_{mn} z} \sinh(\Gamma_{mn} d') & ; \text{ if } z > d' \\ e^{-\Gamma_{mn} d'} \sinh(\Gamma_{mn} z) & ; \text{ if } z < d' \end{cases} \qquad \text{(III.2.20)}$$

$$E_y = -j \frac{4I_o}{ab \sin(kh)} \sqrt{\frac{\mu_o}{\varepsilon_o}} \sum_{m,n} \sin\frac{m\pi x}{a} \cdot \cos\frac{n\pi y}{b} \cdot$$

$$\cdot \frac{\frac{m\pi}{a} \cdot \frac{n\pi}{b}}{\left(\frac{m\pi}{a}\right)^2 - k^2} \cdot \cos\frac{m\pi a'}{a} \sin\frac{n\pi b'}{b} \cdot \left[\cos\frac{m\pi h}{a} - \cos(kh)\right] \cdot$$

$$\cdot \frac{1}{\Gamma_{mn}} \begin{cases} e^{-\Gamma_{mn} z} \sinh(\Gamma_{mn} d') & ; \text{ if } z > d' \\ e^{-\Gamma_{mn} d'} \sinh(\Gamma_{mn} z) & ; \text{ if } z < d' \end{cases} \qquad \text{(III.2.21)}$$

$$E_z = -j \frac{4I_o}{ab \sin(kh)} \sqrt{\frac{\mu_o}{\varepsilon_o}} \sum_{m,n} \sin \frac{m\pi x}{a} \cdot \sin \frac{n\pi y}{b} \cdot$$

$$\cdot \frac{\frac{m\pi}{a}}{\left(\frac{m\pi}{a}\right)^2 - k^2} \cdot \cos \frac{m\pi a'}{a} \cdot \sin \frac{n\pi b'}{b} \cdot \left[\cos \frac{m\pi h}{a} - \cos(kh)\right] \cdot$$

$$\cdot \begin{cases} -e^{-\Gamma_{mn} z} \sinh(\Gamma_{mn} d') \; ; \text{ if } z > d' \\ e^{-\Gamma_{mn} d'} \cosh(\Gamma_{mn} z) \; ; \text{ if } z < d' \end{cases} \qquad \text{(III.2.22)}$$

$$H_x = 0 \qquad \text{(III.2.23)}$$

$$H_y = -\frac{2k\, I_o}{ab \sin(kh)} \sum_{m,n} \varepsilon_m \cos \frac{m\pi x}{a} \cdot \sin \frac{n\pi y}{b} \cdot$$

$$\cdot \frac{1}{\left(\frac{m\pi}{a}\right)^2 - k^2} \cdot \cos \frac{m\pi a'}{a} \cdot \sin \frac{n\pi b'}{b} \cdot \left[\cos \frac{m\pi h}{a} - \cos(kh)\right] \cdot$$

$$\cdot \begin{cases} -e^{-\Gamma_{mn} z} \sinh(\Gamma_{mn} d') \; ; \text{ if } z > d' \\ e^{-\Gamma_{mn} d'} \cosh(\Gamma_{mn} z) \; ; \text{ if } z < d' \end{cases} \qquad \text{(III.2.24)}$$

$$H_z = \frac{2k\, I_o}{ab \sin(kh)} \sum_{m,n} \epsilon_m \cdot \cos\frac{m\pi x}{a} \cdot \cos\frac{n\pi y}{b} \cdot$$

$$\cdot \frac{\frac{n\pi}{b}}{\left(\frac{m\pi}{a}\right)^2 - k^2} \cdot \cos\frac{m\pi a'}{a} \cdot \sin\frac{n\pi b'}{b} \cdot \left[\cos\frac{m\pi h}{a} - \cos(kh)\right] \cdot$$

$$\cdot \frac{1}{\Gamma_{mn}} \cdot \begin{cases} e^{-\Gamma_{mn} z} \sinh(\Gamma_{mn} d') \ ; \text{ if } z > d' \\ e^{-\Gamma_{mn} d'} \sinh(\Gamma_{mn} z) \ ; \text{ if } z < d' \end{cases} \qquad \text{(III.2.25)}$$

For a y-directed source, we should use these equations interchanging x, a, a' and m with y, b, b' and n, respectively.

(B) Longitudinal Source

In this case, we define the antenna current by

$$\vec{J} = \hat{1}_z J_z = \begin{cases} \hat{1}_z I_o \dfrac{\sin[k(h-|z-d'|)]}{\sin(kh)} \delta(x-a')\delta(y-b') \ ; & |z-d'|<h \\ 0 \ ; & |z-d'|>h \end{cases}$$

$$\text{(III.2.26)}$$

and the resultant electric and magnetic fields are

$$E_x = j \frac{8I_o}{ab \sin(kh)} \sqrt{\frac{\mu_o}{\varepsilon_o}} \sum_{m,n} \cos \frac{m\pi x}{a} \cdot \sin \frac{n\pi y}{b} \cdot$$

$$\cdot \frac{\frac{m\pi}{a}}{\left(\frac{m\pi}{a}\right)^2 + \left(\frac{n\pi}{b}\right)^2} \cdot \sin \frac{m\pi a'}{a} \cdot \sin \frac{n\pi b'}{b} \cdot$$

$$\cdot \left[\cosh(\Gamma_{mn} h) - \cos(kh)\right] \cdot \begin{cases} e^{-\Gamma_{mn} z} \cosh(\Gamma_{mn} d') \; ; \text{ if } z > d' \\ e^{-\Gamma_{mn} d'} \sinh(\Gamma_{mn} z) \; ; \text{ if } z < d' \end{cases}$$

(III.2.27)

$$E_y = j \frac{8I_o}{ab \sin(kh)} \sqrt{\frac{\mu_o}{\varepsilon_o}} \sum_{m,n} \sin \frac{m\pi x}{a} \cdot \cos \frac{n\pi y}{b} \cdot$$

$$\cdot \frac{\frac{n\pi}{b}}{\left(\frac{m\pi}{a}\right)^2 + \left(\frac{n\pi}{b}\right)^2} \cdot \sin \frac{m\pi a'}{a} \cdot \sin \frac{n\pi b'}{b} \cdot$$

$$\cdot \left[\cosh(\Gamma_{mn} h) - \cos(kh)\right] \cdot \begin{cases} e^{-\Gamma_{mn} z} \cosh(\Gamma_{mn} d') \; ; \text{ if } z > d' \\ e^{-\Gamma_{mn} d'} \sinh(\Gamma_{mn} z) \; ; \text{ if } z < d' \end{cases}$$

(III.2.28)

$$E_z = -j \frac{8I_o}{ab \sin(kh)} \sqrt{\frac{\mu_o}{\varepsilon_o}} \sum_{m,n} \sin \frac{m\pi x}{a} \cdot \sin \frac{n\pi y}{b} \cdot$$

$$\cdot \frac{1}{\Gamma_{mn}} \cdot \frac{\Gamma_{mn}^2 - k^2}{\left(\frac{m\pi}{a}\right)^2 + \left(\frac{n\pi}{b}\right)^2} \cdot \sin \frac{m\pi a'}{a} \cdot \sin \frac{n\pi b'}{b}$$

$$\cdot \left[\cosh(\Gamma_{mn} h) - \cos(kh)\right] \cdot \begin{cases} e^{-\Gamma_{mn} z} \cosh(\Gamma_{mn} d') \; ; \text{ if } z > d' \\ e^{-\Gamma_{mn} d'} \cosh(\Gamma_{mn} z) \; ; \text{ if } z < d' \end{cases}$$

(III.2.29)

$$H_x = \frac{8k\, I_o}{ab \sin(kh)} \sum_{m,n} \sin \frac{m\pi x}{a} \cdot \cos \frac{n\pi y}{b} \cdot \frac{1}{\Gamma_{mn}} \cdot$$

$$\cdot \frac{\frac{n\pi}{b}}{\left(\frac{m\pi}{a}\right)^2 + \left(\frac{n\pi}{b}\right)^2} \cdot \sin \frac{m\pi a'}{a} \cdot \sin \frac{n\pi b'}{b} \cdot$$

$$\cdot \left[\cosh(\Gamma_{mn} h) - \cos(kh)\right] \cdot \begin{cases} e^{-\Gamma_{mn} z} \cosh(\Gamma_{mn} d') \; ; \text{ if } z > d' \\ e^{-\Gamma_{mn} d'} \cosh(\Gamma_{mn} z) \; ; \text{ if } z < d' \end{cases}$$

(III.2.30)

$$H_y = -\frac{8k\,I_o}{ab\,\sin(kh)} \sum_{m,n} \cos\frac{m\pi x}{a} \cdot \sin\frac{n\pi y}{b} \cdot \frac{1}{\Gamma_{mn}} \cdot$$

$$\cdot \frac{\frac{m\pi}{a}}{\left(\frac{m\pi}{a}\right)^2 + \left(\frac{n\pi}{b}\right)^2} \cdot \sin\frac{m\pi a'}{a} \cdot \sin\frac{n\pi b'}{b} \cdot$$

$$\cdot \left[\cosh(\Gamma_{mn}h) - \cos(kh)\right] \cdot \begin{cases} e^{-\Gamma_{mn}z}\cosh(\Gamma_{mn}d') \; ; \text{ if } z > d' \\ e^{-\Gamma_{mn}d'}\cosh(\Gamma_{mn}z) \; ; \text{ if } z < d' \end{cases}$$

(III.2.31)

$$H_z = 0 \qquad \text{(III.2.32)}$$

III.2.3 Excitation by an Electrically Small Loop Antenna.

Paralleling the work done in Chapter II, we shall take up the case of a square loop of sides 2D and current I_o. Figures 4 and 5 show the loop configuration for the transverse and longitudinal cases, respectively.

(A) Transverse Loop (Fig. 4)

Using the expressions for the fields generated by a current element, worked out in part (III.2.1) of this section, and applying the superposition principle, we obtain

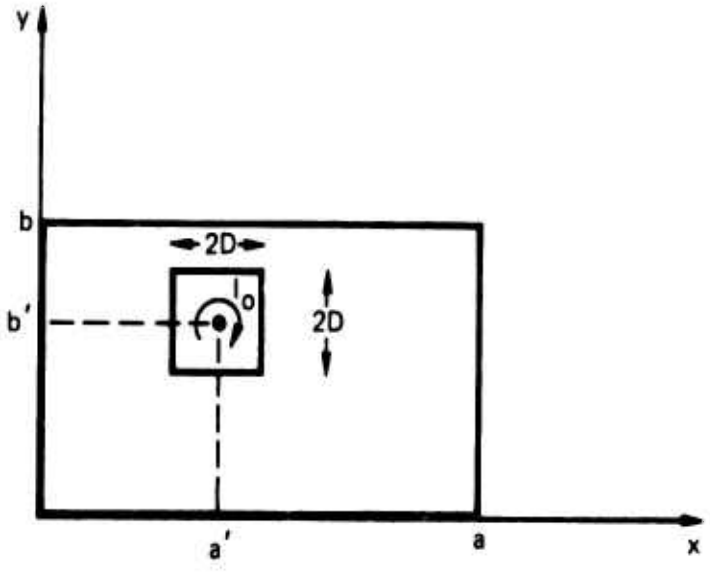

Figure 4
Transverse square loop in semi-infinite
rectangular waveguide (as seen in the plane z=d′)

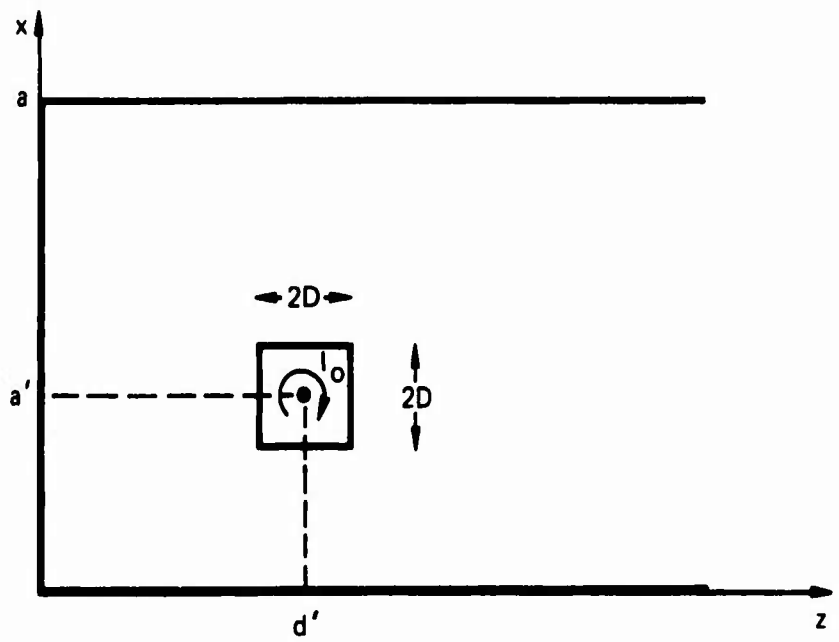

Figure 5
Longitudinal square loop in semi-infinite
rectangular waveguide (as seen in the plane y=b')

$$E_x = j \frac{8k\ I_o}{ab} \sqrt{\frac{\mu_o}{\varepsilon_o}} \sum_{m,n} \varepsilon_m \cos \frac{m\pi x}{a} \cdot \sin \frac{n\pi y}{b} \cdot$$

$$\cdot \frac{a}{m\pi} \cdot \cos \frac{m\pi a'}{a} \cdot \cos \frac{n\pi b'}{b} \cdot \sin \frac{m\pi D}{a} \cdot \sin \frac{n\pi D}{b} \cdot$$

$$\cdot \frac{1}{\Gamma_{mn}} \cdot \begin{cases} e^{-\Gamma_{mn} z} \sinh(\Gamma_{mn} d') \ ; \text{ if } z > d' \\ e^{-\Gamma_{mn} d'} \sinh(\Gamma_{mn} z) \ ; \text{ if } z < d' \end{cases}$$

(III.2.33)

$$E_y = - j \frac{8k\ I_o}{ab} \sqrt{\frac{\mu_o}{\varepsilon_o}} \sum_{m,n} \varepsilon_m \sin \frac{m\pi x}{a} \cdot \cos \frac{n\pi y}{b} \cdot$$

$$\cdot \frac{b}{n\pi} \cdot \cos \frac{m\pi a'}{a} \cdot \cos \frac{n\pi b'}{b} \cdot \sin \frac{m\pi D}{a} \cdot \sin \frac{n\pi D}{b} \cdot$$

$$\cdot \frac{1}{\Gamma_{mn}} \cdot \begin{cases} e^{-\Gamma_{mn} z} \sinh(\Gamma_{mn} d') \ ; \text{ if } z > d' \\ e^{-\Gamma_{mn} d'} \sinh(\Gamma_{mn} z) \ ; \text{ if } z < d' \end{cases}$$

(III.2.34)

$$E_z = 0 \qquad \text{(III.2.35)}$$

$$H_x = -\frac{8I_o}{ab}\sum_{m,n}\varepsilon_n \sin\frac{m\pi x}{a}\cdot\cos\frac{n\pi y}{b}\cdot\frac{b}{n\pi}\cdot$$

$$\cdot\cos\frac{m\pi a'}{a}\cdot\cos\frac{n\pi b'}{b}\cdot\sin\frac{m\pi D}{a}\cdot\sin\frac{n\pi D}{b}\cdot$$

$$\cdot\begin{cases} -e^{-\Gamma_{mn}z}\sinh(\Gamma_{mn}d') \;;\; \text{if } z > d' \\ e^{-\Gamma_{mn}d'}\cosh(\Gamma_{mn}z) \;;\; \text{if } z < d' \end{cases} \qquad \text{(III.2.36)}$$

$$H_y = \frac{8I_o}{ab}\sum_{m,n}\varepsilon_m \cos\frac{m\pi x}{a}\cdot\sin\frac{n\pi y}{b}\cdot\frac{a}{m\pi}\cdot$$

$$\cdot\cos\frac{m\pi a'}{a}\cdot\cos\frac{n\pi b'}{b}\cdot\sin\frac{m\pi D}{a}\cdot\sin\frac{n\pi D}{b}\cdot$$

$$\cdot\begin{cases} -e^{-\Gamma_{mn}z}\sinh(\Gamma_{mn}d') \;;\; \text{if } z > d' \\ e^{-\Gamma_{mn}d'}\cosh(\Gamma_{mn}z) \;;\; \text{if } z < d' \end{cases} \qquad \text{(III.2.37)}$$

$$H_z = -\frac{8I_o}{ab}\sum_{m,n}\cos\frac{m\pi x}{a}\cdot\cos\frac{n\pi y}{b}\cdot\left(\varepsilon_m\frac{\frac{n\pi}{b}}{\frac{m\pi}{a}}-\varepsilon_n\frac{\frac{m\pi}{a}}{\frac{n\pi}{b}}\right)\cdot$$

$$\cdot\cos\frac{m\pi a'}{a}\cdot\cos\frac{n\pi b'}{b}\cdot\sin\frac{m\pi D}{a}\cdot\sin\frac{n\pi D}{b}\cdot$$

$$\cdot\frac{1}{\Gamma_{mn}}\cdot\begin{cases}e^{-\Gamma_{mn}z}\sinh(\Gamma_{mn}d') & ;\ \text{if } z>d'\\ e^{-\Gamma_{mn}d'}\sinh(\Gamma_{mn}z) & ;\ \text{if } z<d'\end{cases}\qquad\text{(III.2.38)}$$

(B) Longitudinal Loop (Fig. 5)

In this case, the generated fields are found to be

$$E_x = j\frac{8kI_o}{ab}\sqrt{\frac{\mu_o}{\varepsilon_o}}\sum_{m,n}\varepsilon_m\cos\frac{m\pi x}{a}\cdot\sin\frac{n\pi y}{b}\cdot\frac{a}{m\pi}\cdot$$

$$\cdot\cos\frac{m\pi a'}{a}\cdot\sin\frac{n\pi b'}{b}\cdot\sin\frac{m\pi D}{a}\cdot\frac{1}{\Gamma_{mn}}\cdot$$

$$\cdot\sinh(\Gamma_{mn}D)\cdot\begin{cases}-e^{-\Gamma_{mn}z}\cosh(\Gamma_{mn}d') & ;\ \text{if } z>d'\\ e^{-\Gamma_{mn}d'}\sinh(\Gamma_{mn}z) & ;\ \text{if } z<d'\end{cases}$$

(III.2.39)

$$E_y = 0\qquad\text{(III.2.40)}$$

$$E_z = j \frac{16kI_o}{ab} \sqrt{\frac{\mu_o}{\epsilon_o}} \sum_{m,n} \sin \frac{m\pi x}{a} \cdot \sin \frac{n\pi y}{b} \cdot$$

$$\cdot \cos \frac{m\pi a'}{a} \cdot \sin \frac{n\pi b'}{b} \cdot \sin \frac{m\pi D}{a} \cdot \frac{1}{\Gamma_{mn}^2} \cdot$$

$$\cdot \sinh(\Gamma_{mn} D) \cdot \begin{cases} e^{-\Gamma_{mn} z} \cosh(\Gamma_{mn} d') \; ; \text{ if } z > d' \\ e^{-\Gamma_{mn} d'} \cosh(\Gamma_{mn} z) \; ; \text{ if } z < d' \end{cases}$$

(III.2.41)

$$H_x = \frac{16I_o}{ab} \sum_{m,n} \sin \frac{m\pi x}{a} \cdot \cos \frac{n\pi y}{b} \cdot \frac{n\pi}{b} \cdot$$

$$\cdot \cos \frac{m\pi a'}{a} \cdot \sin \frac{n\pi b'}{b} \cdot \sin \frac{m\pi D}{a} \cdot \frac{1}{\Gamma_{mn}^2} \cdot$$

$$\cdot \sinh(\Gamma_{mn} D) \cdot \begin{cases} e^{-\Gamma_{mn} z} \cosh(\Gamma_{mn} d') \; ; \text{ if } z > d' \\ e^{-\Gamma_{mn} d'} \cosh(\Gamma_{mn} z) \; ; \text{ if } z < d' \end{cases}$$

(III.2.42)

$$H_y = \frac{8I_o}{ab} \sum_{m,n} \varepsilon_m \cos\frac{m\pi x}{a} \cdot \sin\frac{n\pi y}{b} \cdot \frac{\left(\frac{n\pi}{b}\right)^2 - k^2}{\frac{m\pi}{a}} \cdot$$

$$\cdot \cos\frac{m\pi a'}{a} \cdot \sin\frac{n\pi b'}{b} \cdot \sin\frac{m\pi D}{a} \cdot \frac{1}{\Gamma_{mn}^2} \cdot$$

$$\cdot \sinh(\Gamma_{mn} D) \cdot \begin{cases} e^{-\Gamma_{mn} z} \cosh(\Gamma_{mn} d') \; ; \text{ if } z > d' \\ e^{-\Gamma_{mn} d'} \cosh(\Gamma_{mn} z) \; ; \text{ if } z < d' \end{cases}$$

(III.2.43)

$$H_z = -\frac{8I_o}{ab} \sum_{m,n} \varepsilon_m \cos\frac{m\pi x}{a} \cdot \cos\frac{n\pi y}{b} \cdot \frac{a}{m\pi} \cdot$$

$$\cdot \frac{n\pi}{b} \cdot \cos\frac{m\pi a'}{a} \cdot \sin\frac{n\pi b'}{b} \cdot \sin\frac{m\pi D}{a} \cdot \frac{1}{\Gamma_{mn}} \cdot$$

$$\cdot \sinh(\Gamma_{mn} D) \cdot \begin{cases} -e^{-\Gamma_{mn} z} \cosh(\Gamma_{mn} d') \; ; \text{ if } z > d' \\ e^{-\Gamma_{mn} d'} \sinh(\Gamma_{mn} z) \; ; \text{ if } z < d' \end{cases}$$

(III.2.44)

For a loop in the (yz) plane, we use the same expressions interchanging x, a, a' and m, with y, b, b' and n, respectively.

III.3 Radiation from an Open-Ended Waveguide Excited Below Cutoff

We must now use the tools developed in the first two sections of this chapter, to set up expressions for the radiated fields from an open waveguide excited below cutoff.

First, we shall find a suitable approximation for the fields at the plane of the aperture (i.e., at the "mouth" of the waveguide). After a review of the induction and field-equivalence theorems, we shall make physically reasonable assumptions that will allow us to find the radiated fields under some restrictions.

This section is the least accurate portion of this thesis, but the reader will find ample justifications for the approach taken, not only through reasonable heuristic arguments, but also through experimental confirmation. To put it in another way: since this particular problem cannot be solved exactly, we shall take what we feel is the best possible course under the given circumstances, and rely on the correlation between theory and experiment to pronounce the final verdict.

III.3.1 Electromagnetic Fields at the Open End of a Rectangular Waveguide Excited Below Cutoff.

In Section III.2 of this chapter, we have found expressions for the electromagnetic fields generated inside a semi-infinite waveguide by some simple antennas. The question now arising is: what happens to these fields when the waveguide is cut open at the

plane z = d? Specifically: what are the new field values at the plane z = d?

We should always keep in mind that we are dealing exclusively with non-propagating modes that decay exponentially as we move away from the source. The usual treatment of waveguide radiators, from the pioneering works of Barrow and Greene[9] and Chu[10] to the textbook treatments of Jones[11] and Collin and Zucker[12], assume that the source is sufficiently distant from the aperture, so that any non-propagating modes have decayed to negligible amplitudes and we are left only with the desired propagating mode.

This clearly shows the dichotomy existing in the treatment of radiators, when looked at from the antenna viewpoint or from the point of view of shielding theory. The presence of evanescent waves is ignored in the former and is essential in the latter.

From the above considerations, it is clear that the antenna-aperture distance is the most critical parameter in our case, and since we shall apply our results to typical rectangular cabinets and enclosures, that distance will normally be a fraction of a typical cabinet dimension.

A look at the equations in Section III.2 of this chapter shows that the field generated by a longitudinal dipole consists of TM modes only. As a reasonable approximation, we can assume that the aperture produces a complete reflection of the transverse (x and y in Fig. 3) components of the fields, resulting in the doubling of the transverse magnetic field and the cancellation of the transverse electric field.

Similarly, in the case of a transverse loop, only TE modes are present. This leads to the assumption that the transverse electric field is doubled and the transverse magnetic field cancelled by reflection at the aperture.

For a transverse dipole and a longitudinal loop we have neither TE or TM modes in the z-direction. In these cases, the safest course is to take the fields at the aperture as being identical to those that would exist at the same place in a semi-infinite waveguide.

The next step is to find an answer to the question: how is the antenna affected by the aperture? In order to do this, we must obtain some measure of the decay rate of the fields as we move away from the antenna, and then of the reflected fields as we move from the aperture towards the source.

In Appendix A we show that for a rectangular waveguide of square cross-section, and for physically reasonable sources (thin antennas), the reflected field is at least four orders of magnitude smaller than the incident field (both calculated at the surface of the antenna), when the antenna-aperture distance is greater than 0.1a (where a is a typical dimension of the enclosure). This fact allows us to disregard the effect of the aperture upon the antenna in all cases of interest. (There is no point in shielding a source if we are going to place the source at, or very close to, an aperture in the shield).

We have then determined that the fields at the open end of a rectangular waveguide excited below cutoff are given in terms of the

fields that would exist at the same place in a semi-infinite waveguide, modified according to the assumptions on aperture reflection pertaining to each specific case.

III.3.2 Induction and Field Equivalence Theorems.

As mentioned earlier, the problem of an open rectangular waveguide radiating into space cannot be solved exactly. The assumptions required to obtain an approximate solution can be better understood after a review of the induction and field equivalence theorems, magistrally stated by S. A. Schelkunoff[13], [14], [15], [16]

(A) Induction Theorem (see Fig. 6)

Consider an infinitely long waveguide with a known electromagnetic field in its interior, and let us call this the "incident field" $\vec{E}^i$ and $\vec{H}^i$.

If we now cut the waveguide to a finite length, the internal field will change to the "actual field" $\vec{E}$ and $\vec{H}$.

Let us now imagine a surface S over the waveguide aperture, separating the "inside" of the waveguide (region 1) from its "outside" (region 2). The surface S can be chosen to be any convenient boundary.

We shall call the field in region 2 the "transmitted field" $\vec{E}^t$ and $\vec{H}^t$.

Turning back our attention to region 1, let us call "reflected field" $\vec{E}^r$ and $\vec{H}^r$, the difference between the actual field and the incident field.

Hence, we have:

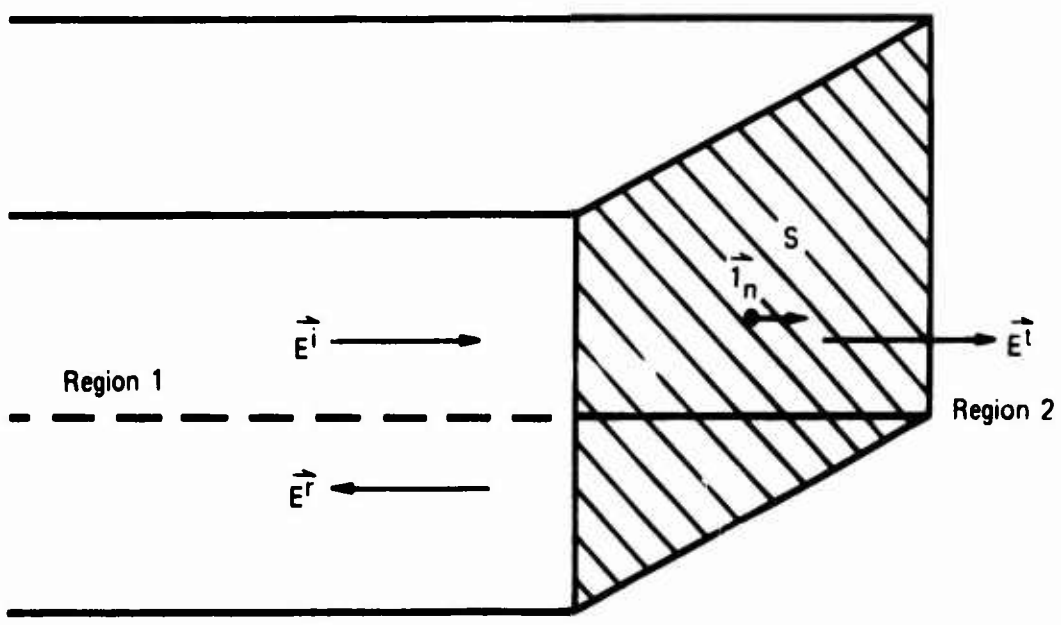

Figure 6
Fields in an open waveguide

$$\text{Region 1} \quad \begin{cases} \vec{E} = \vec{E}^i + \vec{E}^r \\ \vec{H} = \vec{H}^i + \vec{H}^r \end{cases} \tag{III.3.1}$$

$$\text{Region 2} \quad \begin{cases} \vec{E} = \vec{E}^t \\ \vec{H} = \vec{H}^t \end{cases} \tag{III.3.2}$$

If we assume no sources on S, the continuity of the fields $\vec{E}$ and $\vec{H}$ is assured, and their tangential components at the surface S must satisfy:

$$\vec{E}^t_{o,tan} = \vec{E}^i_{o,tan} + \vec{E}^r_{o,tan} \tag{III.3.3}$$

$$\vec{H}^t_{o,tan} = \vec{H}^i_{o,tan} + \vec{H}^r_{o,tan} \tag{III.3.4}$$

Maxwell's equations ensure the continuity of the normal components.

We now define a "scattered field" $\vec{E}^s$, $\vec{H}^s$ made up of the reflected field in region 1 and the transmitted field in region 2

$$\vec{E}^s = \vec{E}^r + \vec{E}^t \tag{III.3.5}$$

$$\vec{H}^s = \vec{H}^r + \vec{H}^t \tag{III.3.6}$$

This scattered field satisfies Maxwell's equations under the boundary conditions imposed by the waveguide, but it is discontinuous across S by the amounts

$$\vec{E}^t_{o,tan} - \vec{E}^r_{o,tan} = \vec{E}^i_{o,tan} \tag{III.3.7}$$

$$\vec{H}^t_{o,tan} - \vec{H}^r_{o,tan} = \vec{H}^i_{o,tan} \tag{III.3.8}$$

These discontinuities may be thought of as arising from the following sources on S:

1) A magnetic current sheet (due to the discontinuity in $\vec{E}^s_{o,tan}$) of density

$$\vec{J}^{\ell}_m = \vec{E}^i_{o,tan} \times \hat{\tau}_n = \vec{E}^i_o \times \hat{\tau}_n \qquad \text{(III.3.9)}$$

2) An electric current sheet (due to the discontinuity in $\vec{H}^s_{o,tan}$) of density

$$\vec{J}^{\ell} = \hat{\tau}_n \times \vec{H}^i_{o,tan} = \hat{\tau}_n \times \vec{H}^i_o \qquad \text{(III.3.10)}$$

The Induction Theorem can then be stated as follows: "The reflected and transmitted fields may be generated by an appropriate distribution of electric and magnetic currents distributed over the "surface of reflection". The linear densities of these currents are given by the tangential components of the incident field."

When using these currents to determine the fields, the environment must be left unchanged, i.e., the waveguide must be left in its place.

(B) Field Equivalence Theorem

When we are interested in calculating only the transmitted field, we may resort to a corollary that follows obviously from the induction theorem: The transmitted field can be obtained by postulating a zero field inside a closed surface S comprised of the surface of the aperture and the outer surface of the waveguide, and a field $\vec{E}^t$, $\vec{H}^t$ outside S. These fields are produced by electric and magnetic

current sheets over S given by expressions (III.3.11) and (III.3.12), but now, in carrying out the calculations, the waveguide must be ignored and the response is obtained by using the "free-space" retarded potentials.

$$\vec{J}_m^{\ell} = \vec{E}_o^{t} \times \hat{\tau}_n \qquad \text{(III.3.11)}$$

$$\vec{J}^{\ell} = \hat{\tau}_n \times \vec{H}_o^{t} \qquad \text{(III.3.12)}$$

III.3.3 Radiation Fields from an Open-Ended Rectangular Waveguide Excited Below Cutoff

The determination of the radiation fields from open-ended parallel-plate waveguides and circular waveguides is essentially a two-dimensional problem, and can be solved exactly by using Wiener-Hopf techniques.[17]

On the other hand, the radiation from an open rectangular waveguide (or horn) poses a much more difficult problem, due to the effect of currents on the outside walls of the waveguide, which are now distributed on a three-dimensional boundary.

The standard procedure[12] is to neglect these currents, which amounts to assuming the existence of a perfectly conducting flange coplanar with the aperture and solving, in essence, the radiation from a rectangular aperture in a perfectly conducting plane.

This approximation worsens at low frequencies, especially if we are interested in the fields at large angles from the axis of the waveguide (i.e., the fields near the imaginary flange). But for points

on, or near the axis, the approximation is acceptable, as borne out by experiments (see Chapter VI).

In the design of electromagnetic shields, the quantity of interest is the worst-case insertion loss (or the worst-case shielding effectiveness). Thus, when we study the "leakage" from an open waveguide, our major concern is with the field intensities along the axis of the waveguide, and the "infinite flange approximation" becomes acceptable.

We are then led to the use of the field equivalence theorem with the closed surface S being now composed of the surface of the aperture, the co-planar infinitely conducting flange and the hemisphere at infinity that does not contain the waveguide.

The radiation field will be that produced by the current sheets (III.3.11) and (III.3.12), repeated below

$$\vec{J}_m^{\ell} = E_o^t \times \vec{1}_n \qquad \text{(III.3.13)}$$

$$\vec{J}^{\ell} = \vec{1}_n \times H_o^t \qquad \text{(III.3.14)}$$

where E_o^t and H_o^t are the assumed aperture fields, whose tangential components are taken to be zero elsewhere on the aperture plane.[12, p.71ff]

Chapter IV

INPUT IMPEDANCE OF A DIPOLE ANTENNA INSIDE A CAVITY WITH APERTURES

In Chapter V we will need to know the input impedance of a dipole antenna inside a cavity with apertures, in order to evaluate the insertion loss of a shielding box when its internal source is fed by a voltage generator.

In most practical circumstances, an electrically short linear antenna is fed by a high-impedance source, whereas a small loop is fed by a low-impedance source. Since the radiated fields from both types of antennas are proportional to their current, it becomes necessary to know the input impedance of the linear antenna if we are to describe the insertion loss of the shielding box in terms of the quantity being kept constant, i.e., the input voltage.

The input impedance of a small loop not only is of little practical interest, but cannot be deduced from our treatment. Obviously, the input impedance of a resistanceless loop enclosed in a perfectly conducting cavity is zero to a first approximation (low-frequency, or quasi-static case).

The antenna impedances are developed in this chapter using the "induced-emf" method[18], i.e., the input impedance of the antenna is given by

$$Z_i = -\frac{1}{I_0^2}\int_L \vec{E}\cdot\vec{I}\,d\ell \qquad (IV.1)$$

where $d\ell$ is a length element along a thin antenna of total length L, and I_0 is the current at the antenna input terminals.

The evaluation of (IV.1) for an infinitely thin antenna leads, in general, to an infinite value of reactance. To obtain a useful result, the finite radius of the wire must be taken into account. This requires that the electric field $\vec{E}$ in (IV.1) be evaluated at a distance ρ (the wire radius) from the axis of the antenna.

IV.1 Dipole Antenna Inside a Cavity with Small Apertures

To the same degree of approximation that we have used in the treatment of the radiation from a cavity with small apertures, we can say that the presence of small apertures will not disturb the fields near the antenna.

Obviously, the most significant error will be introduced in the input resistance of the antenna, whereas the input reactance will be hardly affected. Since we will be dealing with electrically short antennas, for whom the imaginary part of their input impedance is several orders of magnitude greater than the real part, our assumption turns out to be an excellent approximation. In fact, given that our expressions for the fields were derived for the case of infinitely conducting boundaries, we are totally neglecting the input resistance.

Consider a thin dipole antenna oriented in the x-direction, and with a current given by

$$\vec{J} = \vec{i}_x J_x = \begin{cases} \vec{i}_x I_o \dfrac{\sin[k(h-|x-a'|)]}{\sin(kh)} \delta(y-b')\delta(z-d') & ; \ |x-a'|<h \\ 0 & ; \ |x-a'|>h \end{cases} \tag{IV.1.1}$$

The electric field component E_x is obtained from Eq. (II.2.21) after the appropriate coordinate transformation.

Taking

$$y = b' \tag{IV.1.2}$$

$$z = d' + \rho \tag{IV.1.3}$$

we have

$$Z_i = -\frac{1}{I_o^2} \int_{a'-h}^{a'+h} E_x(x)\, I_x(x)\, dx$$

$$= j \frac{2}{ab \sin^2(kh)} \sqrt{\frac{\mu_o}{\varepsilon_o}} \sum_{m,n} \varepsilon_m \cdot \frac{\left(\frac{m\pi}{a}\right)^2 + k^2}{\left(\frac{m\pi}{a}\right)^2 - k^2} \cdot$$

$$\cdot \cos\frac{m\pi a'}{a} \cdot \sin^2\frac{n\pi b'}{b} \left[\cos\frac{m\pi h}{a} - \cos(kh)\right] \cdot$$

$$\cdot \frac{\sinh(\Gamma_{mn} z') \cdot \sinh\left\{\Gamma_{mn}[d-(d'+\rho)]\right\}}{\Gamma_{mn} \cdot \sinh(\Gamma_{mn} d)} \cdot$$

$$\cdot \int_{a'-h}^{a'+h} \sin[k(h-|x-a'|)] \cdot \cos\frac{m\pi x}{a} \cdot dx \tag{IV.1.4}$$

$$Z_i = -j \frac{4k}{ab \sin^2(kh)} \sqrt{\frac{\mu_o}{\varepsilon_o}} \sum_{m,n} \varepsilon_m \cdot \frac{\left(\frac{m\pi}{a}\right)^2 + k^2}{\left[\left(\frac{m\pi}{a}\right)^2 - k^2\right]^2} \cdot$$

$$\cdot \cos^2 \frac{m\pi a'}{a} \cdot \sin^2 \frac{n\pi b'}{b} \cdot \left[\cos(kh) - \cos \frac{m\pi h}{a}\right]^2 \cdot$$

$$\cdot \frac{\sinh(\Gamma_{mn} d') \cdot \sinh\left\{\Gamma_{mn}[d-(d' + \rho)]\right\}}{\Gamma_{mn} \cdot \sinh(\Gamma_{mn} d)} \qquad \text{(IV.1.5)}$$

IV.2 Dipole Antenna Inside an Open Cavity

The approximation used in this case consists in considering that the cavity extends to infinity in the direction of the aperture. As was seen in Chapter III, this is a perfectly acceptable assumption as long as the antenna is located at some small but reasonable distance behind the missing wall.

Thus, we can use the equations developed in Section 2 of Chapter III for a semi-infinite rectangular waveguide.

IV.2.1 Transverse Source

Putting expressions (III.2.19) and (III.2.20) into Eq. (IV.1) we obtain, for an x-directed dipole,

$$Z_i = -j \frac{4k}{ab \sin^2(kh)} \sqrt{\frac{\mu_o}{\varepsilon_o}} \sum_{m,n} \varepsilon_m \cdot \frac{\left(\frac{m\pi}{a}\right)^2 + k^2}{\left[\left(\frac{m\pi}{a}\right)^2 - k^2\right]^2} \cdot$$

$$\cdot \cos^2 \frac{m\pi a'}{a} \cdot \sin^2 \frac{n\pi b'}{b} \cdot \left[\cos(kh) - \cos \frac{m\pi h}{a}\right]^2 \cdot$$

$$\cdot \frac{1}{\Gamma_{mn}} \cdot e^{-\Gamma_{mn}(d' + \rho)} \cdot \sinh(\Gamma_{mn} d') \qquad \text{(IV.2.1)}$$

IV.2.2 Longitudinal Source

For a z-directed dipole, we use Eqs. (III.2.26) and (III.2.29) to obtain

$$Z_i = -j \frac{8}{ab \sin^2(kh)} \sqrt{\frac{\mu_o}{\varepsilon_o}} \sum_{m,n} \frac{1}{\Gamma_{mn}} \cdot \frac{\Gamma_{mn}^2 - k^2}{\left[\left(\frac{m\pi}{a}\right)^2 + \left(\frac{n\pi}{b}\right)^2\right]^2}$$

$$\cdot \sin^2 \frac{m\pi a'}{a} \cdot \sin \frac{n\pi(b'+\rho)}{b} \cdot \sin \frac{n\pi b'}{b} \cdot$$

$$\cdot \left[\cosh(\Gamma_{mn} h) - \cos(kh)\right] \cdot \left\{ \Gamma_{mn} \sin(kh) + \right.$$

$$+ k \left[\frac{1}{2}\left(e^{-2\Gamma_{mn} h} + e^{-2\Gamma_{mn} d'}\right) - \right.$$

$$\left. \left. - \left(1 + e^{-2\Gamma_{mn} d'}\right) \cos(kh) \right] \right\} \qquad \text{(IV.2.2)}$$

Chapter V

INSERTION LOSS OF RECTANGULAR SHIELDING BOXES WITH APERTURES

In the present chapter we shall use all of the tools developed in the previous chapters to find general expressions for the insertion loss of rectangular enclosures with apertures.

As mentioned in Chapter I, we define the "Insertion Loss" of a shield as the ratio of the field strength at a point external to the shield, before and after the insertion of the shield, with the "noise source" driving force maintained constant.

In the light of our present work, the "noise source" is a simple antenna internal to the shield, excited at frequencies below the lowest cutoff mode of the enclosure, and being driven either by a voltage generator or a current generator.

Thus, for the dipole antenna, we shall find two "Insertion Loss" expressions, one for constant current and one for constant voltage at the antenna terminals.

For the loop antenna, the constant-current insertion loss is the only meaningful quantity, as was discussed at the beginning of Chapter IV.

The presence of a conducting plane complicates the situation, since it not only changes the radiation patterns of the antennas and the apertures, but also affects the antenna input impedance. Nevertheless, in many practical applications we cannot disregard the existence of metallic floors or of highly conducting ground. For this purpose, we

are including the necessary equations to deal with this situation.

V.1 Cavity with Small Apertures

V.1.1 Dipole Antenna

(A) Constant Current Insertion Loss

In order to develop insertion loss expressions for the case of a dipole antenna inside a cavity with small apertures, the following steps are necessary:

- Knowledge of the fields inside the cavity, obtained from Eqs. (II.2.19) through (II.2.24).
- Use of Eqs. (II.3.2) and (II.3.3) together with Table I, to find the equivalent aperture source.
- Determine the fields generated by the equivalent aperture source and compare them with the fields produced by the dipole antenna in the absence of the cavity.

We have, by now, all the necessary equations to develop a complete set of insertion loss expressions. Such a task, however, would be not only cumbersome but also pointless. In this and in the following sections, we shall only show some typical examples.

Let us begin by considering a short, thin dipole oriented in the x-direction and centered at the point (a', b', d'). This antenna is enclosed by a perfectly conducting rectangular cavity of sides a, b, and d (see Fig. 1 in Chapter II), having a small aperture on the wall defined by z = 0.

The electric field at the surface of the wall z = 0 is found from Chapter II to be:

$$E_z\Big|_{z=0} = -j\frac{4I_o}{ab\sin(kh)}\sqrt{\frac{\mu_o}{\varepsilon_o}}\sum_{m,n}\sin\frac{m\pi x}{a}\cdot$$

$$\cdot\sin\frac{n\pi y}{b}\cdot\frac{\frac{m\pi}{a}}{\left(\frac{m\pi}{a}\right)^2-k^2}\cdot\cos\frac{m\pi a'}{a}\cdot\sin\frac{n\pi b'}{b}\cdot$$

$$\cdot\left[\cos\frac{m\pi h}{a}-\cos(kh)\right]\cdot\frac{\sinh\left[\Gamma_{mn}(d-d')\right]}{\sinh(\Gamma_{mn}d)} \qquad (V.1.1)$$

The magnetic field at that wall is

$$H_x\Big|_{z=0} = 0 \qquad (V.1.2)$$

$$H_y\Big|_{z=0} = -\frac{2kI_o}{ab\sin(kh)}\sum_{m,n}\varepsilon_m\cos\frac{m\pi x}{a}\cdot\sin\frac{n\pi y}{b}\cdot$$

$$\cdot\frac{1}{\left(\frac{m\pi}{a}\right)^2-k^2}\cdot\cos\frac{m\pi a'}{a}\cdot\sin\frac{n\pi b'}{b}\cdot$$

$$\cdot\left[\cos\frac{m\pi h}{a}-\cos(kh)\right]\cdot\frac{\sinh[\Gamma_{mn}(d-d')]}{\sinh(\Gamma_{mn}d)} \qquad (V.1.3)$$

Expressions (V.1.1) and (V.1.3) were not obtained directly from Eqs. (II.2.19) and (II.2.23), but from equivalent expressions obtained from Eq. (II.1.14) after an appropriate cyclic interchange of the variables.

For computational purposes, it is always advisable to write the equations so that the most critical parameter (in this case the distance d-d') appears in the exponential or hyperbolic functions. It is always possible to do so by using the proper form of Green's function. Throughout this thesis, the Green's functions are expressed as double summations; this provides considerable computational advantage at the cost of lack of symmetry in the equations. However, cyclic interchange of the variables and their associated parameters in the pertinent dyadic Green's function allows us to write any one field expression in three different forms which have, in general, different convergence properties.

Equations (V.1.1) and (V.1.3) provide us with the field intensities at the point (x,y,0), taken to be the center of the small aperture.

The electric and magnetic dipole moments induced on the aperture are given by Eqs. (II.3.2) and (II.3.3).

$$P_z = \alpha_e \, \varepsilon_0 \, E_z\Big|_{z=0} \tag{V.1.4}$$

$$M_y = -\alpha_m \, H_y\Big|_{z=0} \tag{V.1.5}$$

where the appropriate electric and magnetic polarizabilities are to be used.

If we neglect the lateral displacement between the antenna and the aperture, i.e., if we set

$$a' = x \tag{V.1.6}$$

$$b' = y \tag{V.1.7}$$

and,with the help of Appendices B and D, compute the fields with and without the shield at a point directly in front of the aperture, we obtain the following constant current insertion loss expressions for the transverse components of the fields (Fig. 7):

Electric field:

$$\left(I.L.\right)_{I_o} = \frac{\frac{I_o h}{4\pi r'}\sqrt{\frac{\mu_o}{\varepsilon_o}}\left(jk + \frac{1}{r'} + \frac{1}{jkr'^2}\right)}{\frac{k}{4\pi r}\sqrt{\frac{\mu_o}{\varepsilon_o}}\left(jk + \frac{1}{r}\right)|\vec{M}|}$$

$$= \frac{I_o h}{k|\vec{M}|} \cdot \left(\frac{r}{r'}\right) \cdot \frac{jk + \frac{1}{r'} + \frac{1}{jkr'^2}}{jk + \frac{1}{r}} \tag{V.1.8}$$

Magnetic field:

$$\left(I.L.\right)_{I_o} = \frac{\frac{I_o h}{4\pi r'}\left(jk + \frac{1}{r'}\right)}{\frac{k}{4\pi r}\left(jk + \frac{1}{r} + \frac{1}{jkr^2}\right)|\vec{M}|} =$$

$$= \frac{I_o h}{k|\vec{M}|} \cdot \left(\frac{r}{r'}\right) \cdot \frac{jk + \frac{1}{r'}}{jk + \frac{1}{r} + \frac{1}{jkr^2}} \tag{V.1.9}$$

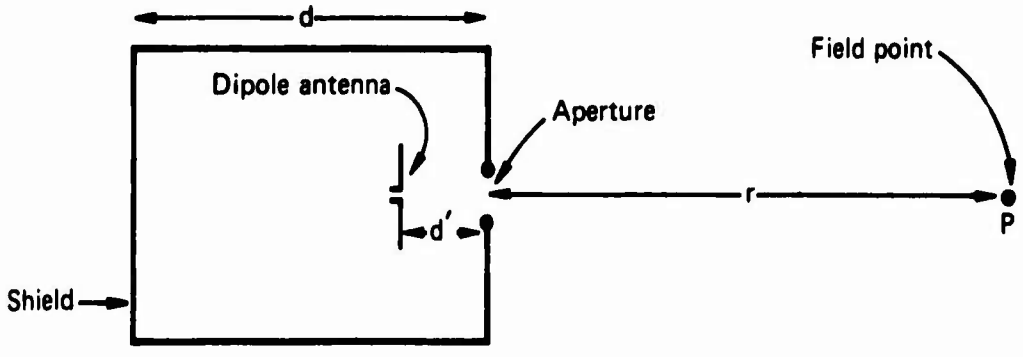

Figure 7

where

$$r' = r + d' \tag{V.1.10}$$

and $|\vec{M}|$ is given by Eq. (V.1.5). Only the absolute value of (I.L.) is of interest.

(B) Constant Voltage Insertion Loss

In Chapter IV and Appendix C we have expressions for the input impedance of a short dipole inside a cavity and in free space, respectively. Thus, we can write the constant voltage insertion loss in terms of the constant current insertion loss and of the impedance ratio:

$$(I.L.)_{V_o} = \frac{Z_i}{Z'_i} (I.L.)_{I_o} \tag{V.1.11}$$

where

Z_i = input impedance of the antenna inside the cavity

Z'_i = input impedance of the antenna in free space

V.1.2 Loop Antenna

The procedure to be followed is obviously the same as in the previous case.

Consider, as before, a cavity with a small aperture on the wall located at z = 0. We shall find the insertion loss expressions for the case of a small square loop whose plane is parallel to the (x,z) plane, centered at the point (a', b', d') internal to the cavity (see Fig. 2 in Chapter II).

We shall use expressions equivalent to (II.2.27), (II.2.28), and (II.2.29), but more convenient from a computational point of view, to describe the fields on the surface z = 0.

$$E_z\Big|_{z=0} = -j\frac{16kI_o}{ab}\sqrt{\frac{\mu_o}{\varepsilon_o}}\sum_{m,n}\sin\frac{m\pi x}{a}\cdot\sin\frac{n\pi y}{b}\cdot\cos\frac{m\pi a'}{a}\cdot$$

$$\cdot\sin\frac{n\pi b'}{b}\cdot\sin\frac{m\pi D}{a}\cdot\frac{\sinh(\Gamma_{mn}D)}{\sinh(\Gamma_{mn}d)}\cdot\frac{1}{\Gamma_{mn}^2}\cdot$$

$$\cdot\cosh\left[\Gamma_{mn}(d-d')\right] \qquad \text{(V.1.12)}$$

$$H_x\Big|_{z=0} = \frac{16I_o}{ab}\sum_{m,n}\sin\frac{m\pi x}{a}\cdot\cos\frac{n\pi y}{b}\cdot\frac{n\pi}{b}\cdot$$

$$\cdot\cos\frac{m\pi a'}{a}\cdot\sin\frac{n\pi b'}{b}\cdot\sin\frac{m\pi D}{a}\cdot\frac{1}{\Gamma_{mn}^2}\cdot$$

$$\cdot\frac{\sinh(\Gamma_{mn}D)}{\sinh(\Gamma_{mn}d)}\cdot\cosh\left[\Gamma_{mn}(d-d')\right] \qquad \text{(V.1.13)}$$

$$H_y\Big|_{z=0} = \frac{8I_o}{ab} \sum_{m,n} \epsilon_m \cos\frac{m\pi x}{a} \cdot \sin\frac{n\pi y}{b} \cdot$$

$$\cdot \frac{\left(\frac{n\pi}{b}\right)^2 - k^2}{\frac{m\pi}{a}} \cdot \cos\frac{m\pi a'}{a} \cdot \frac{n\pi b'}{b} \cdot \sin\frac{m\pi D}{a} \cdot$$

$$\cdot \frac{1}{\Gamma_{mn}^2} \cdot \frac{\sinh(\Gamma_{mn}D)}{\sinh(\Gamma_{mn}d)} \cdot \cosh\left[\Gamma_{mn}(d-d')\right] \qquad \text{(V.1.14)}$$

The use of (II.3.2) and (II.3.3) results in

$$P_z = \alpha_e \epsilon_o E_z\Big|_{z=0} \qquad \text{(V.1.15)}$$

$$\vec{M} = \overleftrightarrow{\alpha}_m \left(\vec{T}_x H_x\Big|_{z=0} + \vec{T}_y H_y\Big|_{z=0} \right) \qquad \text{(V.1.16)}$$

and the corresponding constant current insertion loss expressions may be found with the help of Appendices B and D.

V.2 Open Cavity

V.2.1 Dipole Antenna

(A) Constant Current Insertion Loss

We are now dealing with a cavity, in which the aperture is a missing wall. As we have seen, this case is best treated as a semi-infinite rectangular waveguide truncated (open) at the plane $z = d > d'$ (see Fig. 3 in Chapter III).

The steps to follow are similar to those used in the first section of this chapter, with the main difference that the fields needed

to describe the aperture are the tangential components of $\vec{E}$ and $\vec{H}$, i.e., the components lying in the plane of the aperture.

With reference to Fig. 3 (Chapter III), let us consider an x-directed dipole antenna of length 2h, centered at the point (a', b', d') inside a waveguide section short-circuited at the plane z = 0 and open at z = d > d'.

At the plane of the aperture (z = d), the tangential fields are given by Eqs. (III.2.20), (III.2.21), (III.2.23) and (III.2.24).

$$E_x\Big|_{z=d} = -j\,\frac{2I_o}{ab\,\sin(kh)}\sqrt{\frac{\mu_o}{\varepsilon_o}}\sum_{m,n}\varepsilon_m\cdot\cos\frac{m\pi x}{a}\cdot \sin\frac{n\pi y}{b}\cdot\frac{\left(\frac{m\pi}{a}\right)^2+k^2}{\left(\frac{m\pi}{a}\right)^2-k^2}\cdot\cos\frac{m\pi a'}{a}\cdot \sin\frac{n\pi b'}{b}\cdot\left[\cos\frac{m\pi h}{a}-\cos(kh)\right]\cdot\frac{e^{-\Gamma_{mn}d}}{\Gamma_{mn}}\cdot\sinh(\Gamma_{mn}d') \qquad (V.2.1)$$

$$E_y\Big|_{z=d} = -j\,\frac{4I_o}{ab\,\sin(kh)}\cdot\sqrt{\frac{\mu_o}{\varepsilon_o}}\sum_{m,n}\sin\frac{m\pi x}{a}\cdot\cos\frac{n\pi y}{b}\cdot\frac{\frac{m\pi}{a}\cdot\frac{n\pi}{b}}{\left(\frac{m\pi}{a}\right)^2-k^2}\cdot\cos\frac{m\pi a'}{a}\cdot\sin\frac{n\pi b'}{b}\cdot\left[\cos\frac{m\pi h}{a}-\cos(kh)\right]\cdot\frac{e^{-\Gamma_{mn}d}}{\Gamma_{mn}}\cdot\sinh(\Gamma_{mn}d') \qquad (V.2.2)$$

$$H_x\Big|_{z=d} = 0 \tag{V.2.3}$$

$$H_y\Big|_{z=d} = \frac{2kI_o}{ab\,\sin(kh)} \sum_{m,n} \varepsilon_m \cos\frac{m\pi x}{a} \cdot \sin\frac{n\pi y}{b} \cdot$$

$$\cdot \frac{1}{\left(\frac{m\pi}{a}\right)^2 - k^2} \cdot \cos\frac{m\pi a'}{a} \cdot \sin\frac{n\pi b'}{b} \left[\cos\frac{m\pi h}{a} - \cos(kh)\right] \cdot$$

$$\cdot e^{-\Gamma_{mn} d} \sinh(\Gamma_{mn} d') \tag{V.2.4}$$

We have transverse components of both $\vec{E}$ and $\vec{H}$. Following reference [12, p.71 ff], it is convenient to calculate the fields radiated by the aperture in terms of the assumed transverse electric field. This results in a magnetic current sheet J_m^{ℓ} with the aperture plane replaced by a perfect electric conductor, with the consequence that the effective source has a value $2J_m^{\ell}$. Since we are assuming that the aperture dimensions are small compared to the wavelength, we can integrate Eqs. (V.2.1) and (V.2.2) over x and y and divide them by the area of the aperture to obtain their average values over the opening. Thus, we obtain

$$E_{x_{av}}\Big|_{z=d} = j\,\frac{4I_o}{ab\,\sin(kh)}\cdot\sqrt{\frac{\mu_o}{\varepsilon_o}}\cdot$$

$$\cdot\sum_{n=1,3,5,\ldots}\frac{1}{n\pi}\cdot\sin\frac{n\pi b'}{b}\cdot\left[1-\cos(kh)\right]\cdot$$

$$\cdot\frac{e^{-d\sqrt{\left(\frac{n\pi}{b}\right)^2-k^2}}}{\sqrt{\left(\frac{n\pi}{b}\right)^2-k^2}}\cdot\sinh\left(d'\sqrt{\left(\frac{n\pi}{b}\right)^2-k^2}\right) \qquad (V.2.5)$$

$$E_{y_{av}}\Big|_{z=d} = 0 \qquad (V.2.6)$$

According to Eq. (III.3.13), we have then a magnetic current sheet

$$2J^{\ell}_{my} = 2E_{x_{av}}\Big|_{z=d} \qquad (V.2.7)$$

which produces a magnetic dipole of moment

$$M_y = \frac{2\,ab}{jk\sqrt{\frac{\mu_o}{\varepsilon_o}}}\,E_{x_{av}}\Big|_{z=d} \qquad (V.2.8)$$

The use of Appendices B and D leads to constant current insertion loss expressions identical to (V.1.8) and (V.1.9), where now $|\vec{M}|$ is given by (V.2.8) and $r' = r + (d-d')$.

(B) Constant Voltage Insertion Loss

Just as in Section 1 of this chapter, the constant voltage insertion loss is given by

$$(I.L.)_{V_o} = \frac{Z_1}{Z_T} (I.L.)_{I_o} \qquad (V.2.9)$$

This expression is identical to (V.1.11), but Z_1 is now the input impedance of a dipole inside a semi-infinite waveguide, given in Chapter IV.

V.2.2 Loop Antenna

Let us consider a longitudinal loop such as the one depicted in Fig. 5 (Chapter III), where the waveguide has been cut open at the plane $z = d > d' + D$.

The tangential aperture fields are obtained from Eqs. (III.2.39), (III.2.40), (III.2.42) and (III.2.43). As in the previous case, we shall work only with the tangential electric field and double the resulting magnetic moment.

The tangential electric field at the aperture is

$$E_x\Big|_{z=d} = -j \frac{8kI_o}{ab} \sqrt{\frac{\mu_o}{\varepsilon_o}} \sum \varepsilon_m \cos \frac{m\pi x}{a} \cdot \sin \frac{n\pi y}{b} \cdot$$

$$\cdot \frac{a}{m\pi} \cdot \cos \frac{m\pi a'}{a} \cdot \sin \frac{n\pi b'}{b} \cdot \sin \frac{m\pi D}{a} \cdot \frac{1}{\Gamma_{mn}} \cdot$$

$$\cdot \sinh(\Gamma_{mn} D) \cdot e^{-\Gamma_{mn} d} \cdot \cos(\Gamma_{mn} d') \qquad (V.2.10)$$

Averaging over the aperture results in

$$E_{x_{av}}\Big|_{z=d} = -j\frac{8kI_0D}{ab}\sqrt{\frac{\mu_0}{\varepsilon_0}}\sum_{n=1,3,5,\ldots}\frac{2}{n\pi}\cdot\sin\frac{n\pi b'}{b}\cdot$$

$$\cdot\frac{e^{-d\sqrt{\left(\frac{n\pi}{b}\right)^2-k^2}}}{\sqrt{\left(\frac{n\pi}{b}\right)^2-k^2}}\cdot\sinh\left(D\sqrt{\left(\frac{n\pi}{b}\right)^2-k^2}\right)\cdot$$

$$\cdot\cosh\left(d'\sqrt{\left(\frac{n\pi}{b}\right)^2-k^2}\right) \qquad \text{(V.2.11)}$$

Thus, we take our source to be a magnetic current sheet

$$2J^{\ell}_{my} = 2ab\,E_{x_{av}}\Big|_{z=d} \qquad \text{(V.2.12)}$$

which produces a magnetic dipole of moment

$$M_y = -\frac{2ab}{jk\sqrt{\frac{\mu_0}{\varepsilon_0}}}\cdot E_{x_{av}}\Big|_{z=d} \qquad \text{(V.2.13)}$$

With the help of Appendices B and D we may write the constant current insertion loss expressions. For the electric field (E_x):

$$(I.L.)_{I_o} = \frac{\frac{4I_o D^2 k}{4\pi r'}\sqrt{\frac{\mu_o}{\varepsilon_o}}\left(jk + \frac{1}{r'}\right)}{\frac{k}{4\pi r}\sqrt{\frac{\mu_o}{\varepsilon_o}}\left(jk + \frac{1}{r}\right) M_y}$$

$$= \frac{4I_o D^2}{M_y} \cdot \left(\frac{r}{r'}\right) \cdot \frac{jk + \frac{1}{r'}}{jk + \frac{1}{r}} \qquad \text{(V.2.14)}$$

For the magnetic field (H_y):

$$(I.L.)_{I_o} = \frac{\frac{4I_o D^2 k}{4\pi r'}\left(jk + \frac{1}{r'} + \frac{1}{jkr'^2}\right)}{\frac{k}{4\pi r}\left(jk + \frac{1}{r} + \frac{1}{jkr^2}\right) M_y}$$

$$= \frac{4I_o D^2}{M_y}\left(\frac{r}{r'}\right) \cdot \frac{jk + \frac{1}{r'} + \frac{1}{jkr'^2}}{jk + \frac{1}{r} + \frac{1}{jkr^2}} \qquad \text{(V.2.15)}$$

where, once again

$$r' = r + (d-d') \qquad \text{(V.2.16)}$$

V.3 Effect of a Conducting Ground Plane.

The presence of a conducting plane affects only the last step of our procedure, i.e., the insertion loss expressions. The free-space radiation fields and antenna impedances must be replaced with the half-space fields and impedances.

All the necessary equations have been provided in Appendices B, C and D. Their use should be obvious by now, and nothing could be gained by working out examples.

Chapter VI

APPROXIMATIONS, NUMERICAL RESULTS AND CORRELATION WITH EXPERIMENTS

In this chapter we shall take the cases of a transverse dipole and a longitudinal loop, whose equations we developed in Chapter V, and we shall evaluate the expressions for a source centered on a transverse cross-section and an aperture centered on a wall of the cavity. (For an open box, the "aperture" is already "centered" in its corresponding wall).

This results not only in a high degree of symmetry in the equations, allowing their dramatic simplification, but it also constitutes a good approximation for many practical cases of interest.

In the last section, the predicted results are compared with experimentally obtained values to show the usefulness of the present work.

VI.1 Cavity with Small Apertures.

VI.1.1 Dipole Antenna

Let us take the case of a transverse dipole antenna, worked out in Section 1 of Chapter V, and set

$$a' = \frac{a}{2} \quad ; \quad b' = \frac{b}{2} \tag{VI.1.1}$$

$$x = \frac{a}{2} \quad ; \quad y = \frac{b}{2} \tag{VI.1.2}$$

We are now interested in evaluating the electric field insertion

loss for the above configuration. Equation (V.1.3) becomes

$$H_y\Big|_{z=0} = -\frac{2kI_o}{ab\sin(kh)} \sum_{\substack{m=0,2,4\ldots \\ n=1,3,5\ldots}} \varepsilon_m \cdot \frac{1}{\left(\frac{m\pi}{a}\right)^2 - k^2} \cdot$$

$$\cdot \left[\cos\frac{m\pi h}{a} - \cos(kh)\right] \cdot \frac{\sinh\left[\Gamma_{mn}(d-d')\right]}{\sinh\left(\Gamma_{mn}d\right)} \qquad \text{(VI.1.3)}$$

which may be written as

$$H_y\Big|_{z=0} = -\frac{2kI_o}{ab\sin(kh)} \left\{ \sum_{n=1,3,5\ldots} -\frac{1}{k^2}\left[1-\cos(kh)\right] \cdot \right.$$

$$\cdot \frac{\sinh\left[(d-d')\sqrt{\left(\frac{n\pi}{b}\right)^2 - k^2}\right]}{\sinh\left(d\sqrt{\left(\frac{n\pi}{b}\right)^2 - k^2}\right)} +$$

$$+ \sum_{\substack{m=2,4,6\ldots \\ n=1,3,5\ldots}} \frac{2}{\left(\frac{m\pi}{a}\right)^2 - k^2} \cdot \left[\cos\frac{m\pi h}{a} - \cos(kh)\right] \cdot$$

$$\left. \cdot \frac{\sinh\left[\Gamma_{mn}(d-d')\right]}{\sinh(\Gamma_{mn}d)} \right\} \qquad \text{(VI.1.4)}$$

At frequencies significantly below cutoff we have

$$k \ll \frac{\pi}{a}, \frac{\pi}{b} \qquad \text{(VI.1.5)}$$

and certainly

$$kh << 1 \tag{VI.1.6}$$

Therefore, Eq. (VI.1.4) becomes

$$H_y\Big|_{z=0} = -\frac{2I_o}{abh}\left\{\sum_{n=1,3,5\ldots} -\frac{h^2}{2}\cdot\frac{\sinh\left[\frac{n\pi}{b}(d-d')\right]}{\sinh\left(\frac{n\pi d}{b}\right)}\cdot\right.$$

$$+\sum_{\substack{m=2,4,6\ldots\\ n=1,3,5\ldots}} 2\left(\frac{a}{m\pi}\right)^2\left[\cos\frac{m\pi h}{a}-\cos(kh)\right]$$

$$\left.\cdot\frac{\sinh\left[\Gamma_{mn}(d-d')\right]}{\sinh\left(\Gamma_{mn}d\right)}\right\} \tag{VI.1.7}$$

Assuming that $d \doteq b$ as it should be in a typical cabinet or rectangular shielding box, we can approximate (VI.1.7) by

$$H_y\Big|_{z=0} = -\frac{2I_o}{abh}\left\{\sum_{n=1,3,5,\ldots} -\frac{h^2}{2}\cdot e^{-\frac{n\pi}{b}d'}\right. \quad +$$

$$\left.+\sum_{\substack{m=2,4,6\ldots\\ n=1,3,5\ldots}} 2\left(\frac{a}{m\pi}\right)^2\left[\cos\frac{m\pi h}{a}-\cos(kh)\right]e^{-\Gamma_{mn}d'}\right\} \tag{VI.1.8}$$

Evaluating the first summation[22]

$$H_y\Big|_{z=0} = -\frac{2I_o}{abh}\left\{-\frac{h^{2\cdots}}{4\sinh\frac{\pi d'}{b}}^{80} + \sum_{\substack{m=2,4,6\ldots\\ n=1,3,5\ldots}} 2\left(\frac{a}{m\pi}\right)^2\left[\cos\frac{m\pi h}{a} - \cos(kh)\right] e^{-\Gamma_{mn}d'}\right\} \tag{VI.1.9}$$

If we further make the very reasonable assumption that d', the distance between the antenna and the aperture, is not too small (say, $d' > \frac{b}{10}$), we need only keep the first term (m = 2, n = 1) of the remaining summation.

Thus, we arrive at

$$H_y\Big|_{z=0} = \frac{I_o}{2abh}\left[\frac{h}{\sinh\frac{\pi d'}{b}} - 2\left(\frac{a}{\pi}\right)^2\left(\cos\frac{2\pi h}{a} - 1\right) e^{-\frac{\pi d'}{b}\sqrt{1+4\left(\frac{b}{a}\right)^2}}\right] \tag{VI.1.10}$$

Using Eq. (V.1.5) and inserting the resulting expression in (V.1.8) gives us the desired constant current insertion loss expression.

To determine the constant voltage insertion loss, we must first evaluate the input impedance of the antenna inside the cavity.

To the same degree of approximation used above, Eq. (IV.1.5) becomes

$$Z_i = -j\frac{4}{abkh^2}\sqrt{\frac{\mu_o}{\varepsilon_o}}\left\{\sum_{n=1,3,5\ldots}\frac{k^2h^4}{4}\cdot\frac{e^{-\frac{n\pi}{b}(d'+\rho)}}{\frac{n\pi}{b}}\cdot\sinh\frac{n\pi d'}{b}+\right.$$

$$+\sum_{\substack{m=2,4,6\ldots\\ n=1,3,5\ldots}}2\cdot\left(\frac{a}{m\pi}\right)^2\left[\cos(kh)-\cos\frac{m\pi h}{a}\right]^2\cdot$$

$$\left.\cdot\frac{e^{-\Gamma_{mn}(d'+\rho)}}{\Gamma_{mn}}\cdot\sinh(\Gamma_{mn}d')\right\} \qquad \text{(VI.1.11)}$$

Evaluating the first summation

$$\sum_{n=1,3,5,\ldots}\frac{e^{-\frac{n\pi}{b}(d'+\rho)}}{\frac{n\pi}{b}}\cdot\sinh\frac{n\pi d'}{b} =$$

$$=\frac{b}{2\pi}\sum_{n=1,3,5,\ldots}\frac{1}{n}\left\{\left[e^{-\frac{n\pi\rho}{b}}\right]^n-\left[e^{\frac{\pi}{b}(2d'+\rho)}\right]^n\right\}$$

$$=\frac{b}{2\pi}\left\{\tanh^{-1}\left(e^{-\frac{\pi\rho}{b}}\right)-\tanh^{-1}\left[e^{-\frac{\pi}{b}(2d'+\rho)}\right]\right\}$$

$$=\frac{b}{2\pi}\cdot\left\{\frac{1}{2}\ln\frac{1+e^{-\frac{\pi\rho}{b}}}{1-e^{-\frac{\pi\rho}{b}}}-\tanh^{-1}\left[e^{-\frac{\pi}{b}(2d'+\rho)}\right]\right\}$$

$$\approx\frac{b}{2\pi}\left\{\frac{1}{2}\ln\left(\frac{2}{\frac{\pi\rho}{b}}\right)-\tanh^{-1}\left[e^{-\frac{\pi}{b}(2d'+\rho)}\right]\right\}$$

$$=\frac{b}{2\pi}\left\{\frac{1}{2}\left[\ln\left(\frac{b}{\rho}\right)-0.45\right]-\tanh^{-1}\left[e^{-\frac{\pi}{b}(2d'+\rho)}\right]\right\} \qquad \text{(VI.1.12)}$$

where we have used reference [22, p. 164] and the fact that $\pi\rho << b$.

Putting this result in (VI.1.11) and evaluating the second summation over the index n (see Appendix E), we arrive at

$$Z_1 = -j \frac{1}{abkh^2} \sqrt{\frac{\mu_o}{\varepsilon_o}} \left\{ \frac{k^2 h^4 b}{4\pi} \left[\ell n\left(\frac{b}{\rho}\right) - 0.45 - \right.\right.$$

$$\left. - 2 \tanh^{-1}\left(e^{-\frac{2\pi d'}{b}} \right) \right] +$$

$$+ \frac{2a^2 b}{\pi^3} \sum_{m=2,4,6\ldots} \frac{1}{m^2} \left(1 - \cos\frac{m\pi h}{a}\right)^2 \cdot \left[\ell n \frac{a}{\rho} - \right.$$

$$\left.\left. - 1.84 + \frac{1}{\sqrt{1 + m^2\left(\frac{b}{a}\right)^2}} - \ell n \left(1 + \frac{1}{2}\sqrt{1 + m^2\left(\frac{b}{a}\right)^2} \right) \right] \right\}$$

(VI. 1.13)

This expression, inserted in Eq. (V.1.11), gives us the constant voltage insertion loss.

For frequencies near cutoff, the second summation in (VI.1.11) should be evaluated by computer.

VI.1.2 Loop Antenna

If in Eqs. (V.1.12) through (V.1.14), corresponding to a "longitudinal" square loop inside a cavity, we set

$$a' = \frac{a}{2} \quad ; \quad b' = \frac{b}{2} \qquad \text{(VI.1.14)}$$

$$x = \frac{a}{2} \quad ; \quad y = \frac{b}{2} \qquad \text{(VI.1.15)}$$

The only non-zero field component at the site of the aperture is H_y, which now becomes

$$H_y\Big|_{z=0} = \frac{8I_o}{ab} \sum_{\substack{m=0,2,4\ldots \\ n=1,3,5\ldots}} \frac{\left(\frac{n\pi}{b}\right)^2 - k^2}{\frac{m\pi}{a}} \cdot \sin\frac{m\pi D}{a} \cdot$$

$$\cdot \frac{1}{\Gamma_{mn}^2} \cdot \frac{\sinh(\Gamma_{mn}D)}{\sinh(\Gamma_{mn}d)} \cdot \cosh\left[\Gamma_{mn}(d-d')\right] \qquad \text{(VI.1.16)}$$

Separating the $m = 0$ term and assuming, as before

$$k << \frac{\pi}{a}, \frac{\pi}{b} \qquad \text{(VI.1.17)}$$

$$d \overset{\circ}{=} b \qquad \text{(VI.1.18)}$$

we obtain

$$H_y\Big|_{z=0} = \frac{8I_o}{ab} \left\{ \sum_{n=1,3,5\ldots} D\, e^{-\frac{n\pi d'}{b}} \cdot \sinh\left(\frac{n\pi D}{b}\right) + \right.$$

$$\left. + \sum_{\substack{m=2,4,6\ldots \\ n=1,3,5\ldots}} \frac{\left(\frac{n\pi}{b}\right)^2}{\frac{m\pi}{a}} \cdot \sin\frac{m\pi D}{a} \cdot \frac{e^{-\Gamma_{mn}d'}}{\Gamma_{mn}^2} \cdot \sinh(\Gamma_{mn}D) \right\} \qquad \text{(VI.1.19)}$$

The first summation can be easily evaluated if we write it as

$$\sum_{n=1,3,5\ldots} D \cdot e^{-\frac{n\pi d'}{b}} \cdot \sinh \frac{n\pi D}{b} =$$

$$= \frac{D}{2} \sum_{n=1,3,5\ldots} \left[\left(e^{-\frac{\pi}{b}(d'-D)} \right)^n - \left(e^{-\frac{\pi}{b}(d'+D)} \right)^n \right]$$

$$= \frac{D}{4} \left\{ \operatorname{csch} \left[\frac{\pi}{b}(d'-D) \right] - \operatorname{csch} \left[\frac{\pi}{b}(d'+D) \right] \right\}$$

(VI.1.20)

where we have used reference [22].

In the last summation, if we again assume that (d'-D) is not too small, we may keep only the first term (m = 2, n = 1), so that (VI.1.19) becomes

$$H_y\Big|_{z=0} = \frac{8I_o}{ab} \left\{ \frac{D}{4} \left\{ \operatorname{csch} \left[\frac{\pi}{b}(d'-D) \right] - \operatorname{csch} \left[\frac{\pi}{b}(d'+D) \right] \right\} + \frac{\sin \frac{2\pi D}{a}}{\frac{2\pi}{a}} \cdot \frac{e^{-\frac{\pi d'}{b}\sqrt{1+4\left(\frac{b}{a}\right)^2}}}{1+4\left(\frac{b}{a}\right)^2} \cdot \sinh \left[\frac{\pi D}{b} \sqrt{1+4\left(\frac{b}{a}\right)^2} \right] \right\}$$

(VI.1.21)

Knowledge of the magnetic polarizability of the aperture will allow us to determine the equivalent magnetic dipole moment $\vec{M}$ and the corresponding insertion loss expression.

VI.2 Open Cavity

VI.2.1 Dipole Antenna

Let us set $b' = \frac{b}{2}$ in Eq. (V.2.5), corresponding to the case of a transverse dipole antenna inside an open cavity.

Assuming

$$k << \frac{\pi}{b} \tag{VI.2.1}$$

and

$$kh << 1 \tag{VI.2.2}$$

we obtain

$$E_{x_{av}}\Big|_{z=d} = j \frac{4I_o kh}{\pi^2 a} \sqrt{\frac{\mu_o}{\varepsilon_o}} \sum_{n=1,3,5\ldots} \frac{\left(e^{-\frac{\pi}{b}(d-d')}\right)^n}{n^2} \tag{VI.2.3}$$

This series, although deceptively simple-looking, does not have a closed form [22, p.184]. Fortunately, it is very rapidly convergent and may be truncated after the first few terms. How many terms we must keep depends on the ratio $\frac{d-d'}{b}$, where (d-d') is the distance between the antenna and the aperture.

Inserting Eq. (VI.2.3) in (V.2.8) results in the magnetic dipole moment M_y, and then the constant current insertion loss may be immediately found. To obtain the constant voltage insertion loss, we need the input impedance of the antenna inside the cavity. Setting $a' = \frac{a}{2}$, $b' = \frac{b}{2}$ and assuming

$$k << \frac{\pi}{a}, \frac{\pi}{b} \tag{VI.2.4}$$

$$kh << 1 \tag{VI.2.5}$$

in Eq. (IV.2.1) results in expression (VI.1.11), i.e., the input impedance of a transverse dipole antenna inside a cavity, at frequencies below cutoff, is independent (to a first approximation) of whether the cavity is open or closed.

Hence, expression (VI.1.13) is also valid for our dipole antenna in an open cavity.

VI.2.2 Loop Antenna

Consider the longitudinal loop treated in Chapter V and set

$$b' = \frac{b}{2} \tag{VI.2.6}$$

in Eq. (V.2.11). Assuming

$$k << \frac{\pi}{b} \tag{VI.2.7}$$

we have

$$E_{x_{av}}\Big|_{z=d} = -j \frac{16kI_o D}{\pi^2 a} \sqrt{\frac{\mu_o}{\epsilon_o}} \sum_{n=1,3,5\ldots} \frac{1}{n^2} e^{-\frac{n\pi d}{b}} \cdot \cdot \sinh\left(\frac{n\pi D}{b}\right) \cdot \cosh\left(\frac{n\pi d'}{b}\right) \tag{VI.2.8}$$

Once again, we meet the impossibility of finding a closed form for the series. However, it is rapidly convergent and in most practical cases the first few terms will suffice. Inserting (VI.2.8) in Eq. (V.2.13) results in the magnetic dipole moment M_y, and expressions (V.2.14) and (V.2.15) give us the desired insertion loss.

VI.3 Correlation with Experiments

To verify, to some degree, the validity of the assumptions made

throughout this work, a series of measurements was performed on some simple physical configurations. A cubical shielding box of sides a = b = d was used, having a square aperture centered in the corresponding wall. The antennas were: a dipole of length 2h = a/5, and a square loop of sides 2D = a/5. During the measurements, the antennas were kept centered in the box, to allow the use of the equations developed in the first two sections of this chapter.

The resulting insertion loss expressions are:

VI.3.1 Cavity with a Square Aperture of Side ℓ.

(A) Transverse Dipole Antenna

For the electric field (E_x), we have

$$(I.L.)_{I_o} = \frac{1}{F_1} \cdot \left(\frac{r}{r'}\right) \cdot \frac{jk + \frac{1}{r'} + \frac{1}{jkr'^2}}{jk + \frac{1}{r}} \qquad \text{(VI.3.1)}$$

$$(I.L.)_{V_o} = F_2 \cdot (I.L.)_{I_o} \qquad \text{(VI.3.2)}$$

where

$$F_1 = 10.36\ \pi \left(\frac{\ell}{a}\right)^3 \left(\frac{a}{\lambda}\right) \left[\frac{1}{20 \sinh \frac{\pi d'}{a}} + \frac{1.91}{\pi^2} \cdot e^{-\frac{\pi d'}{a}\sqrt{5}}\right] \qquad \text{(VI.3.3)}$$

and

$$F_2 = \frac{Z_1}{Z_1'} \approx \frac{1}{\ell n(\frac{h}{\rho}) - 1} \cdot \left\{ \frac{\pi^2}{10^3} \left(\frac{a}{\lambda}\right)^2 \cdot \left[\ell n(\frac{a}{\rho}) - 0.45 - 2 \tanh^{-1}\left(e^{-\frac{2\pi d'}{a}}\right)\right] + \right.$$

$$+ \frac{4}{\pi^2}\left(\frac{a}{h}\right) \sum_{\substack{m=2,4,6\ldots \\ n=1,3,5\ldots}} \frac{1}{m^2} \left[\cos(kh) - \cos\frac{m\pi h}{a}\right]^2 \cdot$$

$$\left. \cdot \frac{e^{-\frac{\pi\rho}{a}\sqrt{m^2 + n^2 - 4(\frac{a}{\lambda})^2}}}{\sqrt{m^2 + n^2 - 4(\frac{a}{\lambda})^2}} \right\} \qquad \text{(VI.3.4)}$$

(B) Longitudinal Loop Antenna

For the magnetic field (H_y), the insertion loss is

$$(I.L.)_{I_o} = \frac{1}{F_3} \cdot \left(\frac{r}{r'}\right) \cdot \frac{jk + \frac{1}{r'} + \frac{1}{jkr'^2}}{jk + \frac{1}{r} + \frac{1}{jkr^2}} \qquad \text{(VI.3.5)}$$

where

$$F_3 = 12.95\left(\frac{\ell}{a}\right)^3 \cdot \left\{ \frac{1}{5} \left| \operatorname{csch}\left[\pi\left(\frac{d'}{a} - 0.1\right)\right] - \operatorname{csch}\left[\pi\left(\frac{d'}{a} + 0.1\right)\right]\right| + \frac{0.358}{\pi} \cdot e^{-\frac{\pi d'}{a}\sqrt{5}} \right| \qquad \text{(VI.3.6)}$$

VI.3.2 Open Cavity

(A) Transverse Dipole Antenna

For the electric field (E_x):

$$(I.L.)_{I_o} = \frac{1}{F_4} \cdot \left(\frac{r}{r'}\right) \cdot \frac{jk + \frac{1}{r'} + \frac{1}{jkr'^2}}{jk + \frac{1}{r}} \qquad \text{(VI.3.7)}$$

$$(I.L.)_{V_o} = F_2 \cdot (I.L.)_{I_o} \qquad \text{(VI.3.8)}$$

where

$$F_4 = \frac{8}{\pi}\left(\frac{a}{\lambda}\right) \sum_{n=1,3,5,\ldots} \frac{1}{n^2} \, e^{-\frac{n\pi}{a}(d-d')} \qquad \text{(VI.3.9)}$$

and F_2 is given by Eq. (VI.3.4)

(B) Longitudinal Loop Antenna

For the magnetic field (H_y)

$$(I.L.)_{I_o} = \frac{1}{F_5} \cdot \left(\frac{r}{r'}\right) \cdot \frac{jk + \frac{1}{r'} + \frac{1}{jkr'^2}}{jk + \frac{1}{r} + \frac{1}{jkr^2}} \qquad \text{(VI.3.10)}$$

where

$$F_5 = \frac{80}{\pi^2} \sum_{n=1,3,5,\ldots} \frac{e^{-\frac{n\pi d}{a}}}{n^2} \cdot \sinh\left(\frac{n\pi}{10}\right) \cdot \cosh\left(\frac{n\pi d'}{a}\right) \qquad \text{(VI.3.11)}$$

Figures 8 through 10 show plottings of the above insertion loss expressions in decibels (i.e., 20 log (I.L.)), together with some experimentally obtained values.

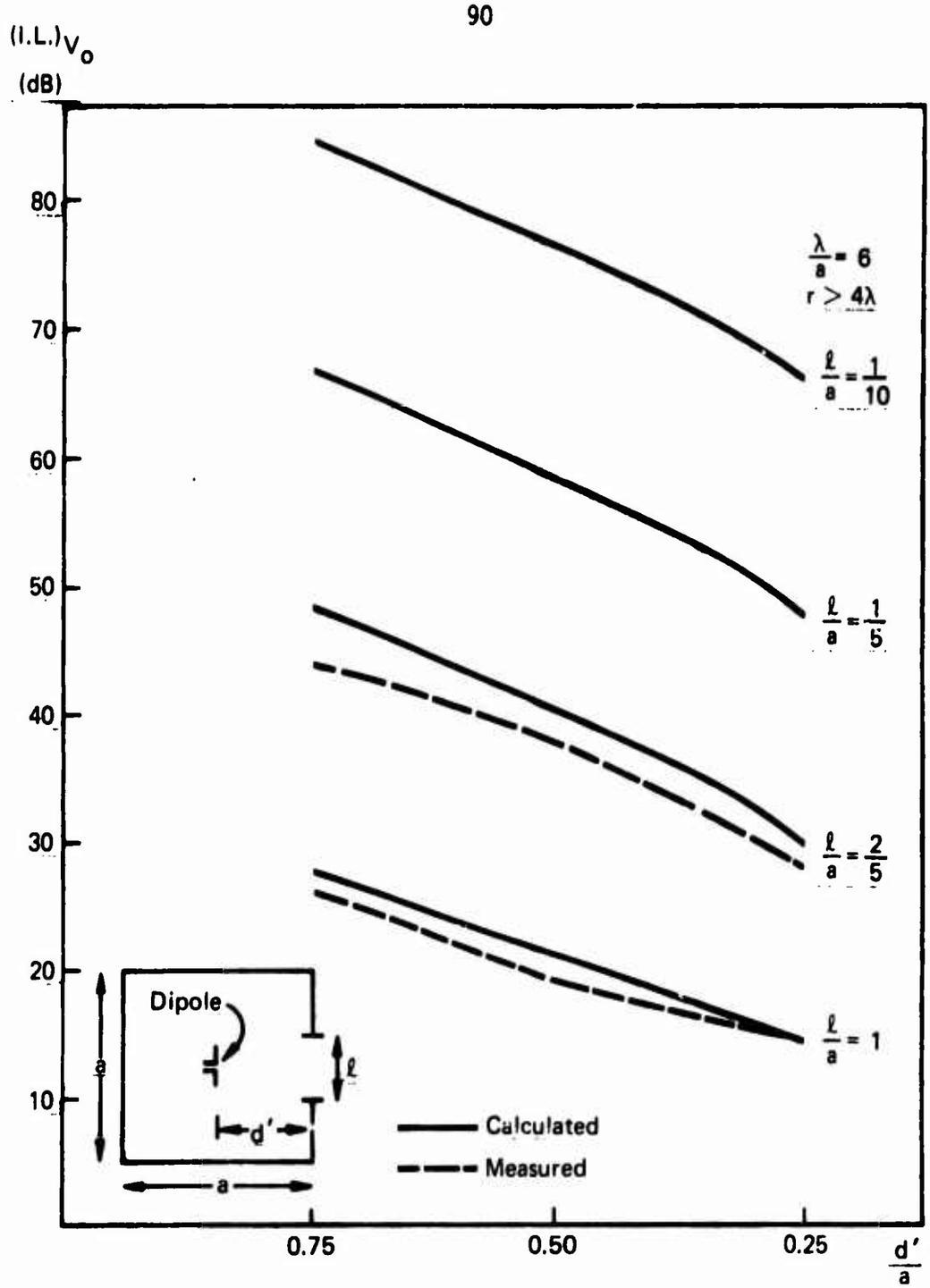

Figure 8
Insertion loss vs. antenna-aperture distance - - dipole antenna

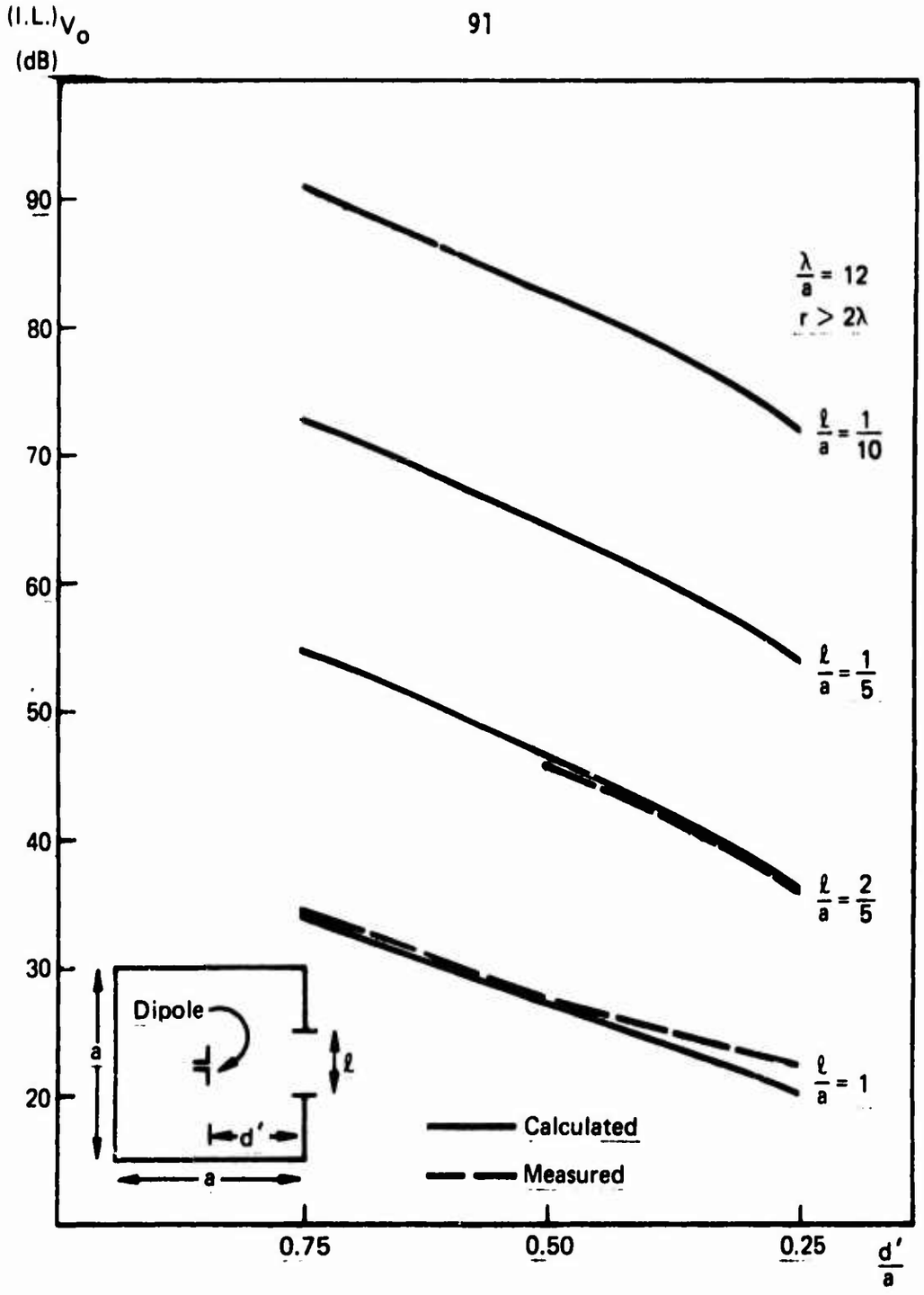

Figure 9
Insertion loss vs. antenna-aperture distance - - dipole antenna

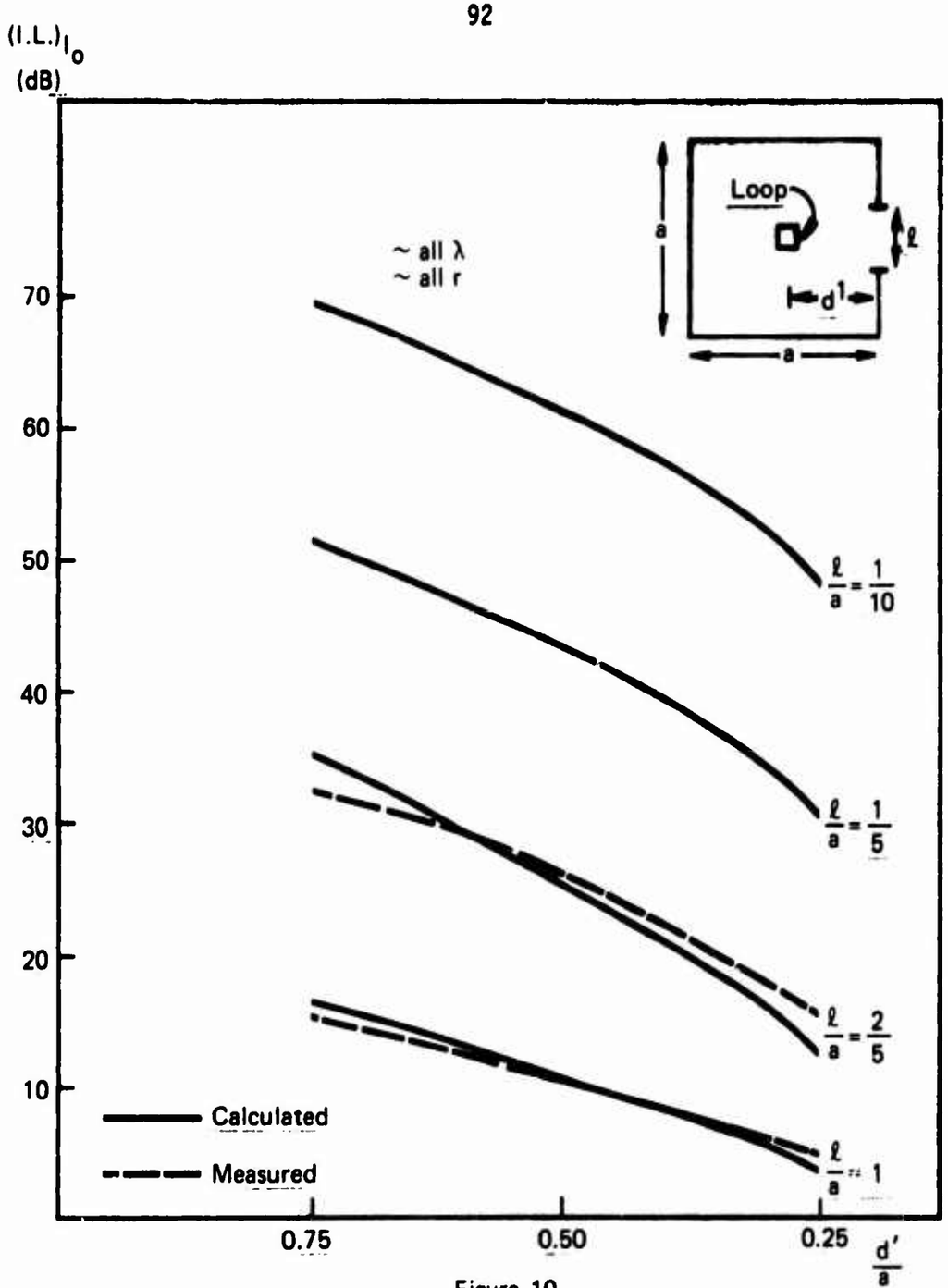

Figure 10
Insertion loss vs. antenna-aperture distance - - loop antenna

It is interesting to note that the results for a longitudinal loop antenna are independent of λ and r (except for the small effect of the difference between r and r'). On the other hand, the insertion loss of the shield for a transverse dipole antenna follows a λ^{-1} behavior in the radiation field ("far-field") and a r^{-1} behavior in the induction field ("near-field").

Also, we note that the input impedance of the dipole antenna is only slightly affected by the presence of the shield. This was to be expected for a relatively small dipole such as the one here used.

The curves in Figs. 8 through 10 were calculated by hand from Eqs. (VI.3.1) through (VI.3.11), which are themselves first-order approximations of the more exact expressions given in Chapter V. For more accurate results, it is advisable to use the latter and evaluate them with the help of a computer, extending the region of applicability up to frequencies slightly below the first resonance.

The curves corresponding to values of $\frac{\ell}{a} = \frac{1}{10}, \frac{1}{5}$, and $\frac{2}{5}$ were obtained using Bethe's method for small apertures. Those labeled $\frac{\ell}{a} = 1$ were calculated using the waveguide methods.

It should be noted that the experimental values were obtained using the upper half of the physical configurations shown in the figures, resting on a conducting plane which provided the other half by image theory. In this way, "free-space" results were simulated.

Due to equipment limitations, the measurements were restricted to insertion losses smaller than 50 dB.

Figure 11 shows schematically how the unshielded and shielded measurements were carried out.

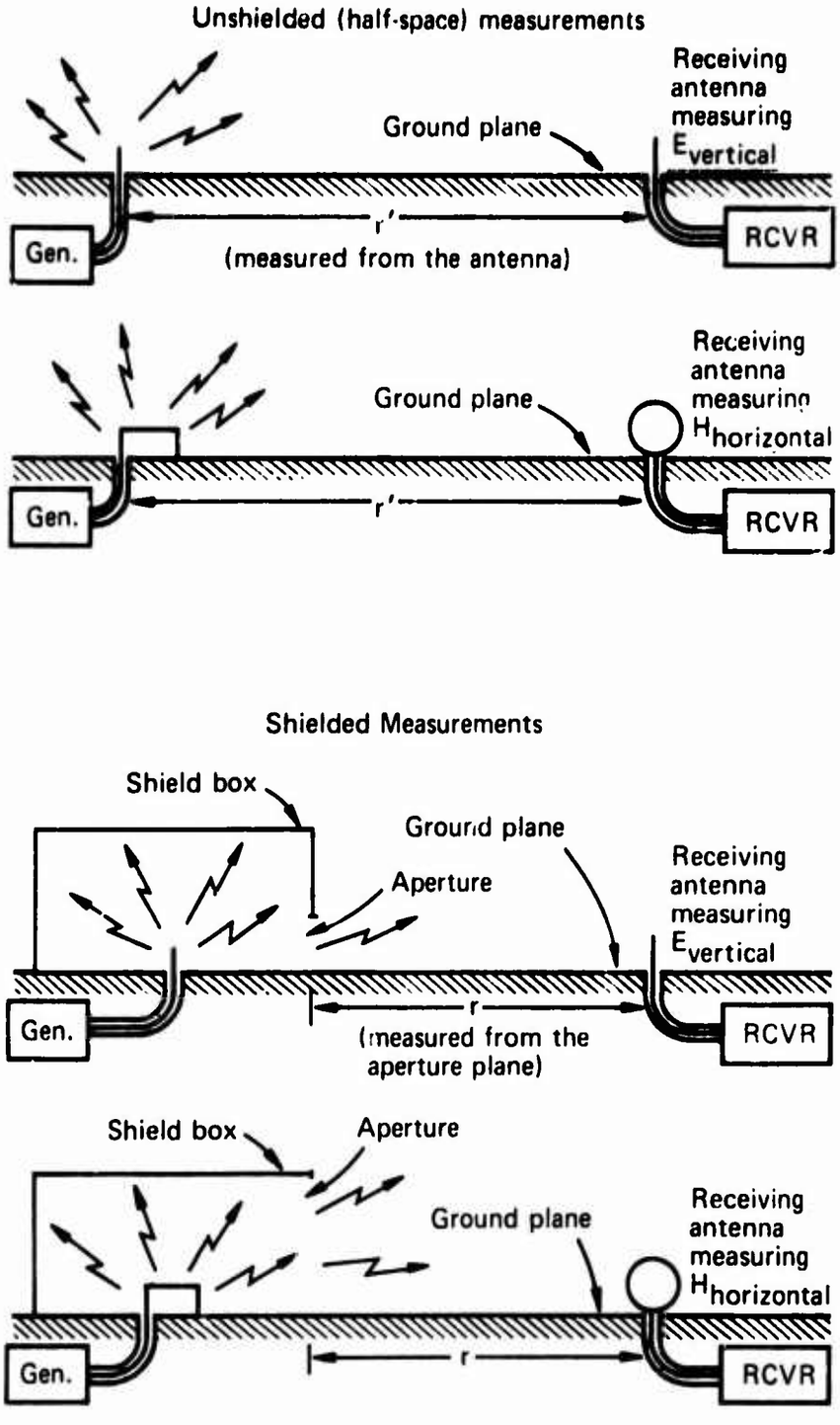
Unshielded (half-space) measurements
Receiving antenna measuring $E_{vertical}$
Ground plane
r'
(measured from the antenna)
Gen.
RCVR
Receiving antenna measuring $H_{horizontal}$
Ground plane
r'
Gen.
RCVR
Shielded Measurements
Shield box
Ground plane
Aperture
Receiving antenna measuring $E_{vertical}$
r
(measured from the aperture plane)
Gen.
RCVR
Shield box
Aperture
Ground plane
Receiving antenna measuring $H_{horizontal}$
r
Gen.
RCVR

Figure 11

Chapter 7

CONCLUSIONS AND RECOMMENDATIONS

The comparison between theory and experiment presented in the last chapter shows very good agreement. The differences are well within the range expected due to experimental errors and the approximations necessary to allow hand computation of the equations.

All the significant features of the analysis have been verified. A disagreement of a few dB's is normally considered negligible in shielding theory, where discrepancies of 50 to 100 dB's in predicted values are not uncommon[26].

We have thus provided a method for predicting, with considerable accuracy, the insertion loss or "attenuation" of a rectangular shielded enclosure with apertures, containing an internal radiating element, at frequencies below the first resonance of the enclosure. Although the detailed analysis was carried out for particularly simple sources - a dipole antenna and a square loop - the inclusion of the solutions for a current element (Hertzian dipole) allows us to solve the problem for an arbitrary current distribution.

Moreover, the results obtained for the chosen examples (selected because of their "worst-case" characteristics) constitute a very reliable indicator of the leakages to be expected from apertures in shields containing "high impedance" or "low impedance" sources (i.e., electric field sources such as dipole antennas,

or magnetic field sources such as current loops, where the electric or magnetic nature of the source is given by the type of field that predominates in the induction region). The insertion loss of shields containing high impedance sources behaves as $1/\lambda$ and is independent of distance in the radiation region, and shows a $1/r$ behavior in the induction region (where it is independent of the wavelength). For low impedance sources, the insertion loss of the shield is essentially independent of wavelength and distance.

Sources having geometries different from the straight center-fed dipole and the square loop here analyzed may be safely approximated by the equations of Chapter V if their dipole moments are known. A dipole, or square loop having the same dipole moment as the given source, and comparable linear dimensions and orientation, should provide a fairly accurate substitute for the real case.

Furthermore, we can expect that enclosures of somewhat different shape but of equal volumes will provide very similar shielding effects, as long as their three dimensions are of comparable magnitude (i.e., if no one dimension is too large or too small compared with the other two). Thus, our results for rectangular enclosures can be applied to other comparable shapes to obtain approximate values for their insertion loss. The critical parameter to be maintained constant is the source-aperture distance. Although the present work has been developed in terms of sources internal to the shield, the theorem of reciprocity[12,pp. 24-25] allows our results to be used for external sources as well. If the external noise source is located at more than a few wavelengths

from the shield, the field incident on the enclosure will have essentially the configuration of a plane wave. Our insertion loss equations provide us with a measure of the effect of the shield upon the "noise pick-up" by sensitive circuits (having high or low impedance, as the case may be) located in its interior, when there are apertures present in the enclosure.

The applicability of the theorem of reciprocity to the insertion loss of shielded enclosures is theoretically and experimentally well established[27]. However, it should be stressed that only the roles of receiving and transmitting equipment should be interchanged for the successful application of the theorem.

A study of the insertion loss equations here developed should provide enough information to achieve optimum shielding performance for a given piece of equipment and its metallic enclosure. The location of "noisy" (or sensitive) circuits with respect to the shield apertures, the physical layout of those circuits, the choice of currents and impedances, the size, shape and location of the required apertures, etc., can all be optimized by analyzing their influence on the insertion loss expressions.

Our analysis may be easily paralleled for geometries other than rectangular, and it should be a straightforward procedure in the case of those regular geometries for which the Green functions are already available.

All of the above considerations indicate that the present

work will represent a valuable tool for EMC* engineers and to all others interested in electromagnetic shields. The accurate prediction of insertion loss (or shield attenuation) for equipment enclosures should be very useful for the electronic industry.

Much theoretical and experimental work can be done to complement this research. Some suggestions that readily come to mind are:

- Effect of low-conductivity material covering the apertures (e.g. conducting glass).

- Analysis of seam apertures formed by doors and covers.

- Description (possibly statistical) of the general electromagnetic field inside a metallic enclosure containing a large number of radiating sources (subsystems, cables, etc.).

- Development of nomograms to solve our expressions in some typical circumstances.

- Include the effect of the finite conductivity of the enclosure material to ascertain the conditions under which the leakage through the aperture ceases to be dominant.

- Critical review of current techniques for shielding effectiveness measurements, in the light of the present work.

---

*Electromagnetic compatibility

Appendix A

BEHAVIOR OF THE FIELDS IN A SEMI-INFINITE WAVEGUIDE

From the treatment of semi-infinite waveguides excited by internal sources at frequencies below cutoff (Chapter III, Section 2), we see that the fields decay, in the z-direction, at least as fast as

$$\sum_{m,n} e^{-\Gamma_{mn} z} \sinh(\Gamma_{mn} d') \tag{A.1}$$

for $z > d'$ ($z=d'$ is the plane of the source). Let $z = d$ be the plane at which we will cut open the waveguide (i.e., $z = d$ will be the plane of the aperture).

The ratio of the field at $z = d$ to that at $z = d' + \rho$ is then

$$\frac{\sum_{m,n} e^{-\Gamma_{mn} d} \sinh(\Gamma_{mn} d')}{\sum_{m,n} e^{-\Gamma_{mn}(d' + \rho)} \sinh(\Gamma_{mn} d')} =$$

$$\frac{\sum_{m,n} \left[e^{-\Gamma_{mn}(d-d')} - e^{-\Gamma_{mn}(d+d')} \right]}{\sum_{m,n} \left[e^{-\Gamma_{mn}\rho} - e^{-\Gamma_{mn}(2d'+\rho)} \right]} \tag{A.2}$$

Thus, it is necessary to evaluate a double summation of the form

$$S = \sum_{\substack{m=0,1,2... \\ n=0,1,2...}} e^{-z\sqrt{\left(\frac{m\pi}{a}\right)^2 + \left(\frac{n\pi}{b}\right)^2}} \tag{A.3}$$

where we have assumed

$$k << \frac{\pi}{a}, \frac{\pi}{b} \tag{A.4}$$

and m and n are not both zero simultaneously.

For computational ease, let us set

$$a = b \tag{A.5}$$

Hence,

$$S = \sum_{m,n} e^{-\frac{z\pi}{a}\sqrt{m^2 + n^2}} \tag{A.6}$$

This double summation, although convergent, cannot be evaluated in closed form. Nevertheless, an approximation can be found by considering the m,n space of Fig. A.1. Each one of the grid crossings is at a distance

$$r = \sqrt{m^2 + n^2} \tag{A.7}$$

from the origin.

For m and n sufficiently large, the total number of crossings (modes) up to a radius R is given to a good degree of approximation by

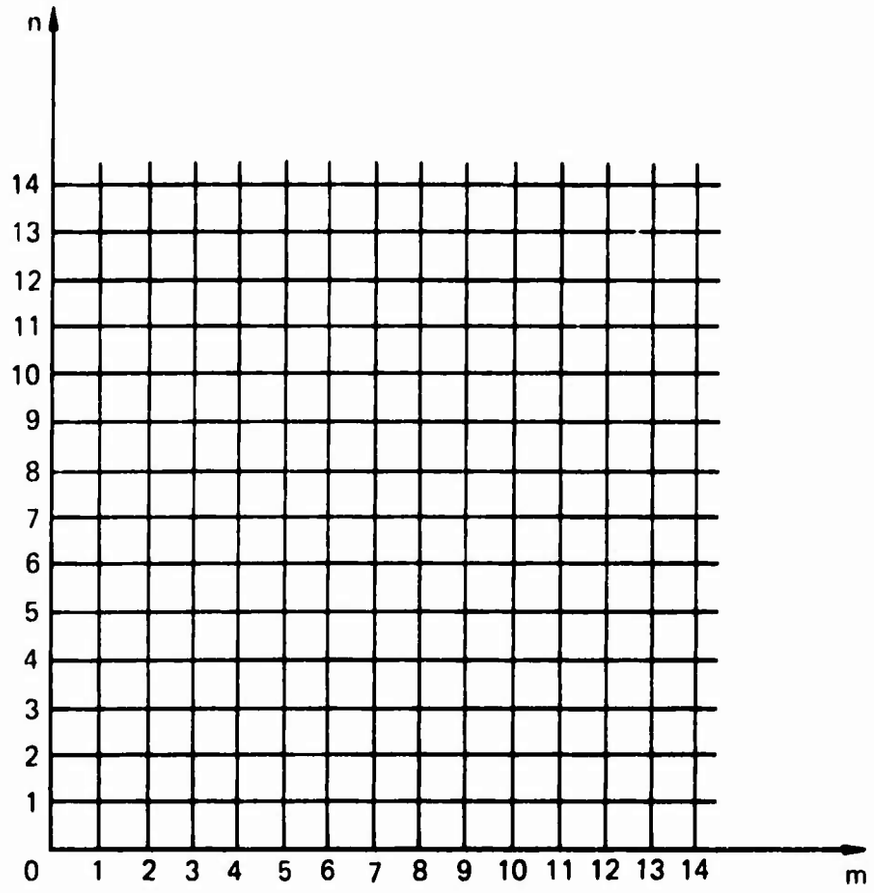

Figure A.1

$$q = \frac{1}{4}\,\pi\,R^2 = \frac{\pi}{4}\left(m^2 + n^2\right) \tag{A.8}$$

Thus, in our summation (A.6), we can replace $\sqrt{m^2 + n^2}$ by $2\sqrt{\frac{q}{\pi}}$ where q = 0,1,2,...

$$S \cong \sum_{q=0}^{\infty} e^{-2\sqrt{\pi}\ \frac{z}{a}\sqrt{q}} \tag{A.9}$$

To evaluate this series, we shall use a graphical comparison between the summation and the integral of the function, i.e.,

$$\sum_{q=0}^{\infty} e^{-K\sqrt{q}} \tag{A.10}$$

and

$$\int_{o}^{\infty} e^{-K\sqrt{q}}\, dq \tag{A.11}$$

From Fig. A.2 we see that the difference between the summation and the integral is the solid shaded area. The approximate value of this area A may be obtained from

$$\begin{aligned} A \cong\ & \frac{1}{2}\left[f(o)-f(1)\right] + \frac{1}{2}\left[f(1)-f(2)\right] + \ldots \\ & \ldots + \left[f(q)-f(q+1)\right] + \ldots \\ =\ & \frac{1}{2}\,f(o) + \frac{1}{2}\left[f(1)-f(1)\right] + \frac{1}{2}\left[f(2)-f(2)\right] + \ldots \\ & \ldots + \frac{1}{2}\left[f(q)-f(q)\right] + \ldots \end{aligned} \tag{A.12}$$

and since

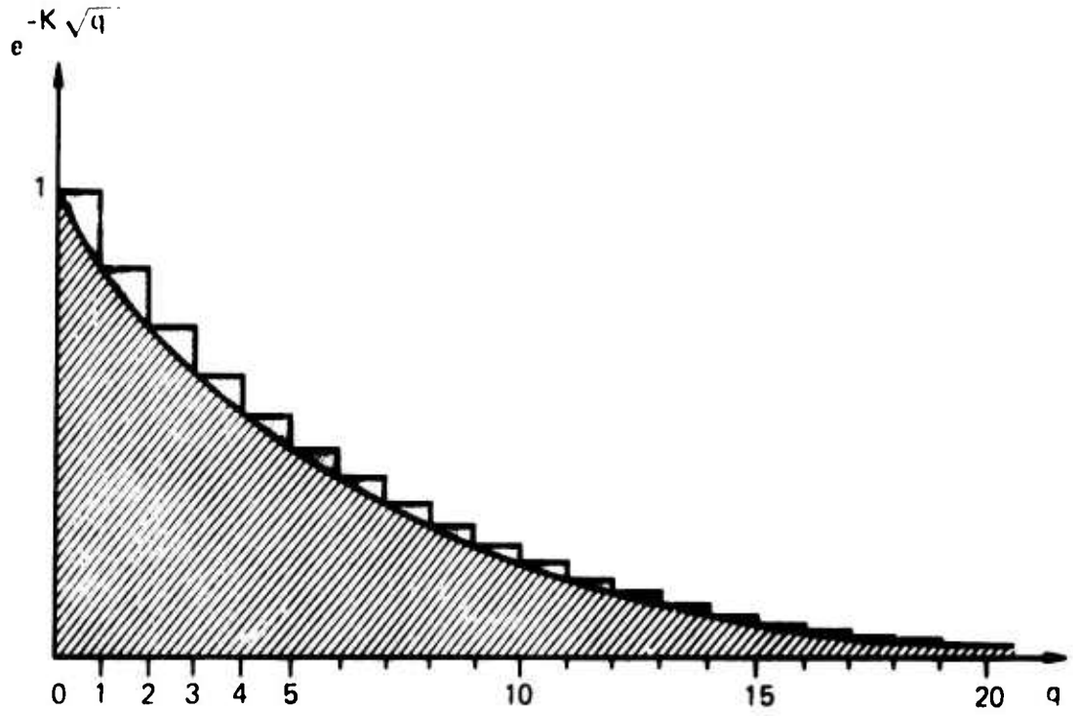

Figure A.2

$$f(q) = e^{-K\sqrt{q}} \longrightarrow 0 \text{ as } q \to \infty \qquad (A.13)$$

we have

$$A \cong \frac{1}{2} f(o) \qquad (A.14)$$

This can also be seen from Fig. A.3, where the area representing the summation has been shifted to the left by a half unit. Except for the solid shaded portion, the area overshoots and undershoots approximately cancel each other. The solid shaded area is clearly given by Eq. (A.14). Therefore

$$\sum_{q=0}^{\infty} e^{-2\sqrt{\pi}\,\frac{z}{a}\sqrt{q}} \cong \frac{1}{2} + \int_{o}^{\infty} e^{-2\sqrt{\pi}\,\frac{z}{a}\sqrt{q}}\, dq$$

$$= \frac{1}{2}\left(\frac{a^2}{\pi z^2} + 1\right) \qquad (A.15)$$

and we can write

$$S \cong \frac{1}{2}\left(\frac{a^2}{\pi z^2} + 1\right) \qquad (A.16)$$

Let us now evaluate

$$S(d-d') = \sum_{m,n} e^{-\Gamma_{mn}(d-d')} \qquad (A.17)$$

for $(d-d') = a, \frac{a}{\pi}$ and $\frac{a}{10}$ i.e., $z = a, \frac{a}{\pi}$ and $\frac{a}{10}$ in Eq. (A.16)

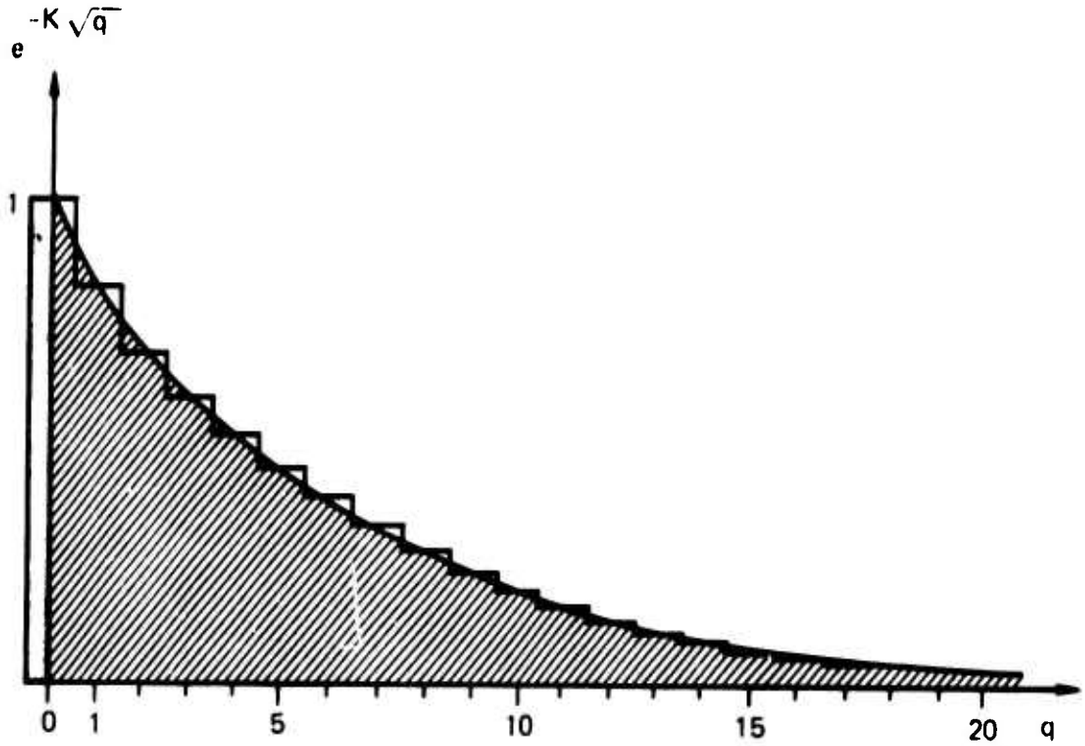

Figure A.3

$$S(a) = 0.659 \tag{A.18}$$

$$S(\frac{a}{\pi}) = 2.07 \tag{A.19}$$

$$S(\frac{a}{10}) = 16.4 \tag{A.20}$$

On the other hand, the radius of the antenna (wire radius) is of the order of $\frac{a}{100}$ or less, so that the relative magnitude of the field next to the antenna is approximately

$$S(\frac{a}{100}) = 1590 \tag{A.21}$$

What this means is that if the semi-infinite waveguide is cut (terminated into space) at a distance $(d-d') = \frac{a}{10}$ from the source, the magnitude of the fields at the plane of the cut is down by approximately two orders of magnitude from that next to the antenna.

Any reflections from the open end will be further attenuated by another factor of 100 before reaching the antenna.

Hence, we can say that the antenna "does not see" the aperture.

Appendix B

RADIATION FROM SMALL ANTENNAS

A.1 Antennas in Free Space

A.1.1 Dipole Antenna (See Fig. B.1)

A short, thin, center-fed dipole antenna of length

$$2h << \lambda$$

and having a current I_o at its terminals, has essentially a triangular current distribution, and may be represented by a Hertzian dipole (current element) of the same length and constant current $I_o/2$.

Thus the phasor expressions for the fields from such an antenna are given, in spherical coordinates, by [18, pp. 322-323]

$$E_r = \frac{I_o h}{4\pi r}\sqrt{\frac{\mu_o}{\epsilon_o}}\left(\frac{2}{r}+\frac{2}{jkr^2}\right)\cos\theta\cdot e^{-jkr} \qquad (B.1)$$

$$E_\theta = \frac{I_o h}{4\pi r}\sqrt{\frac{\mu_o}{\epsilon_o}}\left(jk+\frac{1}{r}+\frac{1}{jkr^2}\right)\sin\theta\cdot e^{-jkr} \qquad (B.2)$$

$$H_\phi = \frac{I_o h}{4\pi r}\left(jk+\frac{1}{r}\right)\sin\theta\cdot e^{-jkr} \qquad (B.3)$$

where θ is the angle between the direction of the dipole and the radius vector to the field point (r,θ,ϕ). The dipole antenna is at the center of the coordinate system.

A.1.2 Loop Antenna (See Fig. B.2)

Consider a loop antenna, whose dimensions are small compared

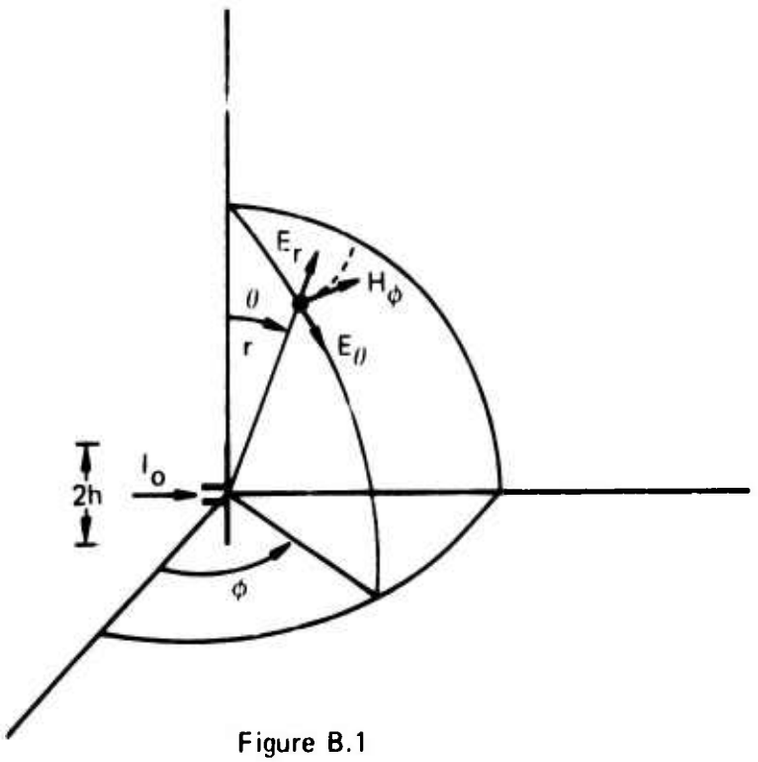

Figure B.1

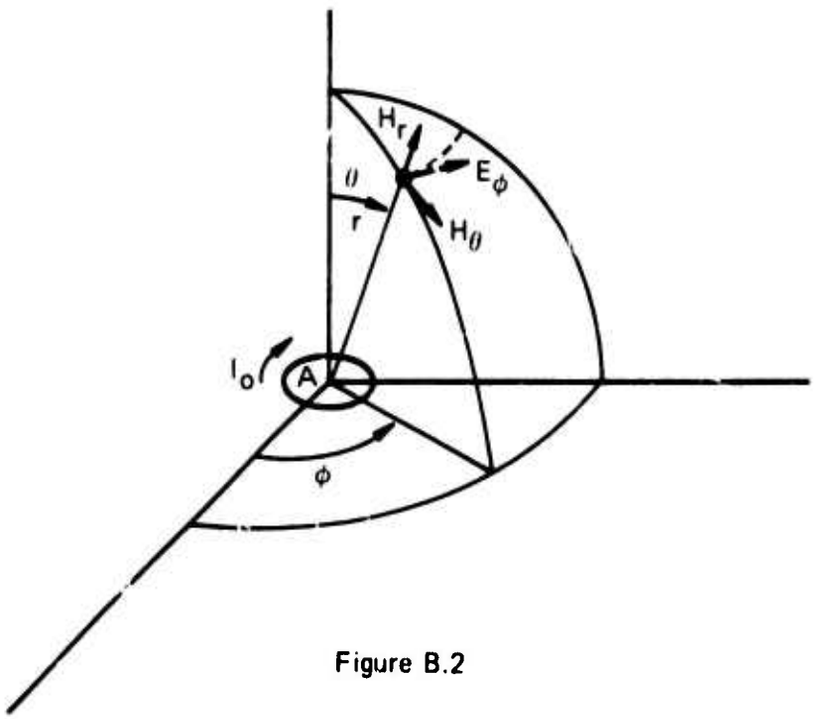

Figure B.2

to the wavelength, having a constant current I_o and enclosing an area A. The radiated field is given by [12, p.37]

$$H_r = j \frac{I_o A k}{4\pi r} \left(\frac{2}{r} + \frac{2}{jkr^2} \right) \cos\theta \cdot e^{-jkr} \tag{B.4}$$

$$H_\theta = j \frac{I_o A k}{4\pi r} \left(jk + \frac{1}{r} + \frac{1}{jkr^2} \right) \sin\theta \cdot e^{-jkr} \tag{B.5}$$

$$E = -j \frac{I_o A k}{4\pi r} \sqrt{\frac{\mu_o}{\varepsilon_o}} \left(jk + \frac{1}{r} \right) \sin\theta \cdot e^{-jkr} \tag{B.6}$$

B.2 Antennas Over a Perfectly Conducting Plane

The electromagnetic fields from small dipoles and loops located over a perfectly conducting plane can best be obtained by describing the radiation in terms of the Hertz vectors. Using Collin and Zucker's[19] treatment and letting the conductivity of the ground plane approach infinity, we obtain the following field expressions (see Fig. B.3) where cylindrical coordinates are used for convenience.

B.2.1 Vertical (z-directed) Electric Dipole

$$E_\rho = \frac{I_o h \rho}{4\pi} \sqrt{\frac{\mu_o}{\varepsilon_o}} \left[\frac{(z-z_o)}{R^3} \left(jk + \frac{3}{R} + \frac{3}{jkR^2} \right) e^{-jkR} + \right.$$

$$\left. + \frac{(z+z_o)}{R'^3} \left(jk + \frac{3}{R'} + \frac{3}{jkR'^2} \right) e^{-jkR'} \right] \tag{B.7}$$

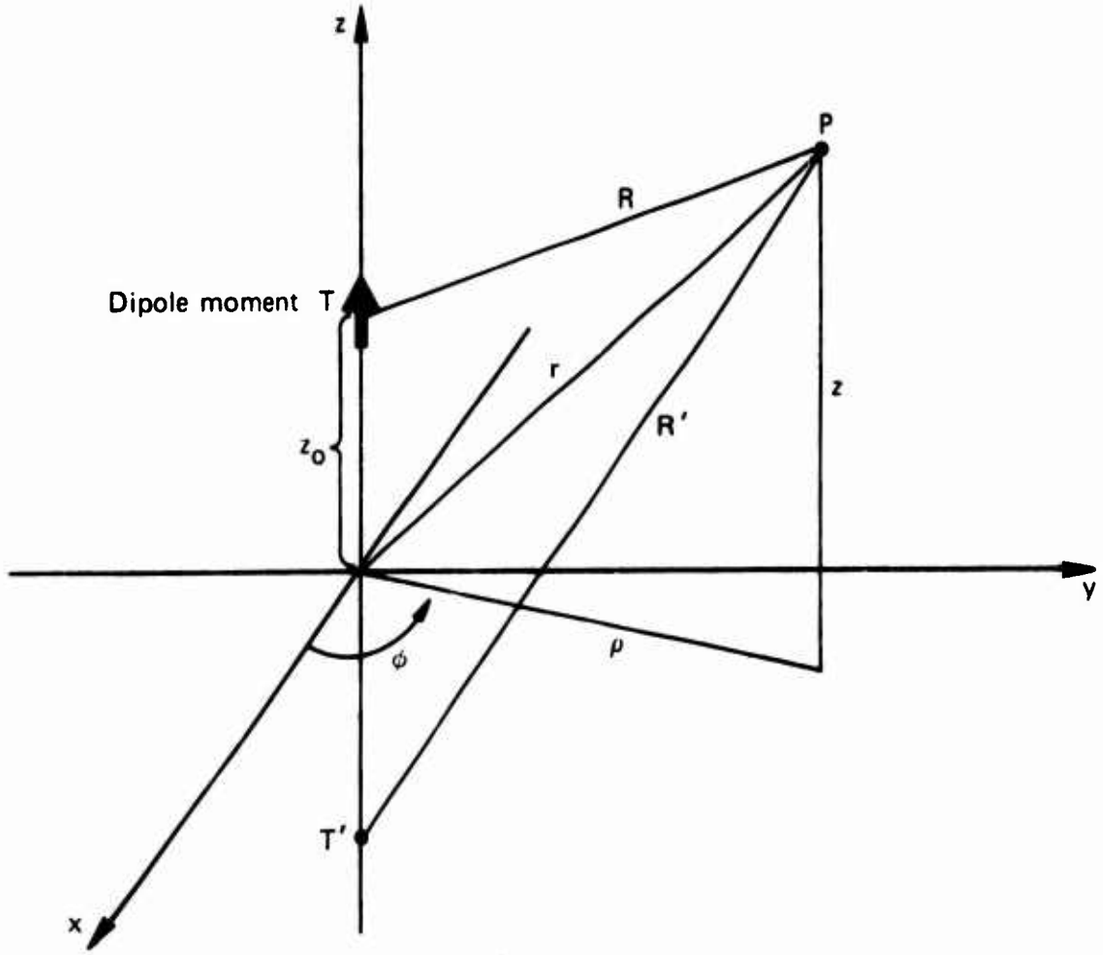

Figure B.3
Elementary dipole over a
perfectly conducting plane (the x,y plane)

$$E_z = \frac{I_o h}{4\pi}\sqrt{\frac{\mu_o}{\varepsilon_o}}\left\{\left[-\frac{1}{R}+\frac{(z-z_o)^2}{R^3}\right]\left(jk+\frac{1}{R}+\frac{1}{jkR^2}\right)e^{-jkR}+\right.$$

$$\left.+\left[-\frac{1}{R'}+\frac{(z+z_o)^2}{R'^3}\right]\left(jk+\frac{1}{R'}+\frac{1}{jkR'^2}\right)e^{-jkR'}\right\} \qquad (B.8)$$

$$H_\phi = \frac{I_o h\rho}{4\pi}\left[\frac{1}{R^2}\left(jk+\frac{1}{R}\right)e^{-jkR}+\right.$$

$$\left.+\frac{1}{R'^2}\left(jk+\frac{1}{R'}\right)e^{-jkR'}\right] \qquad (B.9)$$

$$E_\phi = H_\rho = H_z = 0$$

B.2.2 Horizontal (x-directed) Electric Dipole

$$E_\rho = \frac{I_o h\cos\phi}{4\pi}\sqrt{\frac{\mu_o}{\varepsilon_o}}\left\{\left[\frac{\rho^2}{R^2}\left(jk+\frac{3}{R}+\frac{3}{jkR^2}\right)-\right.\right.$$

$$\left.-\left(jk+\frac{1}{R}+\frac{1}{jkR^2}\right)\right]\cdot\frac{e^{-jkR}}{R}-$$

$$-\left[\frac{\rho^2}{R'^2}\left(jk+\frac{3}{R'}+\frac{3}{jkR'^2}\right)-\right.$$

$$\left.\left.-\left(jk+\frac{1}{R'}+\frac{1}{jkR'^2}\right)\right]\cdot\frac{e^{-jkR'}}{R'}\right\} \qquad (B.10)$$

$$E_\phi = \frac{I_o h \sin\phi}{4\pi}\sqrt{\frac{\mu_o}{\varepsilon_o}}\left[\left(jk + \frac{1}{R} + \frac{1}{jkR^2}\right)\cdot\frac{e^{-jkR}}{R} - \left(jk + \frac{1}{R'} + \frac{1}{R'^2}\right)\frac{e^{-jkR'}}{R'}\right] \tag{B.11}$$

$$E_z = \frac{I_o h\,\rho\cos\phi}{4\pi}\sqrt{\frac{\mu_o}{\varepsilon_o}}\left[\frac{(z-z_o)}{R^3}\left(jk + \frac{3}{R} + \frac{3}{jkR^2}\right)e^{-jkR} - \frac{(z+z_o)}{R'^3}\left(jk + \frac{3}{R'} + \frac{3}{jkR'^2}\right)e^{-jkR'}\right] \tag{B.12}$$

$$H_\rho = \frac{I_o h \sin\phi}{4\pi}\left[\frac{(z-z_o)}{R^2}\left(jk + \frac{1}{R}\right)e^{-jkR} - \frac{(z+z_o)}{R'^2}\left(jk + \frac{1}{R'}\right)e^{-jkR'}\right] \tag{B.13}$$

$$H_\phi = -\frac{I_o h\cos\phi}{4\pi}\left[\frac{(z-z_o)}{R^2}\left(jk + \frac{1}{R}\right)e^{-jkR} - \frac{(z+z_o)}{R'^2}\left(jk + \frac{1}{R'}\right)e^{-jkR'}\right] \tag{B.14}$$

$$H_z = -j\frac{I_o hk\,\rho\sin\phi}{4\pi}\left[\left(jk + \frac{1}{R} + \frac{1}{jkR^2}\right)\frac{e^{-jkR}}{R} - \left(jk + \frac{1}{R'} + \frac{1}{jkR'^2}\right)\frac{e^{-jkR'}}{R'}\right] \tag{B.15}$$

B.2.3 Vertical (z-directed) Magnetic Dipole

$$H_\rho = j \frac{I_o A k \rho}{4\pi} \left[\frac{(z-z_o)}{R^3} \left(jk + \frac{3}{R} + \frac{3}{jkR^2} \right) e^{-jkR} - \right.$$

$$\left. - \frac{(z+z_o)}{R'^3} \left(jk + \frac{3}{R'} + \frac{3}{jkR'^2} \right) e^{-jkR'} \right] \qquad (B.16)$$

$$H_z = j \frac{I_o A k}{4\pi} \left\{ \left[- \frac{1}{R} + \frac{(z-z_o)^2}{R^3} \right] \left(jk + \frac{1}{R} + \frac{1}{jkR^2} \right) e^{-jkR} - \right.$$

$$\left. - \left[- \frac{1}{R'} + \frac{(z+z_o)^2}{R'^3} \right] \left(jk + \frac{1}{R'} + \frac{1}{jkR'^2} \right) e^{-jkR'} \right\} \qquad (B.17)$$

$$E_\phi = - j \frac{I_o A k \rho}{4\pi} \sqrt{\frac{\mu_o}{\varepsilon_o}} \left[\frac{1}{R^2} \left(jk + \frac{1}{R} \right) e^{-jkR} - \right.$$

$$\left. - \frac{1}{R'^2} \left(jk + \frac{1}{R'} \right) e^{-jkR'} \right] \qquad (B.18)$$

$$H_\phi = E_\rho = E_z = 0$$

B.2.4 Horizontal (x-directed) Magnetic Dipole

$$H_\rho = j \frac{I_o A k \cos\phi}{4\pi} \left\{ \left[\frac{\rho^2}{R^2} \left(jk + \frac{3}{R} + \frac{3}{jkR^2} \right) - \left(jk + \frac{1}{R} + \frac{1}{jkR^2} \right) \right] \frac{e^{-jkR}}{R} + \left[\frac{\rho^2}{R'^2} \left(jk + \frac{3}{R'} + \frac{3}{jkR'^2} \right) - \left(jk + \frac{1}{R'} + \frac{1}{jkR'^2} \right) \right] \frac{e^{-jkR'}}{R'} \right\} \quad (B.19)$$

$$H_\phi = j \frac{I_o A k \sin\phi}{4\pi} \left[\left(jk + \frac{1}{R} + \frac{1}{jkR^2} \right) \frac{e^{-jkR}}{R} + \left(jk + \frac{1}{R'} + \frac{1}{jkR'^2} \right) \frac{e^{-jkR'}}{R'} \right] \quad (B.20)$$

$$H_z = j \frac{I_o A k \rho \cos\phi}{4\pi} \left[\frac{(z-z_o)}{R^3} \left(jk + \frac{3}{R} + \frac{3}{jkR^2} \right) e^{-jkR} + \frac{(z+z_o)}{R'^3} \left(jk + \frac{3}{R'} + \frac{3}{jkR'^2} \right) e^{-jkR'} \right] \quad (B.21)$$

$$E_\rho = j \frac{I_o Ak \sin\phi}{4\pi} \sqrt{\frac{\mu_o}{\varepsilon_o}} \left[\frac{(z-z_o)}{R^2} \left(jk + \frac{1}{R} \right) e^{-jkR} + \right.$$

$$\left. + \frac{(z+z_o)}{R'^2} \left(jk + \frac{1}{R'} \right) e^{-jkR'} \right] \qquad (B.22)$$

$$E_\phi = j \frac{I_o Ak \cos\phi}{4\pi} \sqrt{\frac{\mu_o}{\varepsilon_o}} \left[\frac{(z-z_o)}{R^2} \left(jk + \frac{1}{R} \right) e^{-jkR} + \right.$$

$$\left. + \frac{(z+z_o)}{R'^2} \left(jk + \frac{1}{R'} \right) e^{-jkR'} \right] \qquad (B.23)$$

$$E_z = - \frac{I_o Ak^2 \rho \sin\phi}{4\pi} \sqrt{\frac{\mu_o}{\varepsilon_o}} \left[\left(jk + \frac{1}{R} + \frac{1}{jkR^2} \right) \frac{e^{-jkR}}{R} + \right.$$

$$\left. + \left(jk + \frac{1}{R'} + \frac{1}{jkR'^2} \right) \frac{e^{-jkR'}}{R'} \right] \qquad (B.24)$$

In the above equations, we are assuming that the electric dipole consists of a current element of length 2h and current $I_o/2$, and the magnetic dipole is a small loop of area A and current I_o.

Appendix C

SELF-IMPEDANCE OF SMALL ANTENNAS

C.1 Antennas in Free Space

C.1.1 Dipole Antenna

The self-impedance of a small dipole of length

$$2h << \lambda$$

and of wire radius ρ is approximately given by[20]

$$Z_i' = 20 \frac{\ln\left(\frac{h}{\rho}\right) - 1}{\ln\left(\frac{h}{\rho}\right) - 0.81} k^2h^2 - j \frac{120}{kh} \left[\ln \frac{h}{\rho} - 1\right] \text{ ohms} \quad (C.1)$$

C.1.2 Loop Antenna

The leading terms in the driving-point impedance of a small loop of area A and wire radius ρ are[20]

$$Z_i' = 20\, k^4A^2 + j\, 120 \sqrt{\pi}\, k \sqrt{A} \left[\ln \frac{\sqrt{A}}{\rho} - \frac{1}{2}\right] \text{ ohms} \quad (C.2)$$

In expressions (C.1) and (c.2), the resistance of the wire has been neglected.

C.2 Antennas Over a Perfectly Conducting Plane

Using the procedure indicated by Collin and Zucker[19, p. 392 ff.], we have obtained the self-impedance of elementary dipoles over a conducting plane. The electric dipole is taken as a current element of length 2h, and the magnetic dipole as a small loop enclosing an area A.

In both cases, the radius of the wire is ρ.

In the following equations,

$$\alpha = 2 z_o \tag{C.3}$$

where z_o is the height of the dipole over the conducting plane (Fig. B.3, Appendix B).

C.2.1 Vertical Electric Dipole

$$Z'_i = 40(kh)^2 - j \frac{60}{kh} \left\{ 2 \ln\left(\frac{h}{\rho}\right) - 2 - \frac{h^3}{\alpha^3}\left[1 + \frac{k\alpha^2}{2}\right] \right\} \text{ ohms} \tag{C.4}$$

C.2.2 Horizontal Electric Dipole

$$Z'_i = \frac{15}{4}(kh)^2(k\alpha)^2 - j \frac{60}{kh} \left\{ 2 \ln\left(\frac{h}{\rho}\right) - 2 - \frac{h^3}{2\alpha^3}\left[1 - \frac{(k\alpha)^2}{2}\right] \right\} \text{ ohms} \tag{C.5}$$

C.2.3 Vertical Magnetic Dipole

$$Z'_i = 2(kA)^2(k\alpha)^2 + j\, 120\sqrt{\pi}\, k\sqrt{A} \left\{ \ln\left(\frac{\sqrt{A}}{\rho}\right) - \right.$$

$$\left. - \frac{1}{2} - \frac{1}{2\sqrt{\pi}} \left(\frac{\sqrt{A}}{\alpha}\right)^3 \left[1 + \frac{(k\alpha)^2}{2}\right] \right\} \text{ ohms} \tag{C.6}$$

C.2.4 Horizontal Magnetic Dipole

$$Z'_1 = 40\, k^4 A^2 + j\, 120\, \sqrt{\Pi}\, k\, \sqrt{A} \left\{ \ln \frac{\sqrt{A}}{\rho} - \right.$$

$$\left. - \frac{1}{2} - \frac{1}{2\sqrt{\Pi}} \left(\frac{\sqrt{A}}{\alpha}\right)^3 \left[1 - \frac{(k\alpha)^2}{2}\right] \right\} \text{ ohms} \qquad (C.7)$$

The resistance of the wire has been neglected in all of the above expressions.

Appendix D

RADIATION FROM DIPOLE MOMENTS

The electromagnetic field produced by an electric dipole moment $\vec{P}$ has components[21]

$$E_r = j \frac{k}{4\pi\epsilon_0 r} \left(\frac{2}{r} + \frac{2}{jkr^2} \right) |\vec{P}| \cos\theta \cdot e^{-jkr} \tag{D.1}$$

$$E_\theta = j \frac{k}{4\pi\epsilon_0 r} \left(jk + \frac{1}{r} + \frac{1}{jkr^2} \right) |\vec{P}| \sin\theta \cdot e^{-jkr} \tag{D.2}$$

$$H_\phi = j \frac{kc}{4\pi r} \left(jk + \frac{1}{r} \right) |\vec{P}| \sin\theta \cdot e^{-jkr} \tag{D.3}$$

and that produced by a magnetic dipole moment $\vec{M}$ is[21, p.437]

$$H_r = j \frac{k}{4\pi r} \left(\frac{2}{r} + \frac{2}{jkr^2} \right) |\vec{M}| \cos\theta \cdot e^{-jkr} \tag{D.4}$$

$$H_\theta = j \frac{k}{4\pi r} \left(jk + \frac{1}{r} + \frac{1}{jkr^2} \right) |\vec{M}| \sin\theta \cdot e^{-jkr} \tag{D.5}$$

$$E_\phi = -j \frac{k}{4\pi r} \sqrt{\frac{\mu_0}{\epsilon_0}} \left(jk + \frac{1}{r} \right) |\vec{M}| \sin\theta \cdot e^{-jkr} \tag{D.6}$$

All of the above are phasor expressions. The time-dependence has been taken, in the usual engineering fashion, as $e^{j\omega t}$.

The angle θ is that between the direction of the dipole moment and the radius vector to the field point.

For dipole moments over a perfectly conducting plane, we can use Eqs. (B.7) through (B.24) of Appendix B if we write

$$\frac{I_o h \sqrt{\mu_o \varepsilon_o}}{jk} \equiv |\vec{P}| \tag{D.7}$$

for electric dipoles, and

$$I_o \Lambda \equiv |\vec{M}| \tag{D.8}$$

for magnetic dipoles

Appendix E

EVALUATION OF A SERIES

In Eq. (VI.1.11) for the input impedance of a dipole in a cavity, the last summation is

$$S = \sum_{\substack{m=2,4,6\ldots \\ n=1,3,5\ldots}} 2\left(\frac{a}{m\pi}\right)^2 \left[\cos(kh) - \cos\frac{m\pi h}{a}\right]^2 \cdot$$

$$\cdot \frac{e^{-\Gamma_{mn}(d'+\rho)}}{\Gamma_{mn}} \cdot \sinh(\Gamma_{mn} d') \qquad (E.1)$$

If d' is not too small, e.g.

$$\frac{d'}{b} > 0.1$$

and

$$k << \frac{\pi}{a}, \frac{\pi}{b}$$

Eq. (E.1) becomes

$$S = \sum_{\substack{m=2,4,6\ldots \\ n=1,3,5\ldots}} \left(\frac{a}{m\pi}\right)^2 \left[\cos(kh) - \cos\frac{m\pi h}{a}\right]^2 \cdot$$

$$\cdot \frac{e^{-\frac{\pi\rho}{b}\sqrt{n^2 + m^2\left(\frac{b}{a}\right)^2}}}{\frac{\pi}{b}\sqrt{n^2 + m^2\left(\frac{b}{a}\right)^2}} \qquad (E.2)$$

We wish to evaluate the summation over n, which although convergent, decreases very slowly with n due to the fact that

$$\frac{\rho}{b} << 1$$

Let

$$\sigma_n = \sum_{n=1,3,5\ldots} \frac{e^{-\frac{\pi\rho}{b}\sqrt{n^2+\alpha^2}}}{\frac{\pi}{b}\sqrt{n^2+\alpha^2}} \qquad (E.3)$$

where we have put

$$m^2\left(\frac{b}{a}\right)^2 = \alpha^2 \qquad (E.4)$$

Investigating the function of n and its derivatives, we determine that Euler's summation formula[23] is applicable and that we may keep only the first two terms

$$\sigma_n = \frac{b}{\pi}\left[\frac{1}{2}\cdot\frac{e^{-\frac{\pi\rho}{b}\sqrt{1+\alpha^2}}}{\sqrt{1+\alpha^2}} + \int_0^\infty \frac{e^{-\frac{\pi\rho}{b}\sqrt{(2x+1)^2+\alpha^2}}}{\sqrt{(2x+1)^2+\alpha^2}}\,dx\right] \qquad (E.5)$$

Evaluating the integral

$$I = \int_0^\infty \frac{e^{-\frac{\pi\rho}{b}\sqrt{(2x+1)^2+\alpha^2}}}{\sqrt{(2x+1)^2+\alpha^2}}\cdot dx =$$

$$= \frac{1}{2}\int_1^\infty \frac{e^{-\frac{\pi\rho}{b}\sqrt{\omega^2+\alpha^2}}}{\sqrt{\omega^2+\alpha^2}}\,d\omega$$

$$= \frac{1}{2} \int_0^{\infty} \frac{e^{-\frac{\Pi\rho}{b}\sqrt{\omega^2 + \alpha^2}}}{\sqrt{\omega^2 + \alpha^2}} \, d\omega - \int_0^{1} \frac{e^{-\frac{\Pi\rho}{b}\sqrt{\omega^2 + \alpha^2}}}{\sqrt{\omega^2 + \alpha^2}} \, d\omega$$

$$= \frac{1}{2} \left[I_1 + I_2 \right] \tag{E.6}$$

The first integral is[24]

$$I_1 = \int_0^{\infty} \frac{e^{-\frac{\Pi\rho}{b}\sqrt{\omega^2 + \alpha^2}}}{\sqrt{\omega^2 + \alpha^2}} \, d\omega = K_0\left(\frac{\Pi\rho}{b}\,\alpha\right) \tag{E.7}$$

where $K_0(x)$ is the modified Bessel function of the third kind and order zero. For small arguments[25]

$$K_0(x) \sim - \ln x \tag{E.8}$$

For large arguments[25, p.378]

$$K_0(x) \sim \sqrt{\frac{\Pi}{2x}} \cdot e^{-x} \left[1 - \frac{1}{8x} + \frac{3^2}{2!(8x)^2} - \ldots \right] \tag{E.9}$$

In the second integral of (E.6), $\frac{\Pi\rho}{b}$ is very small. But the

m^{-2} factor in Eq. (E.2), plus the effects of $\alpha^2 = m^2\left(\frac{b}{a}\right)^2$ in the exponent and in the denominator of I_2, will make the contribution from this integral very small for $m \gg 1$. We may then approximate

$$I_2 \cong \int_0^1 \frac{d\omega}{\sqrt{\omega^2 + \alpha^2}} - \frac{\Pi\rho}{b} \int_0^1 d\omega$$

$$= \ell n \left(\frac{1}{\alpha} + \sqrt{1 + \frac{1}{\alpha^2}} \right) - \frac{\Pi\rho}{b} \qquad \text{(E.10)}$$

Hence,

$$\sigma_n = \frac{b}{2\Pi} \left[\frac{e^{-\frac{\Pi\rho}{m}} \sqrt{1 + m^2\left(\frac{b}{a}\right)^2}}{\sqrt{1 + m^2\left(\frac{b}{a}\right)^2}} + K_o\left(\frac{\Pi\rho}{a} \cdot m\right) + \right.$$

$$\left. + \frac{\Pi\rho}{b} - \ell n \left(\frac{a}{b} \cdot \frac{1}{m} + \sqrt{1 + \left(\frac{a}{b}\right)^2 \cdot \frac{1}{m^2}} \right) \right] \qquad \text{(E.11)}$$

Essentially for the same reasons given above, we can safely assume that the significant contribution from σ_n in expression (E.2) will happen for values of m such that we still have

$$\frac{2\Pi\rho}{a} m \ll 1$$

and the use of (E.8) is justified.

With $kh \ll 1$, so that

$$\cos(kh) \cong 1$$

we finally have

$$S = \frac{a^2 b}{2\pi^3} \sum_{m=2,4,6\ldots} \frac{1}{m^2} \left(1 - \cos \frac{m\pi h}{a}\right)^2 \cdot$$

$$\cdot \left[\ln \frac{a}{\rho} - 1.84 - \ln \left(1 + \frac{1}{2} \sqrt{1 + m^2 \left(\frac{b}{a}\right)^2}\right) + \right.$$

$$\left. + \frac{1}{\sqrt{1 + m^2 \left(\frac{b}{a}\right)^2}} \right] \qquad (\Gamma.12)$$

List of Symbols

$\vec{A}$	Magnetic vector potential
$\vec{B}$	Magnetic flux density
D	One-half the side of a square loop
$\vec{E}$	Electric field intensity
$G(\vec{r}/\vec{r}_o)$	Scalar Green's function
$\overleftrightarrow{G}(\vec{r}/\vec{r}_o)$	Dyadic Green's function
$\vec{H}$	Magnetic field intensity
I_o	Electric current at antenna input terminals
$(I.L.)_{I_o}$	Constant-current Insertion Loss
$(I.L.)_{V_o}$	Constant-voltage Insertion Loss
$\vec{J}$	Electric current density
$\vec{J}^{\ell}$	Electric current sheet density
$\vec{J}_m^{\ell}$	Magnetic current sheet density
L	Length of Herzian dipole
$\vec{M}$	Magnetic dipole moment
$\vec{P}$	Electric dipole moment
TE	Transverse-electric, or H-mode
TM	Transverse-magnetic, or E-mode
Z_i	Antenna input impedance
a,b,d	Enclosure dimensions
a',b',d'	Source position
h	Half-length of dipole antenna
j	$\sqrt{-1}$
k	Wave number = $2\pi/\lambda$
ℓ	Aperture dimension

m,n,p	Mode integers
$\vec{r}$	Field-point position
r	Source-field point distance
$\vec{r}_c$	Source position
r,θ,ϕ	Spherical coordinates
$\overleftrightarrow{U}$	Idemfactor (unit dyadic)
x,y,z	Rectangular coordinates
$\vec{1}_n$	Normal unit vector
$\vec{1}_x,\vec{1}_y,\vec{1}_z$	Rectangular unit vectors
α_e	Electric polarizability scalar
$\overleftrightarrow{\alpha}_m$	Magnetic polarizability tensor
ϵ_o	Free-space permittivity
ϵ_m	Neumann factor ($\epsilon_{m=o}=1$; $\epsilon_{m\neq o}=2$)
λ	Wavelength
μ_o	Free-space permeability
ρ	Wire radius. Electric charge density
ρ,z,ϕ	Cylindrical coordinates
τ	Volume
ω	Angular frequency
$\vec{\nabla}$	Del (nabla) operator
∇^2	Laplacian operator

REFERENCES

[1] H. A. Bethe, "Theory of Diffraction by Small Holes," Phys. Rev., 2nd Series, 66, 163-182 (1944).

[2] F. E. Borgnis and C. H. Papas, Randwertprobleme der Mikrowellenphysik, Springer-Verlag, Berlin, Chapter II and Appendix D (1955).

[3] H. A. Méndez, "On the Theory of Low-Frequency Excitation of Cavity Resonators," IEEE Trans. Microwave Theory and Techniques, MTT-18, 444-448 (1970).

[4] R. F. Harrington, Time-Harmonic Electromagnetic Fields, McGraw-Hill, N.Y., 365-371 (1961).

[5] C. G. Montgomery, R. H. Dicke and E. M. Purcell, eds., Principles of Microwave Circuits, MIT Radiation Laboratory Series, McGraw-Hill, N.Y., vol. 8, 178 (1948).

[6] S. B. Cohn, "Determination of Aperture Parameters by Electrolytic-Tank Measurements," Proc. IRE, 39, 1416-1421 (1951).

[7] S. B. Cohn, "The Electric Polarization of Apertures of Arbitrary Shape," Proc. IRE, 40, 1069-1071 (1952).

[8] P. M. Morse and H. Feshbach, Methods of Theoretical Physics, McGraw-Hill, N.Y., vol. II, 1824 (1953).

[9] W. L. Barrow and F. M. Greene, "Rectangular Hollow-Pipe Radiators," Proc. IRE, 26, 1498-1519 (1938).

[10] L. J. Chu, "Calculation of the Radiation Properties of Hollow Pipes and Horns," J. Appl. Phys., 11, 603-610 (1940).

[11] D. S. Jones, The Theory of Electromagnetism, Pergamon Press, N.Y., 297 ff. (1964).

[12] R. E. Collin and F. J. Zucker, Antenna Theory, McGraw-Hill, N.Y., Part I Ch. 15 (1969).

[13] S. A. Schelkunoff, "Some Equivalence Theorems of Electromagnetics and Their Application to Radiation Problems," Bell Sys. Tech. J., 15, 92-112 (1936).

[14] S. A. Schelkunoff, "On Diffraction and Radiation of Electromagnetic Waves," Phys. Rev., 56, 308-316 (1939).

[15] S. A. Schelkunoff, Electromagnetic Waves, D. Van Nostrand, N.Y., 158-159 (1943).

[16] S. A. Schelkunoff and H. T. Friis, Antennas: Theory and Practice, John Wiley & Sons, N.Y., 516-519 (1952).

[17] B. Noble, Methods Based on the Wiener-Hopf Technique for the Solution of Partial Differential Equations, Pergamon Press, London (1958).

[18] E. C. Jordan and K. G. Balmain, Electromagnetic Waves and Radiating Systems, 2nd. Ed., Prentice-Hall, N.J., 535 ff. (1968).

[19] R. E. Collin and F. J. Zucker, Antenna Theory, McGraw-Hill, N.Y., Part II Ch. 23 (1969).

[20] R. W. P. King and C. W. Harrison, Jr., Antennas and Waves: A Modern Approach, M.I.T. Press, Mass., p. 187 (1969).

[21] J. A. Stratton, Electromagnetic Theory, McGraw-Hill, N.Y., p. 436 (1941).

[22] L. B. W. Jolley, Summation of Series, 2nd. Revised Ed., Dover, N.Y., p. 174 (1961).

[23] G. F. Carrier, M. Krook and C. E. Pearson, Functions of a Complex Variable: Theory and Technique, McGraw-Hill, N.Y., p. 246 ff. (1966).

[24] I. S. Gradshteyn and I. W. Ryzhik, Tables of Integrals, Series and Products, Academic Press, N.Y., p. 959 (1965).

[25] M. Abramowitz and I. A. Segun, Handbook of Mathematical Functions, Dover, N.Y., p. 375 (1968).

[26] J. E. Bridges and D. A. Miller, "Comparison of Shielding Calculations," IEEE Trans. Electromagnetic Compatibility, EMC-10, 175-176 (1968).

[27] J. Miedzinski, "Electromagnetic Screening: Theory and Practice," Tech. Report. M/T135, The British Electrical and Allied Industries Research Association, Letherhead, Surrey, p. 31 (1959).